Non-Small Cell Lung Cancer utilizes SIRT6 to initiate tumorigenesis and

overcome cellular senescence

Jaclyn Marie D'Innocenzi

A Dissertation Presented to the Graduate Faculty of the University of Virginia

in Candidacy for the Degree of Doctor of Philosophy

Department of Biochemistry and Molecular Genetics

University of Virginia

June 2017

_____

_____

_____

_____

_____

ABSTRACT

Lung cancer is one of the three most common cancers among men and women and causes more cancer-related deaths than any other type of carcinoma. Of the two subtypes, Non-small cell lung cancer (NSCLC) is the most common[1-3]. These tumors are characteristically high grade, PET-positive, indicating heightened glucose uptake and altered cancer metabolism. Sirtuin 6 (SIRT6) is a member of the sirtuin family of histone deacetylases and has previously been shown to be a key regulator of glucose metabolism, DNA damage repair, and aging[4-7]. SIRT6 has been demonstrated to act as a tumor suppressor in colon, pancreatic and liver cancer[4,8]. However, its role in NSCLC remains elusive. Here, we have developed a mouse model to study the role of SIRT6 in NSCLC, utilizing a KRAS[G12D] driver mutation and p53[flox/flox] to drive lung tumorigenesis in response to intranasal deliver of adenovirus expressing Cre recombinase. Work described here indicates that SIRT6 expression is necessary for lung tumor initiation and progression. Loss of SIRT6 expression resulted in a delay of tumor growth leading to decreased tumor burden and prolonged survival compared to animals expressing both wild-type alleles of SIRT6. Utilizing NSCLC developed mouse cell lines, we were able to show that cells lacking SIRT6 exhibited decreased proliferation, decreased formation of colonies of soft agar and increased senescence, providing a possible mechanism for the delay in tumor initiation and formation *in vivo*. Since NSCLC maintain SIRT6 mRNA expression in primary tumors, we sought to identify a potential mechanism by which cancer cells post-translationally regulate SIRT6 activity. In this study, we propose a mechanism where by SIRT6 can be lost in response to the metabolic state

of the cell. Data presented here shows that SIRT6 undergoes a glucose-responsive

N-terminal cleavage that is predicted to result in loss of its chromatin-localization

sequence (CLS), causing it to dissociate from chromatin. More specifically, we found

that SIRT6 is directly O-GlcNAcylated and that the O-GlcNAc transferase (OGT) is

necessary for this cleavage to occur. Our lab has previously shown that OGT also O-

GlcNAcylates the NF-κB subunit, p65, to allow for its full transcriptional activation.

As SIRT6 and NF-κB have been previously shown to physically interact and

antagonize one another in transcription of key metabolic genes, loss of the CLS of

SIRT6 and transcriptional activation of p65 in response to O-GlcNAcylation may

serve as a mechanism for p65-induced transcription of metabolic target genes[9].

Work described in this thesis underscores the importance of SIRT6 as an essential

enzyme required for NSCLC development, yet once carcinoma is established it

becomes dynamically misregulated by altered metabolic flux of the cancer cell.

ACKNOWLEDGEMENTS

TABLE OF CONTENTS

LIST OF FIGURES

LIST OF ABBREVIATIONS

1,3BPG – 1,3-bisphosphoglycerate

2PG – 2-phosphoglycerate

3PG – 3-phosphoglycerate

5mC – 5-methylcytosine

5mhC – 5'-hydroxymethylcytosine

Ad-Cre – Adenovirus expressing Cre

Ad-GFP – Adenovirus expressing GFP

ADC – Adenocarcinoma

AKT – Proto-oncogene AKT

ALDOA – Fructose-1,6-bisphosphate aldolase A

ALDOC – Fructose-1,6-bisphosphate aldolase C

ALK – Anaplastic lymphoma kinase

ALT – Alternative lengthening of telomeres

AMPK – AMP-activated protein kinase

ATM – Ataxia telangiectasia mutated

ATP – Adenosine triphosphate

ATR – Ataxia telangiectasia and Rad3-related protein

BCL10 – B-cell CLL/lymphoma 10

BCR – B-cell receptor

BER – Base excision repair

BMP – Bone morphogenic protein

BRAF – B-Raf proto-oncogene

BTRF – Biorepository and Tissue Research Facility

CARD11 – Caspase recruitment domain family member 11

CBP – CREB-binding protein

CDK – Cyclin-dependent kinase

CE – Cytoplasmic extraction

CHK1 – Checkpoint kinase 1

CHK2 – Checkpoint kinase 2

CHUK – Inhibitor of κB kinase α/Inhibitor of κB kinase 1

CLS – Chromatin localization sequence

CSC – Cancer stem cell

CTGF – Connective tissue growth factor

CtIP – RB-binding protein 8

DDR – DNA damage response

DNA-PK – DNA-activated protein kinase

DNase - Deoxyribonuclease

DRP – Deoxyribose-phosphate

DSB – Double strand break

E3RS$^{I\kappa B/\beta\text{-TRCP}}$ – SCF-type E3 ligase

ECM – Extracellular matrix

EGFR – Epidermal growth factor receptor

Elf3 – E74-like ETS transcription factor 3

EML4 – Echinoderm micrtotubule-associated protein-like 4

EMT – Epithelial-to-mesenchymal transition

Eno1 – Enolase-1

ER – Endoplasmic reticulum

ERK – Extracellular signal-regulated kinase

F6P – Fructose-6-phosphate

FBS – Fetal bovine serum

$FAD/FADH_2$ – Flavin adenine dinucleotide

FBP – Fructose-1,6-bisphosphate

FDG - ^{18}F-fluoro-2-deoxy-glucose

FOXM1 – forkhead box M1

G3P – Glyceraldehyde-3-phosphate

G6P – Glucose-6-phosphate

GAPDH – Glyceraldehyde-3-phosphate dehydrogenase

GCL – Glutathione cysteine ligase

GFAT - Glutamine:fructose-6P aminotransferase

GlcN6P – Glucosamine-6-phosphate

GlcNAc-1P - N-acetylglucosamine-1-phosphate

GlcNAc-6P - N-acetylglucosamine-6-phosphate

GLS – Glutamine deaminase

GLUT1 – Glucose transporter 1

GNPNAT1 - Glucosamine-6-phosphate N-acetyltransferase

GPCR – G-protein-coupled receptor

GPI – Glucose-6-phosphate isomerase

GSH – Glutathione

HAT – Histone acetyltransferase

HBP – Hexosamine biosynthesis pathway

HCF-1 – Host-cell factor-1

HDAC – Histone deacetylase

HEPES - 4-(2-Hydroxyethyl)-1-piperazine ethanesulfonate

HER2 – Human epidermal growth factor receptor 2

HIF1α – Hypoxia-inducible factor-1α

HK - Hexokinase

HR – Homologous recombination

HRE – Hypoxia-responsive element

HSF1 – Heat shock factor 1

HSP – Heat shock protein

hTERT – human telomerase reverse transcriptase

IACUC – Institutional Animal Care and Use Committee

IFNγ – Interferon-γ

IGF – Insulin-like growth factor

IGFR – Insulin-like growth factor receptor

IGFBP – Insulin-like growth factor binding protein

IκB – Inhibitor of κB

IKK – Inhibitor of κB kinase

IKKα – Inhibitor of κB kinase α

IKKβ – Inhibitor of κB kinase β

IL - Interleukin

iPS – Induced pluripotent stem (cells)

IR – Ionizing radiation

IRE1α – Inositol-requiring protein-1α

IRS1 – Insulin receptor substrate-1

ITS-E – Insulin-transferrin-selenium + ethanolamine

JMJD3 – Jumonji domain-containing 3

JunD – JunD proto-oncogene, AP-1 transcription factor subunit

KP – $KRAS^{LSL-G12D}p53^{fl/fl}$

KPS - $KRAS^{LSL-G12D}p53^{fl/fl}SIRT6^{fl/fl}$

KRAS – Kirsten rat sarcoma 2 viral oncogene homolog

LCC – Large cell carcinoma

LDH – Lactate dehydrogenase

LKB1 – Liver kinase B1

LOH – Loss of heterozygosity

LPS - Lipopolysaccharide

MAPK – Mitogen-activated protein kinase

Mcl – Myeloid leukemia cell differentiation protein

Mcl-1 – Myeloid cell leukemia 1

MCT - Monocarboxylate transporters

MDM2 – Double minute 2

MEF – Mouse embryonic fibroblast

MEM-NEAA – Minimal essential medium + non-essential amino acids

MMP – Matrix metalloproteinase

mOGT – Mitochondrial-specific OGT

MRI – Magnetic resonance imaging

MSK – mitogen- and stress-activated protein kinase

mTOR – Mechanistic target of Rapamycin

MyD88 – Myeloid differentiation primary response 88

N-CoR – Nuclear receptor co-repressor

NAD^+/NADH – Nicotinamide adenine dinucleotide

NADPH – Nicotinamide adenine dinucleotide phosphate

NAGK - N-acetylglucosamine kinase

ncOGT – Nucleocytoplasmic OGT

NE – Nuclear extraction

NEMO – Inhibitor of κB kinase γ

NF-κB – Nuclear factor-κB

NFKB1 – p105/p50

NFKB2 – p100/p52

NF1 – Neurofibromin 1

NHEJ – Non-homologous end joining

NLS – Nuclear localization sequence

NSCLC – Non-small cell lung cancer

OGA – O-GlcNAcase

OGA-L – Long OGA

OGA-S – Short OGA

OGT – O-GlcNAc transferase

OIS – Oncogene-induced senescence

PaIN – Pancreatic intraepithelial neoplasm

PARP1 - Poly[adenosine diphosphate (ADP)-ribose] polymerase 1

PBS – Phosphate buffered saline

PDAC – Pancreatic ductal adenocarcinoma

PDK1 – Pyruvate dehydrogenase kinase 1

PD-L1 – Programmed death ligand-1

PD1 – Programmed cell death 1

PDGF – Platelet-derived growth factor

PDH – Pyruvate dehydrogenase

PDK1 – Pyruvate dehydrogenase kinase 1

PEP - Phosphoenolpyruvate

PET-CT - Positron emission tomography and computer tomography

PFK - Phosphofructokinase

PFK1 – Phosphofructokinase-1

PGI – Phosphoglucoisomerase

PGK – Phosphoglycerate kinase

PGM – Phosphoglycerate mutase

PGM3 - Phosphoacetylglucosamine mutase

PIDD - p53- induced death domain factor

PIK3CA – Phosphotidylinositol-4,5-bisphosphate 3-kinase catalytic subunit-α

PIP3 – Phosphatidylinositol-3,4,5-triphosphate

PK – Pyruvate kinase

PKA – Protein kinase A

PKM1 – Pyruvate kinase M1

PKM2 – Pyruvate kinase M2

PMSF - Phenylmethylsulfonyl fluoride

PPP – Pentose phosphate pathway

PTEN – Phosphatase and tensin homolog

PTM – Post-translational modification

Rb - Retinoblastoma

RB1 - Retinoblastoma

RET – Ret proto-oncogene

RHC – Research histology core

RHD – Rel-homology domain

RIP – Receptor interacting protein

ROS – Reactive oxygen species

ROS1 – ROS proto-oncogene 1

SA-β-Gal – Senescence-associated-β-galactosidase

SAHF – Senescence-associated heterochromatic foci

SASP – Senescence-associated secretory phenotype

SCC – Squamous cell carcinoma

SCLC – Small cell lung cancer

SCO2 – Cytochrome C oxidase assembly protein

SIRT6 – Sirtuin 6

SLC – Solute carrier

SMRT – Silencing mediator of retinoic acid and thyroid

Snail1 – Snail family zinc finger 1

SNP – Short nucleotide polymorphism

SOD – Superoxide dismutase

sOGT – Short OGT

TAB1 – Transforming growth factor-β-activated binding protein 1

TAD – Transcription-activating domain

TAK1 – Transforming growth factor-β-activated kinase 1

TCA – Tricarboxylic acid

TCR – T-cell receptor

TET – Ten eleven translocation

TGFβ – Transforming growth factor-β

TIGAR – TP53-induced glycolysis and apoptosis regulator

TKI – Tyrosine kinase inhibitor

TLR – Toll-like receptor

TNF – Tumor necrosis factor

TNFR1 – TNF receptor 1

TPI – Triosephosphate isomerase

TPR – Tetraticopeptide repeat

TRAF2/5 – TNF receptor-associated factor 2/5

UAP1 - UDP N-acetylglucosamine pyrophosphorylase

UDP - GlcNAc - Uridine diphosphate N-acetylglucosamine

UPR – Unfolded protein response

UTP – Uridine-5'-triphosphate

VHL – Von Hippel-Lindau

WNT10B – Wingless-type family member 10B

WRN - Werner Syndrome RecQ-like helicase

Xbp-1 – X-box binding protein 1

XIAP – X-linked inhibitor of apoptosis

CHAPTER I

General Introduction

LUNG CANCER

Lung cancer is the leading cause of cancer-related deaths, accounting for 25% of all cancer-related deaths in the United States. More people die of lung cancer than of breast, colon and prostate cancer combined. Lung cancer is also one of the most prevalent cancers in the world, accounting for approximately 14% of all newly diagnosed cancer cases. The American Cancer Society predicts that there will be 222,500 new cases of lung cancer diagnosed and 155,870 deaths from lung cancer in 2017[2]. Despite the fact that lung cancer incidence is decreasing in many western countries, globally the rate has been increasing. This is thought to be due to an increase in the incidence of lung cancer in most other countries, largely due to tobacco usage. Globally, only about 7-12% of lung cancer patients are alive at 5 years following diagnosis[10].

For smokers, the lifetime risk of developing lung cancer is 16 times that of never smokers. Thus, tobacco usage is the main etiological factor associated with the development of lung cancer. About 85% of all lung cancers occur in past or present smokers[11]. Cigarette smoke contains many known carcinogens, including but not limited to tobacco-specific nitrosamines and polycyclic aromatic hydrocarbons. Exposure to such carcinogens causes formation of DNA adducts, resulting in errors in DNA replication and repair, which eventually accumulate to cause the development of cancer[14]. Other environmental factors are also thought to potentially have a role is being causative of lung cancer, including but not limited to exposure to, asbestos, silica fibers, diesel exhausts, arsenic, nickel, radon, soot and coal fumes[15].

Lung cancer can be categorized into two distinct subtypes based on cell type: small cell lung cancer (SCLC) and non-small cell lung cancer (NSCLC). SCLC comprises approximately 13% of lung cancer cases and occurs almost exclusively in the smoker patient population. It arises from neuroendocrine cells, most of the time located near the bronchi. SCLC is extremely aggressive, and characterized by early metastasis. Only about 6% of patients are alive at 5 years following diagnosis. NSCLC accounts for 84% of all lung cancer cases, including the never smoker lung cancer patient cases, and carries a 5 year survival rate of about 21%. NSCLC can further be divided into three subtypes: adenocarcinoma (ADC), squamous cell carcinoma (SCC) and large cell carcinoma (LCC)[1,12-14]. ADC is the most common subtype of NSCLC, accounting for 40% of lung cancer cases. It is characterized by the formation of glands and presence of intracellular mucin[15,16]. ADC is also the most common subtype of NSCLC in the women, Asian and never smoker patient populations. The initiation of ADC is thought to be slower than that of the other subtypes of NSCLC, but it is also thought to progress and metastasize faster than SCC and LCC[1,3,16]. SCC is the second most common type of NSCLC, accounting for 30% of lung cancer cases. It arises from squamous cells that line the bronchi, and is characterized by the presence of keratin pearls and intercellular bridges[1,13,16]. SCC is more strongly associated with smoking than ADC. SCC is more common in men than women, and grows more slowly than other types of NSCLC. LCC accounts for 15% of lung cancer cases, and does not tend to occur in any one location in the lung. It also is generally poorly differentiated, more aggressive, and tends to grow and metastasize rapidly[1,3]. It is important to note that most patients with NSCLC die due

to metastatic disease. Thus, early detection is one of the most important prognostic factors for these patients. Unfortunately, more than 50% of NSCLC patients are stage IV with distant metastatic disease at diagnosis, and collectively have a 5 year survival rate of less than 5%[16]. Thus, further research is greatly needed to identify molecular targets for therapy in this deadly cancer.

Unfortunately, one single tumorigenic driver mutation for NSCLC has not been identified to date. However, several driver mutations have been identified in select populations of NSCLC patients. EGFR mutations are seen in approximately 10-15% of NSCLC patients, predominantly in patients with adenocarcinomas that are part of the female, Asian, never-smoker patient population[16,17]. Anaplastic lymphoma kinase (ALK) rearrangements are also primarily seen in never-smoker patients with adenocarcinomas over any other patient population. ALK rearrangements occur in approximately 5% of NSCLC tumors, and most commonly, these rearrangements result in an echinoderm microtubule-associated protein-like 4 (EML4)-ALK fusion gene[16]. In addition to EGFR and ALK mutations and rearrangements, alterations in other growth factor signaling proteins, including the human epidermal growth factor receptor 2 (HER2/neu) gene *ERBB2*, hepatocyte growth factor receptor MET gene, ROS proto-oncogene (ROS1) and Ret proto-oncogene (RET) occur in approximately 3%, 7%, 2% and 1% of ADC tumors, respectively[17]. KRAS mutations are yet another set of driver mutations that are present in about 30% of adenocarcinomas and 5% of squamous cell carcinomas. They are often associated with tumors of mucinous pathology, and are present in both the smoker and never-smoker populations[16]. However, the specific KRAS

mutations between these two populations tend to be different from one another[18].

In both populations, most mutations occur in exons 12 and 13 of KRAS, although

transition mutations were much more common in the never smoker population

while transversion mutations were much more common in the current and former

smoker population[18]. It is important to note that the presence of a KRAS mutation

in NSCLC is a strong negative predictor of the presence of EGFR or ALK mutations[16].

Neurofibromin 1 (NF1), a negative regulator of RAS proteins, was also mutated in

approximately 11% of ADC cases. Further down this pathway, BRAF mutations

were also seen in patients with ADC, occurring in about 7% of cases. Lastly,

alterations in the mTOR pathway were also seen. The STK11 gene encoding tumor

suppressor liver kinase B1 (LKB1), a negative regulator of the AMP-activated

protein kinase (AMPK) and mammalian target of rapamycin (mTOR) pathway, is

mutated in approximately 17% of ADC patients[18].

Aside from growth factor signaling, several other pathways are known to be

altered in ADC. These include pathways that impact DNA damage response, cell

cycle progression, and tumor evasion of the immune response. Notably, TP53

encoding the p53 protein and ataxia-telangiectasia (ATM) are mutated 46% and 9%

of ADC patients respectively, and are also mutually exclusive in this population.

Also within this DNA damage response pathway, the negative regulator of p53,

double minute 2 (MDM2), is a known tumor driver and contains an activating

mutation in about 8% of ADC cases[18]. With regard to cell cycle progression, the

CDKN2A gene encoding the cyclin-dependent kinase (CDK) inhibitor p16^{INK4A}, has

been shown to be inactivated in approximately 43% of ADC patients. However, its

downstream effector retinoblastoma (RB1) is only mutated in about 7% of ADC

cases[18]. Recently, it was found that programmed death ligand-1 (PD-L1) may

represent a useful biomarker and/or target for therapy in NSCLC tumors where

>50% of cells express this protein. PD-L1 binds PD-1 expressed on immune cells to

inhibit activation of these cells, and thus PD-L1 expression on cancer cells is thought

to be a mechanism of immune evasion by the tumor[19]. PD-L1 is reported to be

expressed in 13-70% of NSCLC tumors, depending on the study. However, it is

estimated that 30% of NSCLC tumors have high PD-L1 expression (>50% of cells),

making these patients eligible for treatment with a targeted therapy to PD-L1.

Many of the aforementioned genetic alterations observed in ADC also occur

in the SCC subtype of NSCLC, albeit at different frequencies. For genes involved in

growth factor signaling, EGFR and ERBB2 are mutated in only 9% and 4% of SCC,

respectively[12]. KRAS and HRAS mutations are each present in only 3% of SCC

patients, while BRAF and NF1 mutations occurred in 4% and 11% of these tumors,

respectively. Additionally, mutations resulting in activation of phosphatidylinositol-

4,5-bisphosphate 3-kinase catalytic subunit-α (PIK3CA) signaling are more frequent

in SCC than ADC. Activating mutations in PIK3CA occur in 16% of SCC tumors while

inactivating mutations in its inhibitor PTEN occur in 15% of SCC cases. Further

down this pathway, AKT3 is activated in 16% of SCC patients[12]. Despite knowing

and developing targeted therapies to many of the aforementioned genetic

alterations observed in NSCLC, to date, we still do not know the driver mutations

responsible for greater than 70% of NSCLC tumors[9,20].

Clinically, surgical resection with neoadjuvant and/or adjuvant chemotherapy remains the mainstay of potentially curative treatment in patients with early-stage (Stage I and II), local disease confined to the lung and local lymph nodes that does not involve the mediastinum. The five year survival rates of stage IA, IB, IIA an IIB patients are 50%, 43%, 30% and 25% respectively[2,21]. However, the combined rate of recurrence, local or distant, following surgical resection in these patients with local disease is approximately 42%[22,23]. Although post-operative radiation therapy is only indicated for patients with unclean tumor margins, adjuvant chemotherapy following surgical resection is indicated for all patients with Stage IB-II disease, but not in Stage IA patients with a local tumor measuring ≤3 cm[11,21]. Currently, adjuvant chemotherapy consists of a Cisplatin-based doublet with permetrexed for tumors with non-squamous histology, and one of either vinorelbine, docetaxel or gemcitabine for tumors with squamous histology[13,14,24]. With such a high rate of recurrence in patients with only local disease, it is imperative to develop new treatment strategies to combat this deadly cancer.

For NSCLC patients with Stage III disease, surgical resection is not always an option, and chemotherapy and radiation, with or without molecular targeted therapies, are the mainstay of treatment[15,25]. Currently, overall 5-year survival is only between 8-18%[1,21]. Concurrent chemotherapy and radiation has been shown to have a survival benefit over sequential chemotherapy and radiation. Currently, the two most effective chemotherapy regimens have been shown to be cisplatin and etoposide, or carboplatin and paclitaxel[16,25]. For patients with advanced Stage IV

disease, cytotoxic chemotherapy with Cisplatin and permetrexed (for tumors with non-squamous pathology) or Cisplatin and vinorelbine, docetaxel or gemcitabine (for tumors with squamous histology) become the first-line of treatment[2,10]. Metastases to the brain, bone and adrenal glands are common in NSCLC patients with advanced disease. Currently, overall survival is dismal (2%) for these patients[21,22]. If a known driver mutation is not present and the tumor shows non-squamous histology, adding bevacizumab has been shown to increase progression-free survival and overall survival in patients with advanced disease[10,11]. For patients with EGFR mutations, use of the TKIs erlotinib, gefitinib and afatinib are indicated. Erlotinib has been shown to increase progression-free survival, to 13.1 months from 4.6 months with chemotherapy alone, in patients with advanced NSCLC[13,14,26]. For patients with an ALK fusion protein present in their tumor, use of one of the ALK TKIs, crizotinib or ceritinib, is recommended. Crizotinib has been shown to have a positive effect on progression-free survival in patients with advanced NSCLC that contains an ALK fusion proteins, increasing progression-free survival to 10.9 months vs. 7 months with chemotherapy alone[15,27]. For patients with high PD-L1 expression, first-line therapy can include use of the anti-PD-L1 inhibitor pembrolizumab. Pembrolizumab was recently approved in the United States for use in patient with advanced NSCLC that has high expression of PD-L1 as it was shown to increase progression-free survival to 10.3 months compared to 6 months in patients receiving chemotherapy alone[1,28]. Although the advent of molecularly targeted therapies for advanced-stage NSCLC patients has had a significant effect on patient survival, the overall survival rates for patients with late-

stage disease have not improved in over thirty years. Thus, there is an unmet need

for new effective therapies to combat advanced NSCLC.

SENESCENCE

Cellular senescence is a process of cell aging whereby the cell suffers a

reduction in proliferative capacity despite its continued viability. The process of

senescence has thus been said to make cells "mortal", by way of the fact that normal

non-cancerous cells have a limited replicative lifespan. Thus, in order for cancer

cells to proliferate indefinitely, they must overcome senescence. Moreover, they

must also be able to overcome senescence-induced cell death caused by many

chemotherapeutic agents as a result of DNA damage.[16,29] As such, senescence

represents a cellular process that has the potential to be exploited as a therapy to

combat cancer.

There are several different types of senescence. The most well known type is

replicative senescence, whereby senescence is induced in response to shortened

telomeres in actively proliferating cells. Single-stranded DNA at telomeric ends is

normally protected by the formation of a T-loop by the shelterin complex. The t-

loop prevents the single-stranded telomeric DNA from eliciting a DNA damage

response (DDR)[1,3,16,30]. Telomere shortening occurs in actively proliferating cells in

response to the "end replication problem", whereby DNA polymerase fails to

completely replicate the ends of the lagging strand, leading to a shortening of the

telomere with each replication process[1,13,16,31,32]. When the telomere reaches a

critically short length, the DDR is triggered as the single stranded DNA at telomeric

ends becomes exposed. Activation of the DDR leads to the formation of γ-H2AX foci

at the shortened telomere, and subsequent activation of ATM and ATR kinases, and

their downstream effectors CHK1 and CHK2. CHK1 and CHK2 then phosphorylate

and activate CDC25 and p53, respectively, to induce cell cycle arrest. Depending on

the cellular response, activated p53 up-regulates p21 to halt the cell cycle, and then

p53 initiates either apoptosis or the senescence program[1,3,33]. In addition to the

p53-dependent DDR, replicative senescence can also activate p16[INK4A], which

inhibits CDK4 and CDK6 and subsequently RB to induce senescence[16,34]. Thus,

inactivation or loss of p53 and/or p16[INK4A] can abrogate the replicative senescence

phenotype. However, the effect is temporary; a continuing shortening telomere

eventually results in cell death due to genomic instability[16,17,35]. Over-expression of

human telomerase reverse transcriptase (hTERT) is one method continuously

proliferating cancer cells can exploit to lengthen and/or maintain telomeres[16,36,37].

Tumor cells can also maintain telomere length through the alternative lengthening

of telomeres (ALT) pathway, which allows for homology-directed lengthening of

telomeres by an invading homologous strand[17,30].

Another type of senescence, termed premature senescence, can occur

independent of telomere shortening. One type of premature senescence is stress-

induced senescence, which occurs when environmental factors are sub-optimal for

cell survival and proliferation[16,29,38]. *In vitro*, stress-induced senescence has been

overcome by silencing of p53 and/or RB[18,39,40]. Oncogene-induced senescence (OIS)

is yet another mechanism of senescence that is independent of telomere length and

thus, is not rescued by over-expression of hTERT[18,41]. This form of senescence is

thought to occur through p16[INK4A] and/or p21 –dependent inhibition of CDK4/6,

which in turn fail to phosphorylate and inactivate RB. RB then inhibits E2F-

dependent transcription and thus induces senescence. Contrary to the rescue of

replicative senescence by hTERT, knockout of either p53 and/or p16[INK4A] are

necessary to overcome OIS in transformed cells, depending on the type of

transformation and the specific cell type. For example, murine RAS-transformed

cells have been shown to exhibit p53-dependent OIS while human RAS-transformed

cells have been shown to exhibit more p16[INK4A]-dependent OIS[16,42,43]. As both p53

and p16[INK4A] have been shown to inhibit induction of induced pluripotent stem (iPS)

cells, it has been suggested that OIS may not only inhibit tumor cell proliferation, but

may also inhibit formation of cancer stem cells (CSCs)[18,29]. As oncogenic

transformation can induce OIS, it has also been shown that loss of a tumor

suppressor can induce senescence as well. In both mouse and human cells, loss of

PTEN has been shown to be sufficient to induce senescence in a p53-dependent

manner[18,44].

In particular, KRAS[G12D] mutations, resulting in constitutively active Ras

activity, have been shown to induce OIS, particularly characterized by an

irreversible G1 arrest. Importantly, mouse cells transformed with oncogenic Ras

require inactivation of either p53 or p16[INK4A] to overcome OIS[18,45]. This phenotype

has also been shown to represent the progression from a pre-malignant to

malignant cancerous lesion. For example, pancreatic intraepithelial neoplasms

(PanINs) are a pre-malignant lesion to pancreatic ductal adenocarcinoma (PDAC).

Morton et al. 2010 showed that expression of oncogenic KRAS[G12D] induced

formation of senescent PanINs that rarely progressed to PDAC. However, inactivation of p53 caused a selective outgrowth of cells with both of these phenotypes and formation of PDAC in a p21-dependent manner[19,46].

Due to earlier studies, it was believed that senescence could be classified as being a permanent, irreversible state of reduced proliferative capacity. However, recent studies suggest that this may not be true, and that mechanisms exist to escape the senescent state. Notably, this reversal has been shown to occur in response to p53 inactivation and/or oncogenic KRAS expression[12,47-49]. However, this reversal is p16[INK4A]-dependent and only occurs in cells with low p16[INK4A] expression prior to becoming senescent[12,47]. On the contrary, senescence has been shown to be irreversible in cells with high p16[INK4A] expression that suffer p53 inactivation and/or Ras expression [20,47].

In general, senescent cells often undergo a morphological change and take on a large, flat and/or sometimes multinucleated phenotype. In addition to this morphological change, there are specific molecular markers of cellular senescence. Most notable is the increased activity of senescence-associated-β-galactosidase (SA-β-Gal). The enzyme, β-D-Galactosidase, has activity within the lysosomal compartment at the optimal pH of 4.0 in normal, proliferating cells. However, in senescent cells, the lysosomal compartment expands. β-D-Galactosidase in senescent cells (or SA-β-Gal) is overexpressed and accumulates in the lysosome, thus allowing for notable activity at a suboptimal pH of 6.0[21,29]. Chromatin changes also occur during senescence, particularly deemed senescence-associated heterochromatic foci (SAHF). These foci are enriched for methylation of Lys 9 of

histone H3 with the exclusion of H3K9Ac and H3K4me. Notably, formation of these loci have been noted within the promoters of several E2F target genes[23,29,50,51].

Several cellular mechanisms exist that can modulate OIS. One such mechanism is DNA damage, which can be in response to telomere shortening, chemotherapy, and/or ionizing radiation, amongst other causes. Although the DDR is not essential for OIS, it can induce senescence in a p53-dependent manner[21,52-54]. Another such mechanism is the production of reactive oxygen species (ROS). It has been shown that ROS levels are increased in OIS, and also that exposure to H_2O_2 can induce OIS[24,55,56]. It is thought that ROS can induce OIS through induction of p21[WAF1/CIP1] in response to DNA damage[25,57]. Additionally, p21-induced senescence has been shown to be dependent upon p21-mediated accumulation of ROS[21,58].

Senescence has also been shown to affect cell secretion of different molecules and factors into the microenvironment. Thus, as it pertains to cancer, senescence can modulate the tumor microenvironment via secretion of predominantly pro-inflammatory cytokines. This phenomenon has been termed the senescence-associated secretory phenotype (SASP) [25,34,49,59]. Past studies have shown that cells cultured with senescent fibroblasts show increased oncogenic and tumorigenic phenotypes, with regard to processes including increased proliferation, migration and invasion. Thus, senescence of a given population of cells can promote the oncogenic potential of neighboring transformed cells through modulation of not only pro-oncogenic processes, but also the release of inflammatory cytokines and the extracellular matrix (ECM) proteins into the tumor microenvironment[29]. With regard to cell tumorigenicity, senescent fibroblasts co-cultured with pre-malignant

and malignant epithelial cells facilitated cellular proliferation and tumor formation *in vitro*[60]. Recently, it was shown that sustained DNA damage, such as that which occurs in cancer, is required for induction of the SASP[59,61].

Senescent cells themselves were shown to suppress production of ECM proteins while concomitantly increasing levels of ECM-degrading enzymes, thus facilitating invasion. Members of the matrix metalloproteinase (MMP) family of proteases can function to breakdown the ECM and facilitate invasion and migration of cancer cells. MMP-1, MMP-3 and MMP-10 have specifically been shown to be part of the SASP and are up-regulated in senescent cells[62,63].

Growth factors are also part of the SASP, and can contribute to cell proliferation and resistance to cell death in malignant cells. Insulin-like growth factor binding proteins (IGFBP)-2, -3, -4, -5, and -6 have been shown to be secreted by senescent epithelial cells, along with their regulator proteins, the connective tissue growth factor (CTGF) family[49]. Activation of the IGF pathway in NSCLC has been show to potentiate cell proliferation, survival and resistance to apoptosis, and invasiveness, potentially through its downstream activation of the PI3K/AKT/mTOR pathway and/or RAF/RAS/MAPK pathway[64]. Thus, secreted factors involved in the IGF pathway by senescent cells are a double-edged sword – secretion of IGFBPs function to induce senescence and apoptosis by binding and sequestering IGF away from its receptor whereas CTGF expression alone can act in place of IGF1 to promote tumor cell proliferation[65]. Interestingly, SIRT6 is another regulator of this pathway as absence of SIRT6 is correlated with low IGF1 levels in mice. Furthermore, absence of SIRT6 was found to result in increased AKT activity while

recently, SIRT6 itself was shown to undergo AKT-mediated degradation in response to its phosphorylation by AKT on Serine 338. Thus, SIRT6 is directly phosphorylated and down-regulated by AKT, while IGF1-dependent signaling to AKT is negatively regulated by the SIRT6 deacetylase[66].

Perhaps the largest category of molecules that make up the SASP are inflammatory cytokines and chemokines. Interleukin-1 (IL-1) and Interleukin-6 (IL-6) are two prominent pro-inflammatory cytokines secreted as a part of the SASP. Expression of IL-6 has been shown to be regulated and induced by prolonged DNA damage eliciting a DDR response via ATM and CHK2 in a p53-independent manner[49,59]. IL-6 and IL-8 are also part of the SASP, and function in an autocrine manner to positively feedback to reinforce the senescent state. Additionally, these cytokines recruit immune cells to senescent cells for clearance[67,68]. Both IL-1α and IL-1β expression are also induced in senescent cells, especially in response to chemotherapy-induced senescence of cancer cells[49,69]. IL-1 acts as a pro-inflammatory cytokine that can activate the NF-κB pro-survival pathway to promote oncogenesis and tumor cell survival[49,70]. NF-κB was recently shown to be a master regulator of the SASP. OIS cells expressing H-RAS[V12] were found to induce, activate and translocate in to the nucleus the p65 subunit of NF-κB. Furthermore, p65 was found to localize to chromatin with enrichment in factors that are part of the SASP. However, the growth arrest phenotype observed in OIS was found to be dependent on both p65 and p53, due to p16[INK4] accumulation, suggesting that these two proteins co-regulate this process[71]. Additionally, persistent NF-κB activation was shown to inhibit Ras-induced OIS via suppression of the DDR response[72]. Thus,

many of the overlapping pathways that modulate senescence co-regulate the induction and duration of the response linking the DDR with p53 and NF-κB signaling and SASP.

SIRTUIN 6 (SIRT6)

The Sirtuin family of NAD^+-dependent histone deacetylases has been known to be involved in multiple cellular processes involved in cancer development and progression, including regulation of transcription, metabolism, cell division, aging, and DNA damage repair [4,6,7,73,74]. One member of this family, Sirtuin 6 (SIRT6), has been implicated to play a role in all of these processes. It is nuclear-localized, and has been shown to serve as a deacetylase targeting H3K9Ac and H3K56Ac, an ADP-ribosyltransferase, and a long chain fatty acyl hydrolase[73,75,76]. Specifically, SIRT6 has been shown to have a role in regulating metabolism by inhibiting glucose uptake, promoting repair of DNA damage and promoting longevity through telomere stability[4,6,7,74]. In pancreatic, liver and colon cancer, SIRT6 has been shown to function as a tumor suppressor using mouse models [4,8]. However, the role of SIRT6 in lung cancer has remained elusive.

SIRT6 has been implicated as a master regulator of glucose metabolism. The first evidence for this came from the phenotype of SIRT6^{-/-} mice. These mice exhibited osteopenia, lymphopenia, loss of subcutaneous fat and perhaps most striking, hypoglycemia, all of which resulted in a premature death before one month of age[77]. Loss of SIRT6 has been shown to increase glucose uptake, perhaps through increased expression of the glucose transporter, GLUT1. In addition to affecting

glucose uptake, SIRT6 has been shown to modulate expression of the key glycolytic

enzymes, phosphofructokinase-1 (PFK1), Aldolase C (ALDOC), Pyruvate

dehydrogenase kinase 1 (PDK1) and lactate dehydrogenase (LDH), through its role

as a co-repressor of hypoxia-inducible factor-1α (HIF1α). Co-repression of these

glycolytic genes that have been shown to be regulated by both SIRT6 and HIF1α ,

and is proposed to occur through direct binding of SIRT6 to the promoters of these

genes and its subsequent deacetylation of H3K9Ac, a histone H3 mark associated

with active transcription. Thus, in the absence of SIRT6, cells display altered

metabolic profiles consistent with the "Warburg effect"; a phenotype common to

cancer cells whereby the cells up-regulate glucose uptake and switch to lactic acid

fermentation while concurrently inhibiting passage through the TCA cycle and

subsequent oxidative phosphorylation[5].

Perhaps the most striking phenotype of SIRT6 loss is in its modulation of

DNA damage and aging. SIRT6-deficient mice exhibit a degenerative phenotype of

premature aging characterized not only by metabolic effects, such as hypoglycemia,

but also by low levels of IGF1, leading to poor bone development portrayed by thin

bones and lordokyphosis; these are features of many other aging mouse models.

Additionally, these mice show lymphopenia, and eventually these effects lead to a

premature death before one month of age. At a molecular level, loss of SIRT6

induces slowed growth and an increased sensitivity to genotoxic damage, including

that from alkylating agents and oxidative damage. SIRT6-deficient cells also show

increased levels of genomic instability resulting in chromosome breakage[77].

SIRT6 has been shown to modulate two DDR pathways: base excision repair (BER) and double-strand break (DSB) repair. One piece of evidence suggesting that SIRT6 affects BER comes from the increased sensitivity of SIRT6^{-/-} cells to ionizing radiation (IR). SIRT6 is thought to alter the chromatin environment via its deacetylation activity of K3K9Ac and H3K56Ac, such as to affect access of BER factors to chromatin. SIRT6 has also been shown to deacetylate polβ *in vitro*, a requirement for this protein's DRP-lyase activity[77]. The rate-limiting step of BER has been shown to be dependent on cleavage of the 5'-deoxyribose-phosphate domain of polβ – possibly by the DRP-lyase activity [78]. Additionally, re-introduction of a smaller domain of the protein preserving its DRP-lyase activity into SIRT6^{-/-} cells rescues the defective BER phenotype, perhaps because the smaller protein can access chromatin. In addition to BER, SIRT6-deficient cells have also been shown to exhibit defective DSB repair, first observed through increased chromosomal instability in these cells[77,79]. It was then found that SIRT6 binds and stabilizes DNA-PK at sites of DSBs. DNA-PK is required for NHEJ-directed repair of DSBs. Moreover, SIRT6 was found to be essential for deacetylation of H3K9Ac in response to induction of DSBs[79]. Applicable to both BER and non-homologous end joining (NHEJ) DSB repair, SIRT6 has been shown to mono-ADP-ribosylate poly[adenosine diphosphate (ADP)-ribose] polymerase 1 (PARP1) on lysine 521[74]. This activates PARP1's poly-ADP-ribosylase activity, which is essential for its role in recruiting DNA damage repair proteins to sites of DNA breaks[74,80,81]. Lastly, in addition to modulating NHEJ-directed DSB repair, SIRT6 also modulates homologous recombination (HR)-directed repair of DSBs. This occurs through deacetylation of

RB-binding protein 8 (CtIP) by SIRT6, which promotes DNA-end resection of DSBs, a crucial step to allow for HR-directed repair[82,83]. Because SIRT6 has been shown to modulate DNA damage and repair, it may play a role in modulating not only lung cancer progression, but also initiation.

Furthermore, SIRT6 has been shown to have a role in aging by modulation of not only DDR pathways but also telomere stability. This occurs through its deacetylase activity on H3K9Ac. Deacetylation of H3K9Ac by SIRT6 functions to form heterochromatin at telomeric ends, leading to silencing of telomere transcription[6,7]. This results in maintenance of telomeric end length, and in this way, SIRT6 promotes longevity[7]. Loss of SIRT6 in mice induces a progeroid phenotype, portraying a loss of subcutaneous fat, lymphopenia, osteopenia, lordokyphosis, and premature death, all of which are characteristics of aging models. Thus, it seems as though SIRT6 is required to prevent premature aging, perhaps through maintenance of telomeric ends[77]. SIRT6 has been shown to specifically associate with telomeric ends, while its loss results in telomere instability that leads to chromosomal end-to-end fusions and senescence. SIRT6 has been shown to directly interact with Werner Syndrome RecQ-like helicase (WRN), a helicase localized to telomeres that functions in telomeric replication[73,84]. SIRT6 functions to stabilize localization of WRN to the telomere, preferentially during S-phase[73]. Lastly, SIRT6 has also been shown to inhibit aging by its role in HR-directed repair of DNA DSBs. Cells exogenously expressing SIRT6 are able to overcome replicative senescence by restoring HR rather than utilizing error-prone NHEJ to repair DNA DSBs[85].

CANCER METABOLISM

One common feature of cancer cells is that they exhibit altered metabolism thought to support their increased energy demands due to rapid proliferation rates. Cancer cells show increased glucose uptake, followed by an increase in glycolysis and aerobic fermentation with a concomitant decrease in flux through the citric acid cycle (TCA). This effect was first described in the 1920's by Otto Warburg, and was thus deemed the Warburg effect. Although such altered metabolism is less efficient in terms of ATP production, it provides the cancer cell with increased glycolytic intermediates that can be used in protein, lipid and nucleic acid synthesis. This idea is supported by the fact that many cancer cells that undergo Warburg metabolism have unchanged rates of mitochondrial oxidative phosphorylation[86,87]. In addition to altered glucose uptake, many cancer cells also exhibit an increase in glutamine metabolism. Glutamine has a role in maintaining redox homeostasis and replenishing TCA cycle intermediates in a process deemed anaplerosis[88,89]. This feature of cancer cells is exploited today for many types of tumors, including NSCLC, in the imaging modality of positron emission tomography and computer tomography (PET-CT) scan with radiolabeled glucose derivative ^{18}F-fluoro-2-deoxy-glucose (FDG) [86,87].

Glucose crosses the plasma membrane and enters the cytoplasm of the cell through a family of glucose transporters (GLUT). The first step during glycolysis is the phosphorylation of glucose by hexokinase (HK) to form glucose-6-phosphate (G6P). Unlike glucose, G6P is sequestered in the cell. G6P is an important glycolytic

intermediate but also can be shuttled into the pentose phosphate pathway (PPP) to generate NADPH and ribose for nucleotide synthesis[87]. Glycogen catabolism can also generate G6P, which can be use in glycolysis and PPP[90]. The next step in glycolysis is the conversion of G6P into fructose-6-phosphate (F6P) by phosphoglucoisomerase (PGI). Then, key regulatory enzyme phosphofructokinase (PFK) converts F6P into fructose-1,6-bisphosphate (FBP). FBP is then used to make two molecules of glyceraldehyde-3-phosphate (G3P) using the enzyme fructose-1,6-bisphosphate aldolase A (ALDOA). G3P can then have two fates: it may be isomerized by triosephosphate isomerase (TPI) to form dihydroxyacetone or it may be converted into 1,3-bisphosphoglycerate (1,3BPG) by glyceraldehyde-3-phosphate dehydrogenase (GAPDH). 1,3-BPG then feeds into the next step of glycolysis, which is conversion into 3-phosphoglycerate (3PG) by phosphoglycerate kinase (PGK). Phosphoglycerate mutase (PGM) then converts 3PG into 2-phosphoglycerate (2PG), followed by conversion of 2PG into phosphoenolpyruvate (PEP) by enolase. In the final step of glycolysis, PEP is then converted into pyruvate by a key regulatory enzyme, pyruvate kinase (PK). Pyruvate then can have several fates: it can be decarboxylated into acetyl-CoA by pyruvate dehydrogenase (PDH) and enter the TCA cycle, or it can be converted into lactate by lactate dehydrogenase (LDH) for aerobic fermentation and shuttled out of the cell by monocarboxylate transporters (MCT). Such production of lactate and transport of it out of the cell contributes to acidification of the local environment, which can promote cancer invasion. Glycolysis yields two total ATP molecules and two total NADH molecules per molecule of glucose. Aerobic fermentation, which occurs during periods of

hypoxia, then can yield an additional two ATP molecules per molecule of glucose. The TCA cycle occurs in the mitochondria and ultimately converts acetyl-CoA into malate, which can then be recycled into the first step of the cycle again. The TCA cycle has the following intermediates: oxaloacetate, citrate, isocitrate, α-ketoglutarate, succinyl-CoA, succinate, fumarate and malate. Several of these intermediates, including oxaloacetate, α-ketoglutarate, succinyl-CoA and fumarate, have important roles in other biosynthetic pathways. However, passage through the TCA cycle also yields eight NADH, two $FADH_2$, two molecules of ATP and six CO_2 molecules. NADH and $FADH_2$ molecules can then be used as reducing equivalents in oxidative phosphorylation by the electron transport chain in the mitochondrial membrane to generate 38 ATP per one molecule of glucose. Thus, oxidative phosphorylation represents the most efficient breakdown of glucose in terms of energy yield in ATP[86,87].

In addition to altered glucose metabolism, cancer cells also exhibit altered glutamine metabolism. Glutamine is transported into the cell by several families of transporters including solute carrier 1 (SLC1), SLC6-7 and SLC38. Glutamine can have several fates once in the cell: it can be deaminated by glutamine deaminase (GLS) to convert it into α-ketoglutarate, a substrate that can feed into the TCA cycle, or it can be converted into glutathione (GSH) by glutathione cysteine ligase (GCL) to function in redox homeostasis. Thus, increased glutamine uptake fuels the cancer cell by promoting the TCA cycle to provide energy and aid in biosynthesis of necessary macromolecules and by providing the antioxidant GSH that can scavenger

the increased amount of reactive oxygen species (ROS) resulting from increased

metabolism that can be toxic to the cell[88].

There are many pathways altered in cancer cells that contribute to regulation

of glucose metabolism. Activated RAS signaling, as that which occurs in KRAS

mutations, can regulate expression of GLUTs and hexokinase 2 (HK2) activity

through the PI3K/Akt pathway. Additionally, constitutively active RAS can activate

the mammalian target of rapamycin (mTOR) pathway, which can promote lipid and

protein biosynthesis as well as glycolysis through induction of HIF1α. HIF1α is a

key regulator of glucose metabolism under hypoxic conditions, which cancer cells

often encounter. It induces expression of GLUT1, GLUT3, HK1, HK2, lactate

dehydrogenase A (LDHA), pyruvate dehydrogenase kinase 1 (PDK1) and

monocarboxylate transporter 4 (MCT4). PDK1 is a key enzyme that can decrease

oxidative phosphorylation, and thus oxygen consumption, through its inhibitory

kinase activity on pyruvate dehydrogenase (PDH). Additionally, the p53 tumor

suppressor protein induces the expression of HK2 and *TP53*-induced glycolysis and

apoptosis regulator (TIGAR). TIGAR can function to decrease fructose-2,6-

bisphosphate (F26BP), thus inhibiting glycolytic flux and increasing flux through the

PPP. p53 can also induce expression of its own inhibitor, phosphatase and tensin

homolog (PTEN), in a negative feedback loop. PTEN, in turn, can also inhibit

PI3K/Akt signaling. Gain-of-function mutations in p53 is sufficient to induce

Warburg metabolism, in part, by its induction of the protein SCO2, a member of the

electron transport chain. Myc is another oncoprotein that can regulate metabolism.

Myc has been shown to induce pyruvate kinase M2 (PKM2) expression. PKM2 is an

isoenzyme that catalyzes the last rate-limiting step of glycolysis: the conversion of PEP to pyruvate. Compared to PKM1, PKM2 has a much lower activity and thus, results in a buildup of glycolytic intermediates in response to a much less efficient conversion of PEP to pyruvate. Thus, Myc increases glycolytic intermediates and the pool of NADPH through increased flux through the PPP via its induction of PKM2 expression[87]. Myc is also a key regulator of glutamine metabolism and has been shown to directly induce expression of SLC5A1, SLC7A1 and GLS1, which provides more α-ketoglutarate to fuel the TCA cycle. Increased uptake of glutamine also increases the amount of GSH, improving the redox status of highly proliferative cancer cells.[88]

Abnormal activation of oncogenic signaling, as exhibited by most cancer cells, results in an adaptation or "addiction" to the increased amounts of glucose or glutamine. Interestingly, cells with activated Myc activity die under glutamine starvation. Furthermore, targeted inhibition of GLS inhibits Myc-induced oncogenic transformation. [91,92]. In a similar manner, cells with constitutively active RAS and Akt signaling show glucose-addiction, and suffer cell death in response to glucose deprivation as a result of ER stress[93].

THE HEXOSAMINE BIOSYNTHESIS PATHWAY AND O-GLCNACYLATION IN CANCER

The hexosamine biosynthesis pathway (HBP) is a shunt off of glycolysis via the intermediate fructose-6-phosphate (F6P). F6P, with the addition of glutamine, is converted into glucosamine-6-phosphate (GlcN6P) via the rate-limiting enzyme

glutamine:fructose-6P aminotransferase (GFAT) to culminate in production of uridine diphosphate N-acetylglucosamine (UDP-GlcNAc). UDP-GlcNAc is an amino sugar that serves as a necessary co-factor for the enzyme O-GlcNAc transferase (OGT), allowing OGT to glycosylate, or more specifically O-GlcNAcylate proteins to form proteoglycans, glycolipids and glycosylphosphatidylinositol anchors[94]. This is an important modification relevant to cancer and functions in several processes, including modulation of metabolism, induction of pro-survival ER stress responses, secretion of factors that function in invasion and modulation of metastasis[95-97].

The HBP is comprised of four catalyzed steps, the first of which is rate-limiting. This step consists of conversion of F6P and glucosamine to form GlcN6P and glutamate by the enzyme GFAT. This reaction is reversible as GlcN6P can be converted back into F6P by glucosamine-6-phosphate deaminase. However, GlcN6P can also go into the next irreversible step of the HBP where glucosamine-6-phosphate N-acetyltransferase (GNPNAT1) uses acetyl-CoA to acetylate GlcN6P to form N-acetylglucosamine-6-phosphate (GlcNAc-6P). Next, GlcNAc-6P is isomerized by phosphoacetylglucosamine mutase (PGM3) to form N-acetylglucosamine-1-phosphate (GlcNAc-1P). In the last step, UDP N-acetylglucosamine pyrophosphorylase (UAP1) transfers a uriding group onto GlcNAc-1P to generate the final product, UDP-GlcNAc[94].

The cellular level of O-GlcNAc is tightly regulated by the metabolic state of the cell. The amount of glucose, glutamine, acetyl-CoA and UTP are all factors that influence flux through the HBP. Thus, UDP-GlcNAc serves as a key sensor of the metabolic state of the cell. At normal state, 3-5% of glucose that enters the cell is

shunted into the HBP off of glycolysis. However, additional GlcNAc can be obtained

through degradation of previously O-GlcNAcylated products following its

conversion to GlcNAc-6P by N-acetylglucosamine kinase (NAGK) [94,98,99].

Additionally, this pathway is subject to regulation by its own metabolites and

products, including GlcNAc-6P and UDP-GlcNAc. GlcNAc-6P and UDP-GlcNAc, which

can both inhibit the rate limiting enzyme of the first step of the HBP, GFAT1.

However, the other isoform of this enzyme, GFAT2, remains unaffected by feedback

inhibition of its product, UDP-GlcNAc[100-105].

GFAT1 and GFAT2 both can catalyze the first rate-limiting reaction of the

HBP. These two proteins are comprised of 681 amino acids and 682 amino acids,

respectively, and share 78% sequence identity based on BLAST analysis[106].

Importantly, GFAT1 and GFAT2 are expressed in different tissue-specific manners

and are subject to regulation by UDP-GlcNAc in opposite ways. GFAT1 is

ubiquitously expressed throughout at a basal level while a longer form, GFAT-L1, is

expressed specifically in cardiac and skeletal muscle. GFAT1 is subject to regulation

and feedback inhibition by the HBP metabolites GlcNAc-6P and UDP-GlcNAc. In

addition to regulation by HBP intermediates and products, GFAT1 can also be

phosphorylated and inhibited by cAMP-dependent protein kinase A (PKA), an

important effector kinase coupled to G-protein-coupled receptors (GPCRs) that is

responsive to stimuli such as glucagon and adrenaline[105,107]. In a similar fashion,

AMPK has also been shown to phosphorylate GFAT1 to inhibit its enzymatic

activity[108]. GFAT2 expression is limited to the brain and CNS under normal

physiological conditions[109]. In contrast, GFAT2 is not nearly as inhibited by GlcNAc-

6P and UDP-GlcNAc, as the GFAT1 isoform. Additionally, GFAT2 is phosphorylated

and activated by PKA, rather than inhibited[110].

Although there is not a lot known regarding transcriptional regulation of

GFAT1 and GFAT2, there are several proteins important in cancer that can modulate

their expression. For example, EGF overexpression in breast cancer has been shown

to induce GFAT1 transcription and expression[111]. Additionally, KRAS and c-Myc

have also been shown to down-regulate GFAT1 in pancreatic cancer[112]. Hypoxia,

which is often experienced by cancer cells within a tumor, has also been shown to

induce GFAT1 and GFAT2 expression, perhaps via a hypoxia-responsive element

(HRE) contained within the GFAT1 promoter[113]. Lastly, the unfolded protein

response (UPR), another common phenomenon see in cancer cells, was shown to

regulate expression of GFAT1. This occurs via binding of X-box binding protein 1

(Xbp-1) to an X-box motif in the GFAT1 promoter to activate transcription[114,115].

Loss or overexpression of GFAT1 or GFAT2 has been associated with key

phenotypes applicable to cancer. GFAT2 has been shown to promote survival of

neurons in response to oxidative stress, and is also elevated in glioblastoma

tumors[116,117]. Furthermore, overexpression of GFAT1 adipocytes of mice has been

shown to cause insulin resistance and metabolic syndrome[118]. Additionally, varied

short nucleotide polymorphisms (SNPs) have been associated with development of

type II diabetes in humans[119-121]. Recently in breast cancer, high expression of

GFAT1 and GFAT2 was found to be correlated with a poor prognosis[122].

Additionally, increased GFAT2 expression was associated with mesenchymal cells, a

phenotype associated with increased metastasis[123]. Lastly, in lung ADC, ectopic

expression of GFAT2 was linked with increased O-linked glycosylation of fibronectin, a key marker of the mesenchymal state and metastatic cells[124-126].

The end-product of the HBP, UDP-GlcNAc, serves as a necessary co-factor for the enzyme OGT. OGT is responsible for the addition of O-GlcNAcylate to hydroxyl groups on serine and threonine residues of numerous proteins (>4000 identified targets) [95,127,128]. In turn, this post-translational modification (PTM) can be removed by O-GlcNAcase (OGA), the enzyme encoded by the *MGEA5* gene[128]. At the present, OGT and OGA are the only two known enzymes that can add or remove the O-GlcNAc group, respectively. The *OGT* gene is linked to the X-chromosome while the *MGEA5* gene resides on chromosome 10. Complete loss of either OGT or *MGEA5* results in embryonic lethality[129,130]. In humans, there are three OGT splice isoforms: nucleocytoplasmic OGT (ncOGT), short OGT (sOGT) and a mitochondrial-specific OGT (mOGT). All of these isoforms share a common conserved C-terminal glycosyltransferase domain, yet differ in the number of N-terminal tetraticopeptide repeats (TPRs). These TPR motifs determine cellular localization as well as substrate binding[95,131]. OGT also contains a C-terminal PIP3-binding domain that functions in localization to the inner plasma membrane with activated PI3K signaling[132]. Additionally, OGT has been shown to have protease activity and cleave a protein involved in transcriptional regulation of the cell cycle, host-cell factor-1 (HCF-1)[133]. OGA has two splice isoforms: long OGA (OGA-L) that is localized to the cytoplasm and short OGA (OGA-S) that is localized to the nucleus and lipid droplets. These isoforms share a common N-terminal β-N-acetylglucosaminadase enzymatic domain yet differ in the presence of a C-terminal histone acetyltransferase (HAT)

domain contained in the longer isoform[95]. They also differ in their enzymatic

activity: OGA-S shows less enzymatic activity than its longer counterpart *in vitro*.

The amount of O-GlcNAcylation occurring at any given point is primarily

regulated by flux through the HBP and is readily dynamic with changes in glucose

and glutamine levels. This is perhaps because UDP-GlcNAc is essential for OGT

activity, and can modulate both OGT's enzymatic activity and its affinity and

specificity for its substrate. OGT is also regulated by different PTMs.

Phosphorylation of OGT by the activated insulin growth factor (IGF) receptor (IGFR)

potentiates OGT's enzymatic activity[132]. OGT can also be phosphorylated by AMPK,

which causes OGT to localize to the nucleus[96]. Lastly, OGT can modify itself via auto-

O-GlcNAcylation[134].

Protein O-GlcNAcylation often serves as a nutrient sensor of metabolic state

of the cell and generally promotes a pro-survival stress response[95,135]. Under

hyperglycemic conditions, O-GlcNAcylation has been shown to modulate many

pathways involved in cancer and metabolism. Several components of the IGF

pathway, including insulin receptor substrate 1 (IRS1), PIP3-dependent kinase and

Akt, are O-GlcNAcylated by OGT and subsequently re-localized to the plasma

membrane under activation of IGFR signaling. O-GlcNAcylation of these proteins

attenuates the insulin-response; hence, overexpression of OGT can induce insulin

resistance as well as hyperlipidemia[132]. Another target of O-GlcNAcylation by OGT

is transforming growth factor β (TGFβ)-activated binding protein 1 (TAB1), which

transduces signaling via binding of ligands including TGFβ, tumor necrosis factor

(TNF), interleukin-1 (IL-1) and lipopolysaccharide (LPS). TAB1 has been shown to

be O-GlcNAcylated by OGT, and this modification is essential for full activation of its

binding partner TGFβ-activated kinase 1 (TAK1). This step is essential for

downstream signaling to activate nuclear factor kappa B (NF-κB) and mitogen-

activated protein kinase (MAPK)[136]. In a similar fashion, AMPK also requires O-

GlcNAcylation to activate its full enzymatic activity[96]. The O-GlcNAc modification of

proteins can also regulate glycolysis. HK, GPI, PFK1, aldolase A (ALDOA),

triosephosphate isomerase (TPI), glyceraldehyde-3-phosphate dehydrogenase

(GAPDH), PGK2, Enolase-1 (ENO1), PKM2 and LDHA are all enzymes involved in

glycolysis that can also be O-GlcNAcylated to result in a buildup of glycolytic

intermediates, as seen in Warburg metabolism of cancer cells[137,138]. Lastly, O-

GlcNAcylation has recently been shown to act as an epigenetic modification of

chromatin[139]. OGT has been shown to associate with chromatin via its binding to

ten eleven translocation (TET) 2 and 3, where it functions to promote transcription

of H3K4me3 target genes, many of which are involved in regulating pluripotency

and the stem cell state[140-142]. TET proteins promote DNA demethylation by

converting 5-methylcytosine (5mC) to 5-hydroxymethylcytosine (5hmC),

particularly in embryonic stem cells[143].

To promote cell survival, O-GlcNAcylation is often induced in response to

several different stress pathways that are active in cancer cells, including the heat

shock response, heavy metals, DNA damage, endoplasmic reticulum (ER) stress,

hypoxia and starvation[135,144-147]. With regard to the heat shock response, heat shock

factor 1 (HSF1) expression is increased in response to increased O-GlcNAcylation.

HSF1 is a key transcription factor in the heat shock response and induces

transcription of targets including heat shock protein (HSP) 70 and HSP90, both of which act a chaperones for misfolded proteins[135]. Additionally, O-GlcNAcylation of the 26S proteasome inhibits its activity, causing an inhibition of protein degradation[148]. Furthermore, the unfolded protein response (UPR) has been shown to induce O-GlcNAcylation through induction of GFAT1 expression and increased flux through the HBP mediated by X-box binding protein 1 (Xbp1) to promote cell survival[114,115]. In addition to promoting cell survival, O-GlcNAcylation can signal to inhibit apoptosis. This has been shown through O-GlcNAcylation of NF-κB and components of the NF-κB pathway, which leads to its full activation and thus, increased transcription of gene targets, including anti-apoptotic genes[149-152]. Furthermore, loss of p53 has been shown to enhance inhibitor of κB kinase β (IKKβ) activity through O-GlcNAcylation of this protein, causing increased transcription of NF-κB target genes[151].

Hyper-OGlcNAcylation has been associated with cellular transformation and is observed in the majority of cancer types, including but not limited to breast, colon, pancreatic, liver and leukemia, notably chronic lymphocytic leukemia (CLL). Under these circumstances, elevated O-GlcNAcylation causes changes in metabolic flux, as well as de-regulation of OGT and OGA expression[153-157]. Notably, OGT is overexpressed in several cancers *in vitro* and *in vivo*, including prostate, colorectal, breast, pancreatic and lung cancers. In contrast, OGA is down-regulated in brain and ovarian cancers, as well as lymphomas and leukemias[137,153-157]. Elevated and aberrant O-GlcNAcylation has been associated with many processes key to cancer initiation and progression, including cellular proliferation, resistance

to apoptosis, metabolic re-programming, and epithelial-to-mesenchymal transition (EMT), leading to invasion and metastasis[137]. For example, O-GlcNAcylation of the protein forkhead box M1 (FOXM1) has been shown to increase protein stability, allowing signaling to increase cell proliferation and invasion through downstream targets p27[Kip1] and matrix metallopeptidase 2 (MMP2) in breast cancer[157]. The snail family zinc finger 1 (Snail1) transcription factor undergoes O-GlcNAcylation to maintain stability, resulting in a decrease in E-cadherin and thus, induction of EMT in lung and breast cancer cells[158]. To further contribute to invasion and metastasis, the actin-binding protein cofilin is O-GlcNAcylated to alter cytosekeletal dynamics and promote cell migration in breast cancer[159]. Perhaps most notably, the proto-oncogene c-Myc is O-GlcNAcylated and subsequently stabilized, allowing it to increase flux through the HBP. This has been shown to promote pancreatic cancer cell proliferation[160]. In contrast, O-GlcNAcylation of c-Myc has also been show to promote its degradation in prostate cancer cells[161]. In a similar fashion, p53 has also been shown to be O-GlcNAcylated at serine 149. This modification stabilized p53 by inhibiting its subsequent ubiquitin-dependent degradation[162]. In addition to altering the cell cycle, hyper-O-GlcNAcylation of NF-κB has been shown to inhibit apoptosis in cancer cells. Furthermore, silencing OGT and thus, inhibition of O-GlcNAcylation in breast, prostate and colorectal cancer cells has been shown to inhibit cancer initiation, proliferation and invasion *in vivo*[153-157]. In addition to affecting cancer cell proliferation, invasion and apoptosis pathways, O-GlcNAcylation also regulates metabolic pathways. For example, O-GlcNAcylation of HK in cancer cells potentiates its enzymatic activity while O-GlcNAcylation of PFK1

and PKM2 inhibits their activity. Thus together, these modifications further drive

and potentiate the Warburg metabolic state via causing a buildup of glycolytic

intermediates that can be used in pathways including the PPP and HBP[137].

NF-κB IN CANCER

The NF-κB family of transcription factors have diverse functions in regulating

numerous cancer-associated cellular processes, including but not limited to pro-

inflammatory signaling, lymphocyte activation, differentiation, proliferation and

apoptosis. Dysregulation of this pathway is commonly seen across all types of

cancer[120,163-167].

Downstream signaling of all stimuli for the canonical NF-κB pathway results

in activation of the inhibitor of κB (IκB) kinase (IKK) complex, a critical component

of this pathway. The IKK protein complex has two catalytic subunits, IKKα/IKK1

(CHUK) and IKKβ/IKK2 (IKKβ), and a regulatory subunit (NEMO/IKKγ) (IKBKG),

which is essential for modulating NF-κB signaling. Once IKK is activated by

upstream stimuli, IKK can phosphorylate inhibitor of κB (IκB), a complex that binds

and sequesters NF-κB in the cytoplasm by blocking its nuclear localization sequence

(NLS) under baseline conditions[168]. IκB is comprised of the following subunits: IκBα

(NFKBIA), IκBβ (NFKBIB) and IκBε (IKBIE)[168]. IKK-mediated phosphorylation of

IκB induces poly-ubiquitination of IκB by SCF-type E3 ligase (E3RS[IκB/β-TrCP]), which

subsequently targets IκB for degradation by the 26S proteasome. This releases the

sequestered NF-κB complex, allowing it to translocate into the nucleus and induce

expression of transcriptional targets[167-169].

The canonical NF-κB pathway can be induced by a multitude of extracellular stimuli, as well as some intracellular stimuli, all of which converge on activation of IKK. These include B-cell and T-cell receptors (BCRs and TCRs), toll-like receptors (TLRs), pro-inflammatory cytokines, growth factor binding, DNA damage and the UPR. Tumor necrosis factor (TNF) is one such pro-inflammatory cytokine that binds TNF receptor 1 (TNFR1) [163,170]. Upon binding, TNF receptor associated factor 2/5 (TRAF2/5), receptor interacting protein (RIP) and TGFβ-activated kinase 1 (TAK1) are recruited to TNFR1, along with IKK. This convergence allows for activation of IKK and subsequent NF-κB-mediated transcription[163]. In a similar fashion, activation of signaling through toll-like receptors (TLRs) and interleukin-1 receptors (IL-1R) activate IKK through myeloid differentiation primary response 88 (MyD88), TNF receptor associated factor 6 (TRAF6) and TAK1[171]. Growth factor signaling, such as transforming growth factor β (TGFβ), activates IKK through TAK1 and TGFβ-activated kinase binding protein 1 (TAB1)[172]. In contrast, BCRs and TCRs, signal through B-cell CLL/Lymphoma 10 (BCL10) and caspase recruitment domain family member 11 (CARD11) to activate IKK[173]. Intracellularly, DNA damage activates IKK through the nuclear RIP1/NEMO/PIDD complex following phosphorylation of NF-κB-essential modulator (NEMO) by ataxia telangiectasia mutated (ATM). In contrast, IKK is activated by UPR via endoplasmic reticulum (ER) membrane receptor inositol-requiring protein 1α (IRE1α) and TRAF2[174,175].

The family of NF-κB transcription factors is comprised of five proteins that can form homodimers and heterodimers: p65/RelA (RELA), c-Rel (REL), RelB (RELB), p105/p50 (NFKB1) and p100/p52 (NFKB2). These proteins all share a

common N-terminal Rel homology domain (RHD) that mediates dimerization as well as facilitates DNA binding of the NF-κB complex to κB motifs within the enhancers and promoters of transcriptional target genes. p65/RelA, c-Rel and RelB contain an additional C-terminal transcription activation domain (TAD), which functions to recruit co-activators, such as CREB-binding protein (CBP)/p300, to activate transcription of gene targets. Thus, NF-κB heterodimers must contain one of these 3 TAD-containing subunits (p65, c-Rel, or RelB) to drive transcription. In contrast, NF-κB dimers, such as p105/p50 or p100/p52, that do not contain a TAD, repress transcription in the absence of a stimulus[176]. This occurs as these complexes bind κB sites on DNA and tether core repression complexes that are comprised of histone deacetylase 3 (HDAC3) and one of two co-repressors, silencing mediator of retinoic acid and thyroid (SMRT) or nuclear receptor co-repressor (N-CoR). In response to cellular stimulation, these NF-κB repressive complexes are displaced by transcriptionally active NF-κB dimers that recruit HAT-containing co-activator complexes[163].

NF-κB can undergo several post-translational modifications that regulate its transcriptional activity. IKKα and IKKβ can phosphorylate serine 536 of p65[177,178]. Additionally, PKA-mediated phosphorylation of serine 276 of p65 is required for its full transcriptional activation and promotes interaction with other co-activators, notably CBP/p300[179]. This same serine residue can also be phosphorylated by mitogen- and stress-activated protein kinase 1 and 2 (MSK1 and MSK2), which are nuclear-localized effector kinases of the p38/MAPK and ERK signaling pathways. Phosphorylation of serine 276 is necessary for acetylation of lysine 310 on p65 by

CBP/p300, which is a required modification for full transcriptional activation. Furthermore, phosphorylation of p65 at serine 536 further increases acetylation at lysine 310, perhaps by altering binding to co-repressors and the HDAC3/SMRT complex[180].

NF-κB has a wide range of roles in processes that contribute to cancer initiation and progression. In terms of the tumor microenvironment, NF-κB has a key role in promoting inflammation, and in both the innate and adaptive immune responses. Inflammation is a well-known contributor to cancer initiation and progression in a wide range of tumors[181]. In fact, non-steroidal anti-inflammatory drugs (NSAIDs) have been shown to decrease the risk of developing many types of cancer[182-184]. NF-κB is also often activated in cancers and can regulate transcription of many genes with roles in promoting tumorigenicity. These are including, but not limited to: anti-apoptotic genes (Myeloid cell leukemia 1 (Mcl-1), Bcl-xl, Bcl-2 and XIAP), cyclins (cyclin D1, D2 and D3), growth factors (activin A, BMP2, BMP4, WNT10B and PDGF), proto-oncogenes (c-Myc, c-Fos, JunD and c-Rel), inflammatory cytokines (TNF, IL-1, IL-2, IL-6, IL-8, IL-10 and IFNγ) and their receptors (EGFR, *ERBB2*), reactive oxygen scavenger proteins (superoxide dismutase (SOD)1 and SOD2), heat shock proteins (HSP90), molecules involved in cell adhesion (CD44, P-selectin and fibronectin), metabolic enzymes (Eno, GPI, MMP3, MMP9, SCO2 and GLUT3), transcription factors (E74-like ETS transcription factor 3 (Elf3), HIF1α, p53 and Snail) and the histone demethylase jumonji domain-containing 3 (JMJD3)[185].

Constitutive NF-κB activity is a feature of a multitude of cancer types, including lung cancer, and such activity is shown to promote tumorigenesis[167,186-189].

This is supported by the fact that oncogenic transformation of cells often activates this pathway, allowing cells to proliferate and evade apoptosis[165]. In contrast, abrogating NF-κB expression in murine airway epithelial cells has been shown to decrease lung inflammation, inhibit tumor formation and induce apoptosis in response to urethane, possibly due to induction of Bcl-2 expression[188]. Additionally, in a mouse model of lung ADC driven by KRAS mutation and loss of p53, NF-κB was found to be activated[186]. Furthermore, inhibition of NF-κB was found to decrease lung tumor formation in a mouse model driven by KRAS mutation, regardless of p53 status[189]. Consistent with this, another study found that IKK depletion resulted in decreased cell proliferation and increased survival of mice with KRAS-driven lung ADC[187]. These studies were consistent with human data showing that high NF-κB expression in NSCLC patients correlated with higher tumor grade and subsequently, a poorer prognosis[190].

In addition to having an important role in regulating tumorigenesis and resistance to apoptosis, NF-κB has also been shown to modulate cellular metabolism and is also regulated itself by changes in the metabolic state of the cell. NF-κB activity was shown to augment mitochondrial oxidative phosphorylation through induction of synthesis of cytochrome c oxidase (SCO2), an enzyme of the electron transport chain[191]. In addition, inhibition of RelA potentiates Warburg metabolism by increasing aerobic glycolysis, potentiating glucose addiction, and increasing the susceptibility of cells to mitochondrial stress and necrosis as a result of glucose deprivation. These metabolic phenotypes require downstream p53 activity, a transcriptional target of NF-κB[159]. In turn, absence of p53 increases IKK1 and IKK2

activity, thus potentiating NF-κB activity. This potentiation in IKK activity was shown to co-exist with increased aerobic glycolysis in response to p53 loss. Furthermore, it required induction of GLUT3, which could possibly be p65-mediated[192]. O-GlcNAcylation of IKK2 at serine 733, a modification needed to potentiate enzymatic activity, provides yet another metabolic-mediated step to the NF-κB pathway. In the absence of p53 and/or in the presence of high glucose uptake, there are elevated levels of O-GlcNAcylated IKK2, perhaps due to increased flux through the HBP in response to Warburg metabolism[151]. O-GlcNAcylation can also modify NF-κB directly, as several potential O-GlcNAcylation sites have been identified on this protein. It was discovered that O-GlcNAcylation of p65 at serine 352 inhibited IκB binding to p65, resulting in increased NF-κB –mediated transcription of target genes[152]. Furthermore, the Mayo laboratory has shown that O-GlcNAcylation of p65 at threonine 305 is a requirement for acetylation of p65 at lysine 310, a necessary modification to allow for full transcriptional activity of p65[149]. It has also been shown that pancreatic cancer cells experience a hyper-O-GlcNAcylation state under sustained NF-κB activity, and this state was required to allow for anchorage-independent growth[152]. In addition to p65, O-GlcNAcylaion of serine 350 on c-Rel has been shown to augment its transcriptional activity in response to TCR signaling activation[193]. All of this evidence implies that the two processes of O-GlcNAcylation and NF-κB activity are co-regulated, possibly by one another. Indeed, the Mayo laboratory recently showed that NF-κB signaling activated transcription of GFAT2, the rate-limiting enzyme of the HBP, under TNFα/TGFβ treatment of NSCLC and MEK inhibition of KRAS-mutant NSCLC.

Induction of GFAT2 under these conditions was shown to increase O-GlcNAcylation levels and was required to promote invasion and migration of NSCLC cells.

REFERENCES

1. THE DOMINANT MALIGNANCY. 1–2 (2014).
2. *cancer.org*. Available at: http://www.cancer.org. (Accessed: 22nd December 2016)
3. Lung Cancer. 1–14 (2008).
4. Sebastián, C. *et al.* The histone deacetylase SIRT6 is a tumor suppressor that controls cancer metabolism. *Cell* **151,** 1185–1199 (2012).
5. Zhong, L. *et al.* The Histone Deacetylase Sirt6 Regulates Glucose Homeostasis via Hif1α. *Cell* **140,** 280–293 (2010).
6. Tennen, R. I., Bua, D. J., Wright, W. E. & Chua, K. F. SIRT6 is required for maintenance of telomere position effect in human cells. *Nat Comms* **2,** 433 (2011).
7. Michishita, E. *et al.* SIRT6 is a histone H3 lysine 9 deacetylase that modulates telomeric chromatin. *Nature* **452,** 492–496 (2008).
8. Min, L. *et al.* Liver cancer initiation is controlled by AP-1 through SIRT6-dependent inhibition of survivin. *Nature Cell Biology* **14,** 1203–1211 (2012).
9. Kawahara, T. L. A. *et al.* SIRT6 Links Histone H3 Lysine 9 Deacetylation to NF-κB-Dependent Gene Expression and Organismal Life Span. *Cell* **136,** 62–74 (2009).
10. Overview of the treatment of advanced non-small cell lung cancer - UpToDate. *www-uptodate-com.proxy.its.virginia.edu* Available at: https://www-uptodate-com.proxy.its.virginia.edu/contents/overview-of-the-treatment-of-advanced-non-small-cell-lung-cancer?source=search_result&search=NSCLC&selectedTitle=1~150. (Accessed: 28 December 2016)
11. DeVita, V. T., Lawrence, T. S. & Rosenberg, S. A. *DeVita, Hellman, and Rosenberg's Cancer*. (Lippincott Williams & Wilkins, 2008).
12. Hammerman, P. S. *et al.* Comprehensive genomic characterization of squamous cell lung cancers. *Nature* **489,** 519–525 (2012).
13. The Morphological and Molecular Diagnosis of Lung Cancer. 1–8 (2011). doi:10.3238/arztebl.2011.0525
14. Tobacco Smoke Carcinogens and Lung Cancer. 1–17 (1999).
15. Field, R. W. & Withers, B. L. Occupational and Environmental Causes of Lung Cancer. *Clinics in Chest Medicine* **33,** 681–703 (2012).
16. Aisner, D. L. & Marshall, C. B. Molecular Pathology of Non–Small Cell Lung Cancer. *Am J Clin Pathol* **138,** 332–346 (2012).
17. Network, T. C. G. A. R. Comprehensive molecular profiling of lung adenocarcinoma. *Nature* 1–9 (2014). doi:10.1038/nature13385
18. Riely, G. J. *et al.* Frequency and Distinctive Spectrum of KRAS Mutations in Never Smokers with Lung Adenocarcinoma. *Clinical Cancer Research* **14,** 5731–5734 (2008).
19. Ji, M. PD-1/PD-L1 pathway in non-small-cell lung cancer and its relation with EGFR mutation. 1–6 (2015). doi:10.1186/s12967-014-0373-0

20. Non–Small Cell Lung Cancer, PD-L1, and the Pathologist. 1–6 (2016).
21. Goldstraw, P. *et al.* The IASLC Lung Cancer Staging Project: Proposals for the Revision of the TNM Stage Groupings in the Forthcoming (Seventh) Edition of the TNM Classification of Malignant Tumours. *Journal of Thoracic Oncology* **2,** 706–714 (2007).
22. WHO | World Health Organization. *WHO*
23. Kelsey, C. R. *et al.* Local recurrence after surgery for early stage lung cancer. *Cancer* **115,** 5218–5227 (2009).
24. Adjuvant systemic therapy in resectable non-small cell lung cancer - UpToDate. *www-uptodate-com.proxy.its.virginia.edu* Available at: https://www-uptodate-com.proxy.its.virginia.edu/contents/adjuvant-systemic-therapy-in-resectable-non-small-cell-lung-cancer?source=see_link. (Accessed: 28 December 2016)
25. Management of stage III non-small cell lung cancer - UpToDate. *www-uptodate-com.proxy.its.virginia.edu* Available at: https://www-uptodate-com.proxy.its.virginia.edu/contents/management-of-stage-iii-non-small-cell-lung-cancer?source=see_link. (Accessed: 28 December 2016)
26. MD, P. C. Z. *et al.* Articles Erlotinib versus chemotherapy as first-line treatment for patients with advanced. *Lancet Oncology* **12,** 735–742 (2011).
27. Solomon, B. J. *et al.* First-Line Crizotinib versus Chemotherapy in ALK-Positive Lung Cancer. *N Engl J Med* **371,** 2167–2177 (2014).
28. Reck, M. *et al.* Pembrolizumab versus Chemotherapy for PD-L1–Positive Non–Small-Cell Lung Cancer. *N Engl J Med* **375,** 1823–1833 (2016).
29. Kuilman, T., Michaloglou, C., Mooi, W. J. & Peeper, D. S. The essence of senescence. *Genes & Development* **24,** 2463–2479 (2010).
30. Nabetani, A. & Ishikawa, F. Alternative lengthening of telomeres pathway: Recombination-mediated telomere maintenance mechanism in human cells. *Journal of Biochemistry* **149,** 5–14 (2010).
31. AM, O. [Principle of marginotomy in template synthesis of polynucleotides]. *Dokl Akad Nauk SSSR* **201,** 1496–1499 (1971).
32. newbio239197a0. 1–5 (2008).
33. A DNA damage checkpoint response in telomere-initiated senescence. 1–5 (2003).
34. Campisi, J. Senescent Cells, Tumor Suppression, and Organismal Aging: Good Citizens, Bad Neighbors. *Cell* **120,** 513–522 (2005).
35. Shay, J. W. Senescence and immortalization: role of telomeres and telomerase. *Carcinogenesis* **26,** 867–874 (2004).
36. Extension of Life-Span by Introduction of Telomerase into Normal Human Cells. 1–5 (1998).
37. Reconstitution of telomerase activity in normal human cells leads to elongation of telomeres and extended replicative life span. 1–4 (1998).
38. Cellular Senescence: MinireviewMitotic Clock or Culture Shock? 1–4 (2000).
39. Tissue-specific tumor suppressor activity of retinoblastoma gene homologs p107 and p130. 1–11 (2004).
40. Targeted disruption of the three Rb-related genes leads to loss of G. 1–14 (2000).

41. Expression of Catalytically Active Telomerase Does Not Prevent Premature Senescence Caused by Overexpression of Oncogenic Ha-Ras in Normal Human Fibroblasts. 1–5 (1999).

42. Provokes Premature Cell Senescence Associated with Accumulation of p53 and p16. 1–10 (1997).

43. Tumor Suppression at the Mouse. 1–11 (1997).

44. Chen, Z. *et al.* Crucial role of p53-dependent cellular senescence in suppression of Pten-deficient tumorigenesis. *Nature Cell Biology* **436,** 725–730 (2005).

45. Provokes Premature Cell Senescence Associated with Accumulation of p53 and p16. 1–10 (1997).

46. Morton, J. P. *et al.* Mutant p53 drives metastasis and overcomes growth arrest/senescence in pancreatic cancer. *Proc. Natl. Acad. Sci. U.S.A.* **107,** 246–251 (2010).

47. Reversal of human cellular senescence: roles of thep53 and p16 pathways. 1–11 (1912).

48. Dirac, A. M. G. & Bernards, R. Reversal of Senescence in Mouse Fibroblasts through Lentiviral Suppression of p53. *J. Biol. Chem.* **278,** 11731–11734 (2003).

49. Coppé, J.-P. *et al.* Senescence-Associated Secretory Phenotypes Reveal Cell-Nonautonomous Functions of Oncogenic RAS and the p53 Tumor Suppressor. *PLoS Biol* **6,** e301 (2008).

50. Bracken, A. P. *et al.* The Polycomb group proteins bind throughout the INK4A-ARF locus and are disassociated in senescent cells. *Genes & Development* **21,** 525–530 (2007).

51. Kuilman, T. *et al.* Oncogene-Induced Senescence Relayed by an Interleukin-Dependent Inflammatory Network. *Cell* **133,** 1019–1031 (2008).

52. Bartkova, J. *et al.* Oncogene-induced senescence is part of the tumorigenesis barrier imposed by DNA damage checkpoints. *Nature* **444,** 633–637 (2006).

53. Di Micco, R. *et al.* Oncogene-induced senescence is a DNA damage response triggered by DNA hyper-replication. *Nature* **444,** 638–642 (2006).

54. DNA Damage Signaling and p53-dependent Senescence after Prolonged. 1–10 (2006). doi:10.1091/mbc.E05

55. Ras Proteins Induce Senescence by Altering the Intracellular Levels of Reactive Oxygen Species*. 1–6 (1999).

56. Senescence-likegrowth. 1–5 (2004).

57. Passos, J. A. O. F. *et al.* Feedback between p21 and reactive oxygen production is necessary for cell senescence. *Molecular Systems Biology* **6,** 1–14 (2010).

58. Inhibition of p21-mediated ROS accumulation canrescue p21-induced senescence. 1–9 (1911).

59. Rodier, F. *et al.* Persistent DNA damage signalling triggers senescence-associated inflammatory cytokine secretion. *Nature Cell Biology* **11,** 973–979 (2009).

60. Senescent fibroblasts promote epithelial cell growth and tumorigenesis: A link between cancer and aging. 1–6 (2001).

61. Johmura, Y., Yamashita, E., Shimada, M., Nakanishi, K. & Nakanishi, M. Defective DNA repair increases susceptibility to senescence through extension of Chk1-mediated G2 checkpoint activation. *Sci Rep* **6,** 31194 (2016).

62. Coppé, J.-P., Desprez, P.-Y., Krtolica, A. & Campisi, J. The Senescence-Associated Secretory Phenotype: The Dark Side of Tumor Suppression. *Annu. Rev. Pathol. Mech. Dis.* **5,** 99–118 (2010).

63. Liu, D. & Hornsby, P. J. Senescent Human Fibroblasts Increase the Early Growth of Xenograft Tumors via Matrix Metalloproteinase Secretion. *Cancer Res.* **67,** 3117–3126 (2007).

64. Targeting the insulin-like growth factor receptor pathway in lung cancer: problems and pitfalls. 1–10 (2012).

65. Zhou, Y., Capuco, A. V. & Jiang, H. Involvement of connective tissue growth factor (CTGF) in insulin-like growth factor-I (IGF1) stimulation of proliferation of a bovine mammary epithelial cell line. *Domestic Animal Endocrinology* **35,** 180–189 (2008).

66. Thirumurthi, U. *et al.* MDM2-mediated degradation of SIRT6 phosphorylated by AKT1 promotes tumorigenesis and trastuzumab resistance in breast cancer. *Science Signaling* **7,** ra71–ra71 (2014).

67. Xue, W. *et al.* Senescence and tumour clearance is triggered by p53 restoration in murine liver carcinomas. *Nature* **445,** 656–660 (2007).

68. Krizhanovsky, V. *et al.* Senescence of Activated Stellate Cells Limits Liver Fibrosis. *Cell* **134,** 657–667 (2008).

69. Molecular determinants of terminal growth arrest induced in tumor cells by a chemotherapeutic agent. 1–6 (2001).

70. Decoy receptors: a strategy toregulate inflammatory cytokines andchemokines. 1–9 (2001).

71. Chien, Y. *et al.* Control of the senescence-associated secretory phenotype by NF- B promotes senescence and enhances chemosensitivity. *Genes & Development* **25,** 2125–2136 (2011).

72. Batsi, C. *et al.* Chronic NF-κB activation delays RasV12-induced premature senescence of human fibroblasts by suppressing the DNA damage checkpoint response. *Mechanisms of Ageing and Development* **130,** 409–419 (2009).

73. Michishita, E., McCord, R. A., Boxer, L. D. & Barber, M. F. Cell cycle-dependent deacetylation of telomeric histone H3 lysine K56 by human SIRT6. *Cell* (2009).

74. Mao, Z. *et al.* SIRT6 Promotes DNA Repair Under Stress by Activating PARP1. *Science* **332,** 1443–1446 (2011).

75. J. Biol. Chem.-2005-Liszt-jbc.M413296200. 1–19 (2005).

76. Jiang, H. *et al.* SIRT6 regulates TNF-α secretion through hydrolysis of long-chain fatty acyl lysine. *Nature* **496,** 110–113 (2013).

77. Mostoslavsky, R. *et al.* Genomic Instability and Aging-like Phenotype in the Absence of Mammalian SIRT6. *Cell* **124,** 315–329 (2006).

78. Srivastava, D. K. *et al.* Mammalian abasic site base excision repair. Identification of the reaction sequence and rate-determining steps. *J. Biol.*

Chem. **273,** 21203–21209 (1998).

79. User, O. 2. T. D. SIRT6 stabilizes DNA-dependent protein kinase at chromatin for DNA double-strand break repair. 1–15 (2009).

80. Ahel, D. *et al.* Poly(ADP-ribose)-Dependent Regulation of DNA Repair by the Chromatin Remodeling Enzyme ALC1. *Science* **325,** 1240–1243 (2009).

81. El-Khamisy, S. F. A requirement for PARP-1 for the assembly or stability of XRCC1 nuclear foci at sites of oxidative DNA damage. *Nucleic Acids Res* **31,** 5526–5533 (2003).

82. Sartori, A. A. *et al.* Human CtIP promotes DNA end resection. *Nature* **450,** 509–514 (2007).

83. Kaidi, A., Weinert, B. T., Choudhary, C. & Jackson, S. P. Human SIRT6 promotes DNA end resection through CtIP deacetylation. *Science* **329,** 1348–1353 (2010).

84. Multani, A. S. & Chang, S. WRN at telomeres: implications for aging and cancer. *Journal of Cell Science* **120,** 713–721 (2007).

85. Sirtuin 6 (SIRT6) rescues the decline of homologous recombination repair during replicative senescence. 1–6 (2012). doi:10.1073/pnas.1200583109/-/DCSupplemental

86. Vander Heiden, M. G., Cantley, L. C. & Thompson, C. B. Understanding the Warburg Effect: The Metabolic Requirements of Cell Proliferation. *Science* **324,** 1029–1033 (2009).

87. Cairns, R. A., Harris, I. S. & Mak, T. W. Regulation of cancer cell metabolism. 1–11 (2011). doi:10.1038/nrc2981

88. Hensley, C. T., Wasti, A. T. & DeBerardinis, R. J. Glutamine and cancer: cell biology, physiology, and clinical opportunities. *J. Clin. Invest.* **123,** 3678–3684 (2013).

89. Lukey, M. J., Wilson, K. F. & Cerione, R. A. Therapeutic strategies impacting cancer cell glutamine metabolism. *Future Medicinal Chemistry* **5,** 1685–1700 (2013).

90. Kang, J. G. *et al.* O-GlcNAc Protein Modification in Cancer Cells Increases in Response to Glucose Deprivation through Glycogen Degradation. *Journal of Biological Chemistry* **284,** 34777–34784 (2009).

91. Wang, J.-B. *et al.* Targeting Mitochondrial Glutaminase Activity Inhibits Oncogenic Transformation. *Cancer Cell* **18,** 207–219 (2010).

92. Yuneva, M., Zamboni, N., Oefner, P., Sachidanandam, R. & Lazebnik, Y. Deficiency in glutamine but not glucose induces MYC-dependent apoptosis in human cells. *J Cell Biol* **178,** 93–105 (2007).

93. Palorini, R. *et al.* Glucose starvation induces cell deathin K-ras-transformed cells by interfering with the hexosamine biosynthesis pathway and activating the unfolded protein response. **4,** e732–14 (2013).

94. Abdel Rahman, A. M., Ryczko, M., Pawling, J. & Dennis, J. W. Probing the Hexosamine Biosynthetic Pathway in Human Tumor Cells by Multitargeted Tandem Mass Spectrometry. *ACS Chem. Biol.* **8,** 2053–2062 (2013).

95. Bond, M. R. & Hanover, J. A. A little sugar goes a long way: The cell biology of O-GlcNAc. *J Cell Biol* **208,** 869–880 (2015).

96. Bullen, J. W. *et al.* Cross-talk between Two Essential Nutrient-sensitive

Enzymes: O-GlcNAc TRANSFERASE (OGT) AND AMP-ACTIVATED PROTEIN KINASE (AMPK). *Journal of Biological Chemistry* **289,** 10592–10606 (2014).

97.   Slawson, C. & Hart, G. W. O-GlcNAc signalling: implications for cancer cell biology. *Nature Publishing Group* **11,** 678–684 (2011).

98.   Hanover, J. A., Krause, M. W. & Love, D. C. The hexosamine signaling pathway: O-GlcNAc cycling in feast or famine. *Biochimica et Biophysica Acta (BBA) - General Subjects* **1800,** 80–95 (2010).

99.   Metallo, C. M. & Vander Heiden, M. G. Metabolism strikes back: metabolic flux regulates cell signaling. *Genes & Development* **24,** 2717–2722 (2010).

100.   1-s2.0-0005274471901197-main. 1–12 (2002).

101.   Allosteric Control of Glucosamine Phosphate Isomerase from the Adult Housefly and Its Role in the Synthesisof Glucosamine 6-Phosphate. 1–11 (2003).

102.   Feedback Inhibition of L-Glutamine D-Fructose 6-Phosphate Amidotransferase by Uridine DiphosphateN-Acetylglucosamine. 1–7 (2002).

103.   Broschat, K. O. Kinetic Characterization of Human Glutamine-fructose-6-phosphate Amidotransferase I. POTENT FEEDBACK INHIBITION BY GLUCOSAMINE 6-PHOSPHATE. *Journal of Biological Chemistry* **277,** 14764–14770 (2002).

104.   Marshall, S., Nadeau, O. & Yamasaki, K. Dynamic Actions of Glucose and Glucosamine on Hexosamine Biosynthesis in Isolated Adipocytes: DIFFERENTIAL EFFECTS ON GLUCOSAMINE 6-PHOSPHATE, UDP-N-ACETYLGLUCOSAMINE, AND ATP LEVELS. *Journal of Biological Chemistry* **279,** 35313–35319 (2004).

105.   Functional regulation of glutamine:fructose-6-phosphate aminotransferase 1 (GFAT1) of Drosophila melanogaster in a UDP-N-acetylglucosamine and cAMP-dependent manner. 1–12 (1910).

106.   Durand, P., Golinelli-Pimpaneau, B., Mouilleron, S., Badet, B. & Badet-Denisot, M.-A. Highlights of glucosamine-6P synthase catalysis. *Archives of Biochemistry and Biophysics* **474,** 302–317 (2008).

107.   Chang, Q. *et al.* Phosphorylation of Human Glutamine:Fructose-6-phosphate Amidotransferase by cAMP-dependent Protein Kinase at Serine 205 Blocks the Enzyme Activity. *Journal of Biological Chemistry* **275,** 21981–21987 (2000).

108.   Eguchi, S. *et al.* AMP-activated protein kinase phosphorylates glutamine : fructose-6-phosphate amidotransferase 1 at Ser243 to modulate its enzymatic activity. *Genes to Cells* **14,** 179–189 (2009).

109.   Cloning and partial characterization of the mouse glutamine:fructose-6-phosphate amidotransferase (GFAT) gene promoter. 1–9 (1997).

110.   Hu, Y., Riesland, L., Paterson, A. J. & Kudlow, J. E. Phosphorylation of Mouse Glutamine-Fructose-6-phosphate Amidotransferase 2 (GFAT2) by cAMP-dependent Protein Kinase Increases the Enzyme Activity. *Journal of Biological Chemistry* **279,** 29988–29993 (2004).

111.   Paterson, A. J. & Kudlow, J. E. Regulation of glutamine: fructose-6-phosphate amidotransferase gene transcription by epidermal growth factor and glucose. *Endocrinology* (1995).

112. Ying, H. *et al.* Oncogenic Kras Maintains Pancreatic Tumors through Regulation of Anabolic Glucose Metabolism. *Cell* **149,** 656–670 (2012).
113. Strengthened glycolysis under hypoxia supportstumor symbiosis and hexosamine biosynthesisin pancreatic adenocarcinoma. 1–6 (2013). doi:10.1073/pnas.1219555110/-/DCSupplemental
114. Denzel, M. S. *et al.* Hexosamine Pathway Metabolites Enhance Protein Quality Control and Prolong Life. *Cell* **156,** 1167–1178 (2014).
115. Wang, Z. V. *et al.* Spliced X-Box Binding Protein 1 Couples the Unfolded Protein Response to Hexosamine Biosynthetic Pathway. *Cell* **156,** 1179–1192 (2014).
116. Zitzler, J. High-throughput Functional Genomics Identifies Genes That Ameliorate Toxicity Due to Oxidative Stress in Neuronal HT-22 Cells: GFPT2 Protects Cells Against Peroxide. *Molecular & Cellular Proteomics* **3,** 834–840 (2004).
117. Verbovšek, U. *et al.* Expression Analysis of All Protease Genes Reveals Cathepsin K to Be Overexpressed in Glioblastoma. *PLoS ONE* **9,** e111819 (2014).
118. 980930. 1–7 (1996).
119. Zhang, H. *et al.* Common Variants in Glutamine:Fructose-6-Phosphate Amidotransferase 2 (GFPT2) Gene Are Associated with Type 2 Diabetes, Diabetic Nephropathy, and Increased GFPT2 mRNA Levels. *J. Clin. Endocrinol. Metab.* **89,** 748–755 (2004).
120. Elbein, S. C. *et al.* Molecular screening of the human glutamine–fructose-6-phosphate amidotransferase 1 (GFPT1) gene and association studies with diabetes and diabetic nephropathy. *Molecular Genetics and Metabolism* **82,** 321–328 (2004).
121. Srinivasan, V. *et al.* Glutamine fructose-6-phosphate amidotransferase (GFAT) gene expression and activity in patients with type 2 diabetes: Inter-relationships with hyperglycaemia and oxidative stress. *Clinical Biochemistry* **40,** 952–957 (2007).
122. Simpson, N. E., Tryndyak, V. P., Beland, F. A. & Pogribny, I. P. An in vitro investigation of metabolically sensitive biomarkers in breast cancer progression. *Breast Cancer Res Treat* **133,** 959–968 (2011).
123. Shaul, Y. D. *et al.* Dihydropyrimidine Accumulation Is Required for the Epithelial-Mesenchymal Transition. *Cell* **158,** 1094–1109 (2014).
124. Involvement of O-glycosylation defining oncofetal fibronectin in epithelial-mesenchymaltransition process. 1–12 (2011). doi:10.1073/pnas.1115191108/-/DCSupplemental
125. Ding, Y., Gelfenbeyn, K., Freire-de-Lima, L., Handa, K. & Hakomori, S.-I. Induction of epithelial-mesenchymal transition with O-glycosylated oncofetal fibronectin. *FEBS Letters* **586,** 1813–1820 (2012).
126. Alisson-Silva, F. *et al.* Increase of O-Glycosylated Oncofetal Fibronectin in High Glucose-Induced Epithelial-Mesenchymal Transition of Cultured Human Epithelial Cells. *PLoS ONE* **8,** e60471 (2013).
127. Glycosylation of NucleocytoplasmicProteins: Signal Transduction and O-GlcNAc. 1–4 (2001).

128. Bond, M. R. & Hanover, J. A. O-GlcNAc Cycling: A Link Between Metabolism and Chronic Disease. *Annu. Rev. Nutr.* **33,** 205–229 (2013).

129. The O-GlcNAc transferase gene resides on theX chromosome and is essential for embryonicstem cell viability and mouse ontogeny. 1–5 (2000).

130. Conditional Knock-out Reveals a Requirement for O-Linked N-Acetylglucosaminase (O-GlcNAcase) in MetabolicHomeostasis. 1–17 (2015).

131. Janetzko, J. & Walker, S. The Making of a Sweet Modification: Structure and Function of O-GlcNAc Transferase. *Journal of Biological Chemistry* **289,** 34424–34432 (2014).

132. Yang, X. *et al.* Phosphoinositide signalling links O-GlcNAc transferase to insulin resistance. *Nature* **451,** 964–969 (2008).

133. Lazarus, M. B. *et al.* HCF-1 Is Cleaved in the Active Site of O-GlcNAc Transferase. *Science* **342,** 1235–1239 (2013).

134. Butkinaree, C., Park, K. & Hart, G. W. O-linked β-N-acetylglucosamine (O-GlcNAc): Extensive crosstalk with phosphorylation to regulate signaling and transcription in response to nutrients and stress. *Biochimica et Biophysica Acta (BBA) - General Subjects* **1800,** 96–106 (2010).

135. Zachara, N. E. *et al.* Dynamic O-GlcNAc Modification of Nucleocytoplasmic Proteins in Response to Stress: A SURVIVAL RESPONSE OF MAMMALIAN CELLS. *Journal of Biological Chemistry* **279,** 30133–30142 (2004).

136. Pathak, S. *et al.* O-GlcNAcylation of TAB1 modulates TAK1-mediated cytokine release. *EMBO J* **31,** 1394–1404 (2012).

137. Li, Z. & Yi, W. Regulation of cancer metabolism by O-GlcNAcylation. *Glycoconj J* **31,** 185–191 (2013).

138. Jang, H. *et al.* O-GlcNAc Regulates Pluripotency and Reprogramming by Directly Acting on Core Componentsof the Pluripotency Network. *Stem Cell* **11,** 62–74 (2012).

139. β-N-acetylglucosamine (O-GlcNAc) is part of the histone code. 1–6 (2010). doi:10.1073/pnas.1009023107/-/DCSupplemental

140. Chen, Q., Chen, Y., Bian, C., Fujiki, R. & Yu, X. TET2 promotes histone O-GlcNAcylation during gene transcription. *Nature* **493,** 561–564 (2012).

141. Pietro Vella *et al.* Tet Proteins Connect the O-Linked N-acetylglucosamine Transferase Ogt to Chromatin in Embryonic Stem Cells. *Molecular Cell* **49,** 645–656 (2013).

142. Deplus, R. *et al.* TET2 and TET3 regulate GlcNAcylation and H3K4 methylation through OGT and SET1/COMPASS. *EMBO J* **32,** 645–655 (2013).

143. Cimmino, L., Abdel-Wahab, O., Levine, R. L. & Aifantis, I. TET Family Proteins and Their Rolein Stem Cell Differentiation and Transformation. *Stem Cell* **9,** 193–204 (2011).

144. Chatham, J. C., Nöt, L. G., Fülöp, N. & Marchase, R. B. HEXOSAMINE BIOSYNTHESIS AND PROTEIN O-GLYCOSYLATION. *Shock* 1 (2007). doi:10.1097/shk.0b013e3181598bad

145. Zachara, N. E., Molina, H., Wong, K. Y., Pandey, A. & Hart, G. W. The dynamic stress-induced 'O-GlcNAc-ome' highlights functions for O-GlcNAc in regulating DNA damage/repair and other cellular pathways. *Amino Acids* **40,** 793–808 (2010).

146. Groves, J. A., Lee, A., Yildirir, G. & Zachara, N. E. Dynamic O-GlcNAcylation and its roles in the cellular stress response and homeostasis. *Cell Stress and Chaperones* **18,** 535–558 (2013).

147. Glucose Deprivation Stimulates O-GlcNAc Modification of Proteins through Up-regulation of O-LinkedN-Acetylglucosaminyltransferase. 1–9 (2008).

148. O-GlcNAc Modification Is an Endogenous Inhibitor of the Proteasome. 1–11 (2003).

149. Allison, D. F. *et al.* Modification of RelA by O-linked N-acetylglucosamine links glucose metabolism to NF-κB acetylation and transcription. (2012).

150. Ma, Z., Vocadlo, D. J. & Vosseller, K. Hyper-O-GlcNAcylation Is Anti-apoptotic and Maintains Constitutive NF- B Activity in Pancreatic Cancer Cells. *Journal of Biological Chemistry* **288,** 15121–15130 (2013).

151. Loss of p53 enhances catalytic activity of IKK through O-linked -N-acetylglucosamine modification. 1–6 (2009).

152. NF B activation is associated with itsO-GlcNAcylation state underhyperglycemic conditions. 1–6 (2008).

153. Champattanachai, V. Aberrant O-GlcNAcylated proteins: new perspectives in breast and colorectal cancer. 1–10 (2014). doi:10.3389/fendo.2014.00193/abstract

154. O-Linked -N-Acetylglucosaminylation (O-GlcNAcylation) in Primary and Metastatic Colorectal Cancer Clones and Effect of N-Acetyl- . 1–15 (2012).

155. Onodera, Y., Nam, J.-M. & Bissell, M. J. Increased sugar uptake promotes oncogenesis via EPAC/RAP1 and O-GlcNAc pathways. *J. Clin. Invest.* **124,** 367–384 (2013).

156. Lynch, T. P. *et al.* Critical Role of O-Linked -N-Acetylglucosamine Transferase in Prostate Cancer Invasion, Angiogenesis, and Metastasis. *Journal of Biological Chemistry* **287,** 11070–11081 (2012).

157. Caldwell, S. A. *et al.* Nutrient sensor O-GlcNAc transferase regulates breast cancer tumorigenesis through targeting of the oncogenic transcription factor FoxM1. *Oncogene* **29,** 2831–2842 (2010).

158. Park, S. Y. *et al.* Snail1 is stabilized by O-GlcNAc modification in hyperglycaemic condition. *EMBO J* **29,** 3787–3796 (2010).

159. Huang, X. *et al.* O-GlcNAcylation of Cofilin Promotes Breast Cancer Cell Invasion. *Journal of Biological Chemistry* **288,** 36418–36425 (2013).

160. Glycosylation. 1–5 (2005).

161. Itkonen, H. M. *et al.* O-GlcNAc Transferase Integrates Metabolic Pathways to Regulate the Stability of c-MYC in Human Prostate Cancer Cells. *Cancer Res.* **73,** 5277–5287 (2013).

162. Yang, W. H. *et al.* Modification of p53 with O-linked N-acetylglucosamine regulates p53 activity and stability. *Nature Cell Biology* **8,** 1074–1083 (2006).

163. Napetschnig, J. & Wu, H. Molecular Basis of NF-κB Signaling. *Annu. Rev. Biophys.* **42,** 443–468 (2013).

164. Tak, P. P. & Firestein, G. S. NF-κB: a key role in inflammatory diseases. *J. Clin. Invest.* **107,** 7–11 (2001).

165. Perkins, N. D. The diverse and complex roles of NF-κB subunits in cancer.

Nature Publishing Group (2012). doi:10.1038/nrc3204

166. Karin, M., Cao, Y., Greten, F. R. & Li, Z.-W. NF-κB IN CANCER: FROM INNOCENT BYSTANDER TO MAJOR CULPRIT. *Nat. Rev. Cancer.* **2,** 301–310 (2002).

167. Karin, M. Nuclear factor-κB in cancer development and progression. *Nature Cell Biology* **441,** 431–436 (2006).

168. Karian, M. E. A. B kinase (IKK) and NF. 1–14 (2000).

169. Missing Pieces in the NF. 1–16 (2002).

170. J. Biol. Chem.-1990-Hohmann-22409-17. 1–9 (2001).

171. Burns, K. *et al.* Inhibition of Interleukin 1 Receptor/Toll-like Receptor Signaling through the Alternatively Spliced, Short Form of MyD88 Is Due to Its Failure to Recruit IRAK-4. *J Exp Med* **197,** 263–268 (2003).

172. induces p65 acetylation to enhance bacteria-induced NF. 1–13 (2007).

173. Perkins, N. D. Integrating cell-signalling pathways with NF-κB and IKK function. *Nat Rev Mol Cell Biol* **8,** 49–62 (2007).

174. Janssens, S. & Tschopp, J. Signals from within: the DNA-damage-induced NF-κB response. *Cell Death Differ* **13,** 773–784 (2006).

175. Tam, A. B., Mercado, E. L., Hoffmann, A. & Niwa, M. ER Stress Activates NF-κB by Integrating Functions of Basal IKK Activity, IRE1 and PERK. *PLoS ONE* **7,** e45078 (2012).

176. Huxford, T. & Ghosh, G. A Structural Guide to Proteins of the NF- B Signaling Module. *Cold Spring Harbor Perspectives in Biology* **1,** a000075–a000075 (2009).

177. IKK-i/IKK Controls Constitutive, Cancer Cell-associated NF- B Activity via Regulation of Ser-536p65/RelA Phosphorylation. 1–10 (2006).

178. Kumar, A. & Narayan, C. Constitutive over expression of IL-1β, IL-6, NF-κB, and Stat3 is a potential cause of lung tumorgenesis in urethane (ethyl carbamate) induced Balb/c mice. *J Carcinog* **11,** 9 (2012).

179. Essential role of RelA Ser311 phosphorylation byzPKC in NF-kB transcriptional activation. 1–9 (1912).

180. Huang, B., Yang, X.-D., Lamb, A. & Chen, L.-F. Posttranslational modifications of NF-κB: Another layer of regulation for NF-κB signaling pathway. *Cellular Signalling* **22,** 1282–1290 (2010).

181. Ben-Neriah, Y. & Karin, M. Inflammation meets cancer, with NF-κB as the matchmaker. *Nat Immunol* **12,** 715–723 (2011).

182. Increased Expression of Cyclooxygenase 2 Occurs Frequently in Human Lung Cancers, Specifically in Adelincarcinomas1. 1–4 (2006).

183. 1471-2407-2-31. 1–7 (2002).

184. Shebl, F. M. *et al.* Non-Steroidal Anti-Inflammatory Drugs Use Is Associated with Reduced Risk of Inflammation-Associated Cancers: NIH-AARP Study. *PLoS ONE* **9,** e114633 (2014).

185. NF-kB Target Genes » NF-kB Transcription Factors | Boston University. *bu.edu* Available at: http://www.bu.edu/nf-kb/gene-resources/target-genes/. (Accessed: 10 February 2017)

186. Meylan, E. *et al.* Requirement for NF-κB signalling in a mouse model of lung adenocarcinoma. *Nature* **462,** 104–107 (2009).

187. Xia, Y. *et al.* Reduced cell proliferation by IKK2 depletion in a mouse lung-cancer model. *Nature Cell Biology* **14,** 257–265 (2012).
188. Epithelial NF- B activation promotes urethane-induced lung carcinogenesis. 1–6 (2007).
189. Basseres, D. S., Ebbs, A., Levantini, E. & Baldwin, A. S. Requirement of the NF- B Subunit p65/RelA for K-Ras-Induced Lung Tumorigenesis. *Cancer Res.* **70,** 3537–3546 (2010).
190. NIH Public Access. 1–20 (2013).
191. Mauro, C. *et al.* NF-κB controls energy homeostasis and metabolic adaptation by upregulating mitochondrial respiration. *Nature Cell Biology* **13,** 1272–1279 (2011).
192. Kawauchi, K., Araki, K., Tobiume, K. & Tanaka, N. p53 regulates glucose metabolism through an IKK-NF-κB pathway and inhibits cell transformation. *Nature Cell Biology* **10,** 611–618 (2008).
193. Ramakrishnan, P. *et al.* Activation of the Transcriptional Function of the NF- B Protein c-Rel by O-GlcNAc Glycosylation. *Science Signaling* **6,** ra75–ra75 (2013).

CHAPTER II

Materials and Methods

MATERIALS AND METHODS

Generation of KP and KPS mice

      All animal experiments for this study were approved by the Institutional

Animal Care and Use Committee (IACUC), University of Virginia. Mice carrying the

KRAS[LSL-G12D]*p53*^{fl/fl} (KP) alleles were kindly provided by Tyler Jacks, and were

described previously in DuPage *et al.* 2009[1]. *SIRT6*^{fl/fl} mice were obtained from the

Jackson Laboratory. KP and *SIRT6*^{fl/fl} mice were bred to create *KRAS*[LSL-

G12D]*p53*^{fl/fl}*SIRT6*^{fl/fl} (KPS) mice. Mice were backcrossed to generate mixed strains

FVB/NJ, 129, C57BL/6, and SWR/J.

Conditional knockout of SIRT6 and formation of lung tumors

      At 6-12 weeks of age, KP and KPS mice were administered adenovirus

expressing either GFP (Ad-GFP) or Cre recombinase (Ad-Cre) via intranasal delivery

in accordance with the protocol outlined in DuPage *et al.* 2009 and in accordance

with ACUC guidelines. Mice were imaged weekly using MRI starting at 4 weeks

post-adenovirus delivery and continuing until the appropriate survival endpoint

was met at approximately 8-10 weeks post-adenovirus delivery. The survival

endpoint was determined by the condition of the mouse: overall appearance,

hunching, weight loss, ruffled fur, decreased activity and respiratory distress were

all physical parameters considered in determination of the survival endpoint.

Overall survival curves were determined for each experimental group. The

Institutional Animal Care and Use Committee (IACUC) at the University of Virginia approved all animal experiments for this study.

Tissue Staining

Tissue samples were collected from mice at their survival endpoint and immediately washed in phosphate buffered saline (PBS) before being fixed in 10-times the volume of either 10% buffered formalin, zinc formalin or Bouin's solution. Fixed tissue was then paraffin-embedded, sectioned, and stained with H&E using the UVA Research Histology Core (RHC). Immunohistochemistry analysis of mouse NSCLC tissue sections were examined for changes in protein expression of Ki67 (Epitomics 4203-1), p53 (LifeSpan Biosciences B722) and SIRT6 (Sigma S4322) using the UVA Biorepository and Tissue Research Facility (BTRF). Bright-field photomicroscopy was carried out using the Olympus BX41TF with 12 megapixel digital camera. H&E and IHC images we taken at 40, 100, 200 and 400X.

Generation of Cell Lines

Lung tumors harvested from KP and KPS mice were minced in a solution of 1 mg/mL type IV collagenase (Sigma C5138), 100 μg/mL type V hyaluronidase (Sigma H6254) and 20 μg/mL type IV DNase (Sigma D5025), and incubated for 30 minutes. Cells and tissue pieces were re-suspended and plated in DMEM/F-12 50:50 + L-Glutamine + 15 mM HEPES media (Gibco®) containing 1% fetal bovine serum (FBS), 2mM GlutaMAX™ (Gibco®), 1X minimal essential medium with non-essential

amino acids (MEM-NEAA) (Gibco®), 1X sodium pyruvate (Gibco®), 1X insulin-transferrin-selenium – ethanolamine (ITS-E), 0.5 µg/mL hydrocortisone, 5 ng/mL epidermal growth factor (EGF) and 1X Antibiotic-Antimycotic (Gibco®) in CellBIND®-coated flasks (Corning®). Cells and tissue pieces were continuously passaged first by scraping for 1-2 passages, and then by using TrypLE Express (Gibco®), and were deemed stable cell lines at passage 15 or when homogeneous. Once cell lines were established, the media formulation was adjusted to exclude the hydrocortisone and antibiotic-antimycotic for the JaDI4T and JaDI23T cell lines. The JaDI3T cell line was then cultured in DMEM (Cellgro) supplemented with 10% FBS, 2mM GlutaMAX, 1X MEM-NEAA and 10mM HEPES. A clonal population of representative cells from each of these pools was then designated as the cell lines used for experiments in this study. Light micrograph images of the resultant cell lines were taken at 80-90% confluency.

KRAS Mutational Analysis

JaDI3, JaDI4 and JaDI23 cell lines were grown to 70-80% confluency on a 10 cm dish, washed with PBS and then collected. Genomic DNA was extracted from these samples using PureLink® Genomic DNA Mini Kit (Invitrogen) according to the manufacturer's protocol. PCR directed at Exon 3 of KRAS was performed using primers listed in Table 1 with MyFi™ DNA polymerase (Bioline), according to the manufacturer's protocol. PCR purification was performed using QIAquick PCR Purification Kit (Qiagen). Purified PCR product was then combined with sequencing

primers listed in Table 1, and sequencing was performed by Genewiz to reveal mutations in Exon 3 of KRAS.

Cre recombinase treatment of SIRT6$^{fl/fl}$ NSCLC lines

At 50-70% confluency 18-24 hours after plating, cells were treated with adenovirus expressing either GFP (Ad-GFP) or Cre recombinase (Ad-Cre) at an MOI of 125. Two to three days post-treatment, cells were passaged and used for experiments within one week of Cre exposure. The characterization of cells in an "acute" manner reduced the chances of secondary effects of cell growth in the absence of SIRT6 expression. For select experiments, cells were treated with Ad-Cre allowed to recover and then passaged 4-6 times before being used in experiments to measure how the "chronic" loss of SIRT6 impacted proliferation.

Western Blot Analysis

Cells were plated and grown to approximately 80% confluency, and then collected and lysed in RIPA buffer containing 0.15 M NaCl, 1% NP40, 0.005 g/mL Sodium Deoxycholate, 0.1% SDS, 50 mM Tris, 0.4 mM EDTA, 10% glycerol, 1 mM DTT and protease inhibitor cocktail. Tumor and adjacent lung tissue samples were treated similarly. After incubation for 30 minutes, the supernatant containing protein was collected and protein concentration obtained by bicinchoninic acid (BCA) protein assay (Thermo Scientific Pierce). Protein samples (25 μg per sample)

were loaded on 2-5% Bis-Tris SDS-PAGE gels (Invitrogen) and transferred to

Immobilon-P membranes. The membranes were hybridized with the following

antibodies: SIRT6 (N-terminus) (Cell Signaling Technology, D8D12), SIRT6 (C-

terminus) (Cell Signaling Technology), α-tubulin (Sigma, T9026), p21 (Santa Cruz

SC-397), Cyclin D1 (Cell Signaling 92G2), Flag (Sigma), O-GlcNAc (Thermo Scientific

MA1-072) and OGT (Sigma O6264). Secondary species-specific horseradish

peroxidase-labeled antibodies were added and membranes were incubated for 1

hour at room temperature in 3% milk/TBS. Detection was achieved using

Immobilon Western Chemiluminescent HRP Substrate (Millipore).

Cell Proliferation Assays

For growth curve assays, cells were plated in triplicate in 6-well plates at a

concentration of 5,000 cells/well. Cells were then trypsinized and counted on days

2, 4, 6 and 8 post-plating using a hemacytometer.

qRT-PCR

Cells were plated and grown to approximately 80% confluency, and then

collected. RNA was isolated using Quick-RNA™ MidiPrep kit (Zymo Research). RNA

yield was quantified and cDNA was synthesized using SensiFAST™ cDNA synthesis

kit (Bioline). qRT-PCR was performed using SensiMix™ SYBR® and Fluoroscein kit

(Bioline). qRT-PCR was carried out as previously described[2]. Primers directed at

SIRT6 and HPRT were used at a concentration of 10 μM.

Senescence-Associated-β-Galactosidase (SA-β-Gal) Assay

Cells were plated in triplicate on 6- well plates at a concentration of 5,000 cells/well. Cells were then fixed and stained using senescence β-galactosidase staining kit (Cell Signaling) at 72 and 96 hours post-plating, according to the manufacturer's protocol. Senescence-associated β-galactosidase (SA-β-Gal) positive cells were identified as blue-stained cells and quantified under light microscopy.

Soft Agar Assays

Seaplaque® agarose (1.5%) was prepared in deionized water and autoclaved on liquid cycle for 20 minutes. 2X DMEM/F-12 media was prepared as followed: 2X DMEM/F-12 powder + L-glutamine + 15 mM HEPES (Sigma), 4 mM GlutaMAX™ (Gibco®), 2X MEM-NEAA (Gibco®), 2X sodium pyruvate (Gibco®), 2X ITS-E and 2% FBS. Media was filter-sterilized prior to use. Media and agarose were combined in a 50:50 ratio for a final agarose concentration of 0.75%. Media/agarose mixture (3 mL) was plated onto 6 cm plates and allowed to solidify at room temperature. Agarose plates were then allowed to equilibrate in a 37°C incubator for 3 hours to overnight. Cells were then plated in a 3 mL top layer of media/agarose mixture at a concentration of 1000 cells/plate. Plates were then incubated in a 37°C incubator for 2-4 weeks until colonies were easily visible (~ 1 mm or larger). Colonies were then fixed and stained with 0.005% crystal violet (0.2% crystal violet stock in 5% absolute ethanol) for 1 hour. Photos were taken and quantification of colony number and size was determined using Image J software.

In vitro Deacetylation Assay

HEK293T cells were transfected with pcDNA3.1-Flag-p65 with or without pcDNA3.1-HA-p300 using PolyFect reagent (Qiagen) according to the manufacturer's protocol. These cells were collected and lysed in 500 μL RIPA buffer containing 0.15 M NaCl, 1% NP40, 0.005 g/mL Sodium Deoxycholate, 0.1% SDS, 50 mM Tris, 0.4 mM EDTA, 10% glycerol, 1 mM DTT and protease inhibitor cocktail. Immunoprecipitation was performed using anti-Flag (Sigma) antibody and agarose beads in order to immunoprecipitate the Flag-p65 protein. The immunoprecipitated Flag-p65 protein was then combined with deacetylase buffer containing protease inhibitor and 1mM DTT. 500 μM NAD^+ was added to appropriate samples, along with 1.5 μg recombinant SIRT1 and/or recombinant SIRT6 enzyme. Samples were incubated for two hours at 30°C. The supernatant was then aspirated and samples were re-suspended in 35 μL of reducing sample buffer containing LDS sample buffer and 50 μM DTT. Input and IP samples were then subjected to western blot analysis as described previously in the above procedure. Immunoblots were probed with anti-p65 (Santa Cruz, sc-372), anti-Ac-p65 (Cell Signaling 3045) and anti-Flag antibody (Sigma).

In vitro Acetylation Assay

HEK293T cells were transfected with pcDNA3.1-HA-p65 with or without pcDNA3.1-V5-SIRT1, Flag-SIRT6 and/or Myc-OGA using PolyFect reagent (Qiagen) according to the manufacturer's protocol. These cells were collected and lysed in 500 μL RIPA buffer containing 0.15 M NaCl, 1% NP40, 0.005 g/mL Sodium

Deoxycholate, 0.1% SDS, 50 mM Tris, 0.4 mM EDTA, 10% glycerol, 1 mM DTT and

protease inhibitor cocktail. Immunoprecipitation was performed using anti-HA

(Sigma) antibody and agarose beads in order to immunoprecipitate the HA-p65

protein. The immunoprecipitated HA-p65 protein was then combined with

acetylation buffer containing 100 µM acetyl-CoA and recombinant p300 enzyme.

Samples were incubated for two hours at 30°C. The supernatant was then aspirated

and samples were re-suspended in 35 µL of reducing sample buffer containing LDS

sample buffer and 50 µM DTT. Input and IP samples were then subjected to western

blot analysis as outlined in the above procedure, and probed with anti-p65, anti-

K310 Ac-p65, anti-HA, or anti-Myc antibody (Santa Cruz).

Plasmid and siRNA Transfections

All plasmid and siRNA transfections were carried out by seeding HEK293T

cells onto tissue culture plates at a concentration to allow for 70% confluency and

allowed to adhere overnight. Plasmid transfection was performed following

overnight adherence using Polyfect reagent (Qiagen) according to the

manufacturer's protocol. siRNA transfections were performed using oligofectamine

(Invitrogen) according to the manufacturer's protocol. Cells were then incubated

for the appropriate amount of time, washed with PBS, collected by scraping, and

frozen at -80°C or used for experiments.

Isolation of Nuclear and Cytoplasmic Extracts

H1299 cells were cultured to the indicated conditions overnight in low (5 mM) and high (25 mM) glucose conditions with and without glucosamine. Two hours prior to collection, 100 µM of the proteasome inhibitor MG-132 was added to the appropriate samples. Cells were then washed in PBS and collected. Cell pellets were re-suspended in 5 volumes of cytoplasmic extraction (CE) buffer containing 10 mM HEPES (pH 7.6), 60 mM KCl, 1 mM EDTA, 1 mM DTT, 1 mM phenylmethylsulfonyl fluoride (PMSF), protease inhibitor cocktail and 0.3% NP-40. Samples were then incubated on ice for 3 min, and vortexed briefly several times. Nuclei were pelleted by centrifugation at 2000 rpm for 4 minutes at 4°C. The supernatant containing cytoplasmic proteins was then removed and added to a fresh microcentrifuge tube with 20% glycerol by volume. Nuclei were then washed in 5 volumes of CE buffer lacking NP-40, and re-suspended in 1 pellet volume of nuclear extraction (NE) buffer containing 20 mM Tris (pH 8.0), 420 mM NaCl, 1.5 mM $MgCl_2$, 0.2 mM EDTA, 25% glycerol by volume, 0.5 mM PMSF, and protease inhibitor cocktail. Samples were incubated on ice for 10 minutes, and subsequently centrifuged at 14,000 rpm for 10 minutes at 4°C. Supernatant containing nuclear proteins was then transferred to a fresh microcentrifuge tube. Protein concentrations were then quantified by BCA assay, and re-suspended in reducing sample buffer prior to western blot analysis, as described above.

REFERENCES

1. DuPage, M., Dooley, A. L. & Jacks, T. Conditional mouse lung cancer models using adenoviral or lentiviral delivery of Cre recombinase. *Nat Protoc* **4,** 1064–1072 (2009).
2. Allison, D. F. *et al.* Modification of RelA by O-linked N-acetylglucosamine links glucose metabolism to NF-κB acetylation and transcription. (2012).

Table 1. Primer Sequences

Gene/Primer	**Sequence (5'→ 3')**
SIRT6 5'F	CCTGGTCAGCCAGAACGTAG
SIRT6 3'R	TACTGCGTCTTACACTTGGGA
KRAS PCR 5'F	CCTTCTCCCAAGGTGCTTGCC
KRAS PCR 3'R	AGGCCCTGGTGTCAGATAGCAC
KRAS Seq 5'F1	TGGCCACTTGTCTGCTTTGGAG
KRAS Seq 5'F2	CGTGCTTTGCCTGTTTTGAATGGG
SIRT6 Geno 5'F	AGTGAGGGGCTAATGGGAAC
SIRT6 Geno 3'R	AACCCACCTCTCTCCCCTAA
p53 Geno 5'F	CACAAAAACAGGTTAAACCCAG
p53 Geno 3'R	AGCACATAGGAGGCAGAGAC
KRAS Geno 5'F	CTAGCCACCATGGCTTGAGT
KRAS Geno 3'R	TCCGAATTCAGTGACTACAGATG

CHAPTER III

NSCLC utilizes SIRT6 for tumorigenesis by overcoming

oncogene-induced senescence

ABSTRACT

Lung cancer is the leading cause of cancer-related deaths in the United States and worldwide, with non-small cell lung cancer (NSCLC) being the most common type. Since most patients present with metastatic disease upon diagnosis, one of the unmet needs in the lung cancer research field is to identify novel signaling pathways involved in NSCLC initiation and progression[1,2]. SIRT6 is a NAD^+-dependent histone deacetylase that has many important physiological roles in regulating glucose metabolism, genomic stability, and aging[1-4]. While SIRT6 functions as a tumor suppressor in mouse models of colon, liver and pancreatic cancers, the role of SIRT6 in lung cancer remains under studied[1,5]. Here, we create a conditional mouse model for SIRT6 utilizing activation of KRAS and homozygous deletion of p53 for lung tumor formation. Upon intranasal delivery of adenovirus expressing Cre to selectively induce tumor formation and knockout SIRT6 in the lung, we found that loss of SIRT6 delayed lung tumor initiation and formation. Using SIRT6[flox/flox] lung tumor cell lines derived from urethane-induced lung tumors, we were able to determine that an initial loss of SIRT6 decreased cell proliferation and colony formation in soft agar assays. Cells lacking SIRT6 undergo senescence upon initial loss of SIRT6. However, cells lacking SIRT6 evidentially recover demonstrating increased proliferation and the ability to form large soft agar colonies *in vitro*. Thus, we have determined that initial loss of SIRT6 in a mouse model of NSCLC delays lung tumor initiation and formation, possibly due to induction of senescence. However, this delay is later overcome and tumors that form in the absences of SIRT6 have

more aggressive characteristics, such as increased proliferation rates and invasive

carcinoma properties.

INTRODUCTION

Lung cancer is the leading cause of cancer-related deaths in men and women, accounting for approximately 158,080 deaths in 2016. More than 50% of patients have advanced metastatic disease at diagnosis, resulting in a 5-year survival rate of <5%[2,5]. Furthermore, on a global scale, only 7-12% of lung cancer patients are alive at 5 years following diagnosis[1,2,5-7]. Thus, there is a great need for further research into developing therapies to combat this deadly disease.

Non-small cell lung cancer (NSCLC) is the most common subtype of lung cancer. Although 83% of all cancers occur in tobacco smokers, as high as 17% of patients represent the never-smoker NSCLC population. NSCLC is well known to be induced by tobacco smoke, and numerous other environmental chemical carcinogens[1,3,8]. However, it has been proposed that other genetic factors may play a role in modulating not only NSCLC progression, but initiation as well.

Sirtuin 6 (SIRT6) is a member of the sirtuin family of NAD^+-dependent histone deacetylases that acts as a tumor suppressor in colon, pancreatic and liver cancers through its role as a key regulator of glucose metabolism[1,2,5,7]. Through its deacetylase activity on H3K9Ac and H3K56Ac, SIRT6 down-regulates expression of several key glycolytic enzymes and glucose metabolism genes, including glucose transporter 1 (GLUT1), phosphofructokinase-1 (PFK1), Aldolase C (ALDOC), pyruvate dehydrogenase kinase 1 (PDK1) and lactate dehydrogenase (LDH), primarily through its role as a co-repressor of HIF1α-mediated transcription[1,8,9]. High-grade NSCLC tumors demonstrate elevated glucose uptake, which can be

detected by positron emission tomography (PET) scans[10,11]. Thus, since SIRT6 regulates key regulators in glucose uptake and glycolysis, we postulated that SIRT6 might be dysregulated in the initiation and progression of NSCLC.

In addition to its role in metabolism, SIRT6 also has roles in DNA repair and telomere maintenance, both of which contribute to its anti-aging effects and inhibition of senescence. Senescence is a process of cellular aging whereby there is a reduction in proliferative capacity despite continued viability of the cell. Because senescence represents a mechanism by which the cell can exit the cell cycle, it is a targetable pathway in the interest of cancer therapy[12,13]. Oncogene-induced senescence (OIS) and tumor suppressor-induced senescence are mechanisms of tumor suppression whereby activation of an oncogene, as was first observed with KRAS, or loss of a tumor suppressor gene induces senescence as a barrier to tumorigenesis in benign, early stage tumors[14-16]. Tumor suppressor-induced senescence has been shown to occur in a p53-dependent manner following loss of PTEN, and subsequent induction of p21, in prostate cancer[17-19]. Loss of the von Hippel-Lindau (VHL) tumor suppressor has also been shown to induce senescence in a p53-independent manner through activation of retinoblastoma (Rb) and subsequent activation of p27[20,21]. Furthermore, loss of retinoblastoma was found to induce cellular senescence in mice with the background of activated N-Ras, thus further supporting a crucial role for tumor suppressor-induced senescence as a barrier to tumorigenesis[22,23].

Because SIRT6 has been shown to function as a tumor suppressor in other cancers, we sought to investigate its role in lung cancer using a conditional knockout
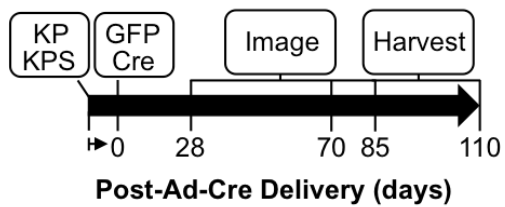
mouse model that induces adenocarcinomas via expression of oncogenic $KRAS^{G12D}$ and loss of *TP53*. Using this system, we discovered that loss of SIRT6 temporarily abrogates lung tumor initiation. *In vitro*, the initial loss of SIRT6 inhibits cell proliferation and formation of soft agar colonies, which is associated with a senescence phenotype. Despite this initial phenotype, some NSCLC SIRT6 null cells escape senescence displaying increased rates of proliferation and soft agar colony formation, compared to isogenic SIRT6$^{flox/flox}$ cells. Therefore, this study implies a novel role for SIRT6 in promoting lung tumor initiation and formation, possibly through its ability to inhibit oncogene-induced senescence. However, our *in vitro* work also supports the notion that loss of SIRT6 activity in late-stage NSCLC is associated with its well-known tumor suppressive properties previously observed in other models of tumorigenesis.
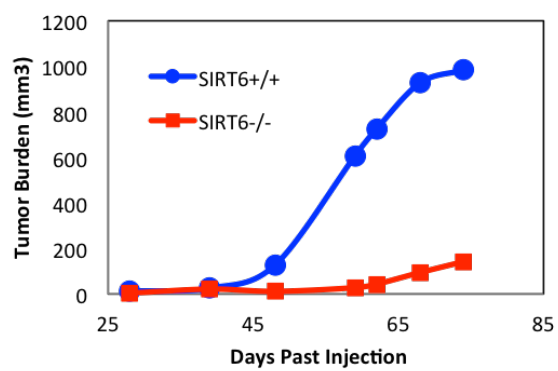
RESULTS

Loss of SIRT6 delays lung tumor formation in a murine model of NSCLC.

KRAS$^{G12D/WT}$p53$^{fl/fl}$ mice have been used as a model for many types of cancer as activation of the constitutively active *KRAS^{G12D}* allele and knockout of the *TP53* gene result in tumor formation. Oncogenic KRAS G12 mutations and loss of heterozygosity (LOH) for *TP53* are present in 35% and 50% of NSCLC tumors respectively. Thus, this genotypic profile represents two of the major driver mutations in this cancer patient population[24,25]. To study the effect of loss of SIRT6 in NSCLC, we utilized KRAS$^{G12D/WT}$p53$^{fl/fl}$ (KP) mice and bred them to SIRT6$^{fl/fl}$ mice to create KRAS$^{G12D/WT}$p53$^{fl/fl}$SIRT6$^{fl/fl}$ (KPS) mice (Supplementary Fig. 1A). Intranasal delivery of adenovirus expressing GFP (Ad-GFP) or Cre (Ad-Cre) was sufficient to induce tumor formation and knockout SIRT6 with Ad-Cre selectively in the lung (Fig. 2B and Supplementary Fig. 1A). Mice were imaged by magnetic resonance imaging (MRI) weekly starting at 4 weeks post-adenovirus delivery until their survival endpoints at approximately 70-110 days post-delivery (Fig. 1A). Contrary to previous mouse cancer models for colon, pancreas and lung, KPS mice lacking SIRT6 in their tumors showed a delay in tumor initiation and formation compared to KP control mice (Fig. 1B and 1C). Moreover, as a consequence of the delay in tumor development KPS mice also had significantly longer overall survival, with a median survival of 102 days, compared to KP mice with a median survival of 80 days (n=12/group, p=0.03) (Fig. 1D).

A.

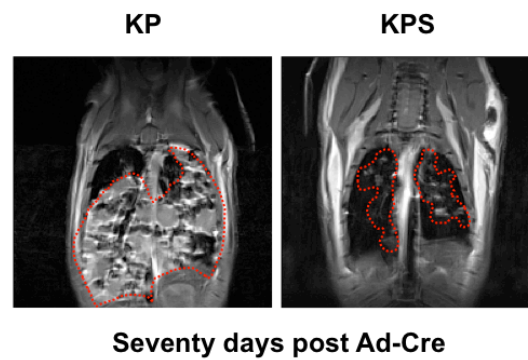
KP KPS | GFP Cre | Image | Harvest

0   28   70 85   110

Post-Ad-Cre Delivery (days)

B.

C.

KP   **KPS**

Seventy days post Ad-Cre

D.

- KP
- KPS

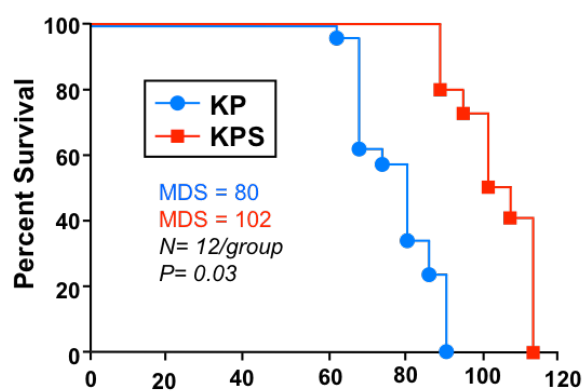MDS = 80
MDS = 102
N= 12/group
P= 0.03

Figure 1. Loss of SIRT6 delays lung tumor formation in a murine model of NSCLC. A) KP and KPS mice were inoculated with Ad-GFP or Ad-Cre intranasally to initiate $KRAS^{G12D}$ expression and to knockout the $TP53$ allele. Mice were imaged weekly by thoracic MRI to assess tumor burden until their respective survival endpoints. Normal and tumor lung tissue were harvested post-mortem. B) Tumor burden observed by MRI in KP and KPS mice post-Ad-GFP or –Ad-Cre delivery reveals that loss of SIRT6 delays lung tumor formation and results in significantly reduced overall tumor burden. C) Representative MR images of KP and KPS mice 68 days post Ad-GFP or Ad-Cre delivery reveal that loss of SIRT6 results in decreased tumor burden. D) KPS mice have increased overall survival relative to KP mice following Ad-Cre administration (n=12/group, p=0.03). Work done by Jaclyn D'Innocenzi and Marty Mayo.

At their respective survival endpoints, lung tumor and adjacent lung tissue was harvested from these mice. Following the same histological classification used by DuPage *et al.* 2009 on the KP mouse model system, H&E staining of tissue samples indeed confirmed pathology consistent with adenocarcinoma of the lung (Fig. 2A). Using the grading system described by DuPage *et al.* 2009, tumors derived from both KP and KPS mice exhibited invasive lung adenocarcinomas (Fig. 2A). Both KP and KPS tumors showed pleiomorphic cells with prominent and atypical nuclei and elevated nuclear-to-cytoplasmic ratios (Fig. 2A). Although the KP tumor shown below appears to exhibit a greater mitotic index than the KPS tumor, which may represent a more invasive adenocarcinoma, it is important to note that these are merely representative images of the tumor burden observed in both the KP and KPS mouse (Fig. 2A). Under careful observation, lung tissues isolated from both KP and KPS mice have multiple foci displaying a heterogeneic plethora of tumor grades that pathologically represent less aggressive "adenoma-like" tumors to those that are high-grade invasive adenocarcinoma tumors. However, staining of the more invasive carcinomas revealed comparable Ki67 staining between the KP and KPS tumors, indicating similar rates of cellular proliferation (Fig. 2B). Moreover, Ki67 staining also identified similar rates of mitotic-index in both KP and KPS tumors, suggesting that at a pathological level tumor growth rates were similar in developed NSCLC. As expected, tumors isolated from both KP and KPS mice both lacked p53 expression by IHC staining, compared to adjacent normal lung tissue. Furthermore, SIRT6 was effectively knocked out in many, but not all, of the tumors isolated from KPS mice, compared to KP controls (Fig. 2B and Supplementary Figure 1A).

A.

H&E

KP

KPS

100x

200x

B.

Ki67

p53

SIRT6

KP

KPS
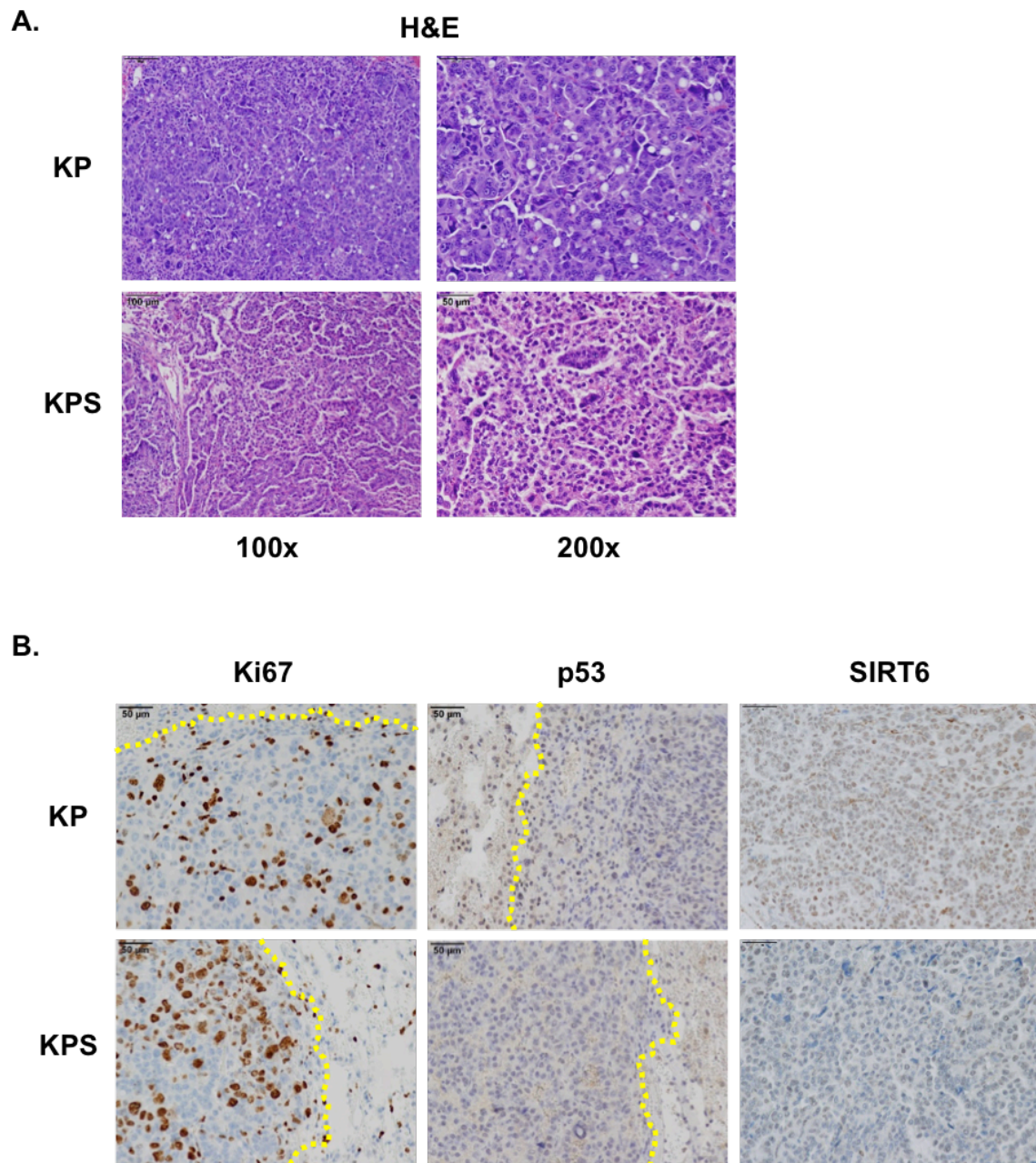
Figure 2. Histopathology of KP and KPS tumors are consistent with high-grade invasive lung adenocarcinomas. A) H&E staining of lung tumor tissue harvested from KP and KPS mice at their respective survival endpoints. B) Immunohistochemistry staining of lung tumor tissue harvested from KP and KPS mice show similar degrees of Ki67 staining while confirming the KP and KPS genotype for p53 and SIRT6 expression. Work done by UVA Histology Core Facility.

Development and characterization of NSCLC cell lines derived urethane-induced lung tumors.
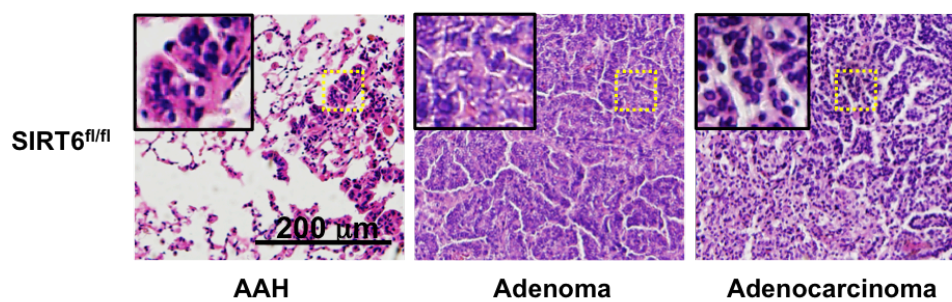
In order to create NSCLC cell lines that can be used to characterize the importance of SIRT6 *in vitro*, we treated SIRT6^{fl/fl} mice with an intraperitoneal (IP) injection of urethane to induce lung adenocarcinomas. At their survival endpoint (approximately 10 months post-injection), lung tumors and adjacent normal lung tissue was harvested (Fig. 3A). Within the lung tumor tissue sample, H&E staining revealed areas of atypical adenomatous hyperplasia (AAH), adenoma and adenocarcinoma (Fig. 3B). Interestingly, SIRT6 protein expression was elevated in the lung tumor sample compared with the adjacent normal lung tissue (Fig. 3C). These results supports the *in vivo* mouse model presented in Figure 1 showing that SIRT6 is required for lung tumor initiation in mice harboring the KPS genotype. Additionally, it suggests that SIRT6 expression is elevated in urethane-induced NSCLC tumors in response to the progression from adenomas to adenocarcinomas. To develop NSCLC cell lines from urethane-induced tumors, lung tumor tissue was mechanically and enzymatically digested at the time of harvest and cultured with continuous passaging until a homogeneous population of cells grew out. Three cell lines were developed and characterized using tumors obtained from 3 different mice.   Cells lines were created as a clonal population derived from the homogeneous population of cells (Fig. 3D). Since 90% of urethane-derived tumors carry KRAS[Q61] mutations[26], we analyzed isolated genomic DNA and sequenced exon 3 of the KRAS allele for gain-of-function mutations. Sequence analysis confirmed

that all three cell lines carried KRAS^{Q61} mutations (Fig. 3E). Additionally, genomic

sequencing confirmed that the lines were in fact clonal isolates.

A.

SIRT6^fl/fl → Urethane → Harvest

Time post-urethane (months)

B.

SIRT6^fl/fl

200 μm

AAH   Adenoma   Adenocarcinoma

C.   Urethane Tumors

Animal	1	2	3	4

A T   A T   A T   A T

SIRT6

Tubulin

D.
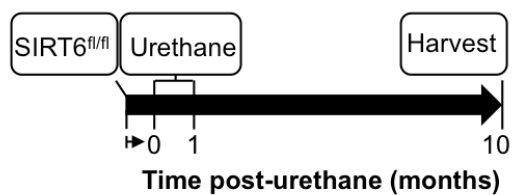
JD3.12T   JD4.18T   JD23.77T
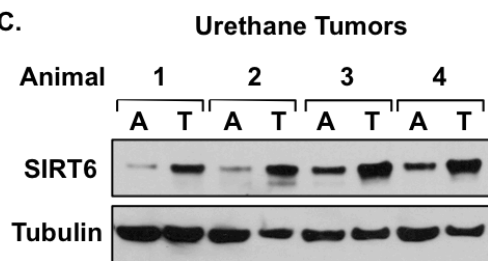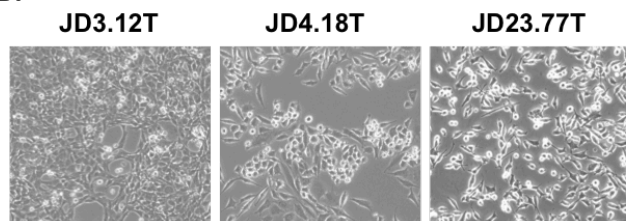
E.

Cell Line	KRAS
JD3.12T	Q61R
JD4.18T	Q61L
JD23.77T	Q61L

Figure 3. Development and characterization of urethane-induced lung adenocarcinoma cell lines. A) SIRT6$^{fl/fl}$ mice were given an IP injection of urethane to induce lung tumor formation. Ten months later, tumor tissue was isolated from mice. B) H&E staining of urethane-induced lung tumor tissue harvested from mice at their survival endpoint. Photomicrographs show lung foci with atypical adenomatous hyperplasia (AAH), adenoma and adenocarcinoma. C) Western blotting reveals that SIRT6 expression is elevated in urethane-induced lung tumor (T) tissue compared to adjacent (A) lung tissue. Tubulin ensures even loading of protein. D) Light microscopy photos of resulting JD.3.12T, JD.4.18T and JD.23.77T urethane-induced murine lung tumor cell lines (10X). E) Genomic DNA sequencing identifies mutations in KRAS^{Q61} in all three cell lines developed. Work done by Jaclyn D'Innocenzi and the UVA Histology Core Facility.

The initial loss of SIRT6 expression results decreased cell proliferation.

To study the role of SIRT6 in NSCLC, JD3.12T, JD4.18T and JD23.77T cell lines were treated with Ad-Cre and SIRT6 protein expression was tracked over time. Treatment of JD3.12T, JD4.18T and JD23.77T cell lines with Ad-Cre resulted in >99% knockdown at the mRNA and protein level by 48 hours post-treatment (Fig. 4A, B and C). The development of these cell lines enabled us to acutely knockdown SIRT6 to near completion and then study the phenotypic differences between isogenic cells that either express or lack SIRT6 expression. First, cell proliferation assays were performed following treatment of the JD3.12T, JD4.18T and JD23.77T cell lines with Ad-GFP or Ad-Cre. Following the first passage after Cre delivery, all three cell lines showed that the loss of SIRT6 expression significantly inhibited cell proliferation over an 8-day period compared to Ad-GFP control treated cells (Fig. 4D). Thus, the knockout of SIRT6 resulted in a slower rate of proliferation, compared to NSCLC cells that expressed endogenous SIRT6.
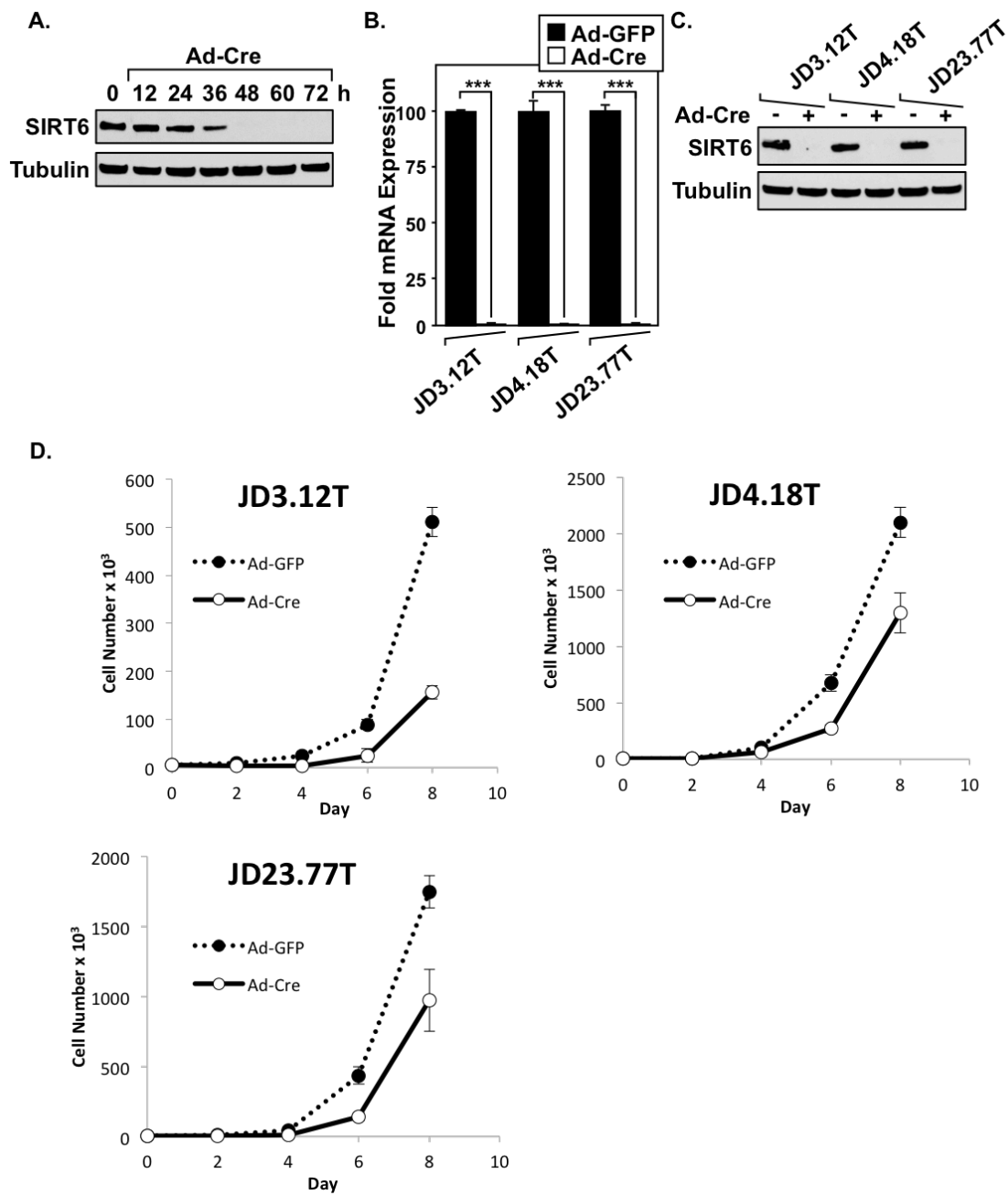
Figure 4. Loss of SIRT6 expression dampens proliferation of NSCLC cells *in*

vitro. A) Treatment of JD3.12T cells with Ad-Cre results in a time-dependent loss of

SIRT6 protein expression, which was undetectable by 48 hrs post-treatment.

Tubulin shows all samples contain even amounts of total protein. B) qRT-PCR

analysis reveals that treatment of the JD3.12T, JD4.18T and JD23.77T cell lines with

Ad-Cre results in >99% knockdown of SIRT6 mRNA expression (n=3 p=0.005). C)

Treatment of the JD3.12T, JD4.18T and JD23.77T cell lines with Ad-Cre effectively

knockdown of SIRT6 protein expression. D) Knockdown of SIRT6 in all three NSCLC

cell lines resulted in a loss of cell proliferation, compared to cell expressing SIRT6

(n=3, p<0.05 on days 6 and 8). Work done by Jaclyn D'Innocenzi and Lisa Gray.

Initial loss of SIRT6 induces a senescence phenotype.

To further assess the mechanism behind the delay in tumor formation shown in Fig. 1B and decreased cellular proliferation shown in Fig. 5D, soft agar assays were performed in JD3.12T cells. As expected by previous results, the JD3.12T cells lacking SIRT6 formed less colonies on soft agar compared to their JD3.12T counterparts that retained SIRT6 expression. However, the cells lacking SIRT6 did form significantly larger colonies (Fig. 5A). Moreover, cells lacking SIRT6 had a visible change in morphology. JD3.12T and JD4.18T cells lacking SIRT6 become large, flattened and multinucleated, which are all morphological changes associated with oncogene-induced senescence (Fig. 5B)[13]. Thus, the JD3.12T and JD4.18T cells were subjected to SA-β-Gal staining 72 hrs following Ad-Cre treatment to determine if these morphological changes and decreased proliferative capacity were due to senescence. Indeed, an increased proportion of JD3.12T and JD4.18T cells lacking SIRT6 stained β-Gal positive (blue) than cells retaining SIRT6 expression, indicating that an acute loss of SIRT6 resulted in cellular senescence (Fig. 5B). To further confirm this phenotype, western blot analysis for the key cell cycle regulators that are induced in response to loss of tumor suppressor-induced senescence, p21 and cyclin D1, was performed. Indeed, the JD3.12T cells lacking SIRT6 show an increase in p21 expression without changes in cyclin D1 expression (Fig 5C). Thus, JD3.12T cells lacking SIRT6 display characteristics of cellular senescence, including increased β-Gal positive cells and elevated expression of the cell cycle inhibitor p21 (Fig. 5B and 5C).

A.
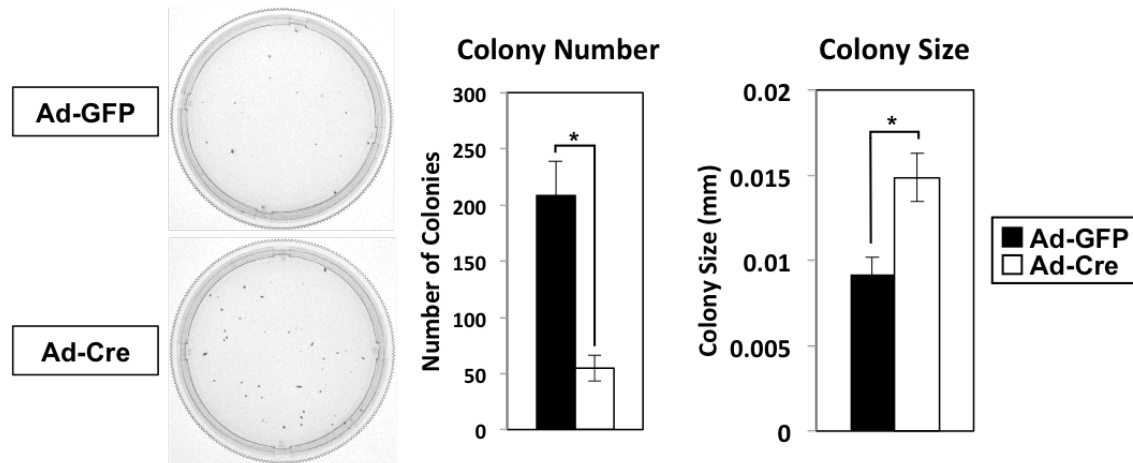
B.
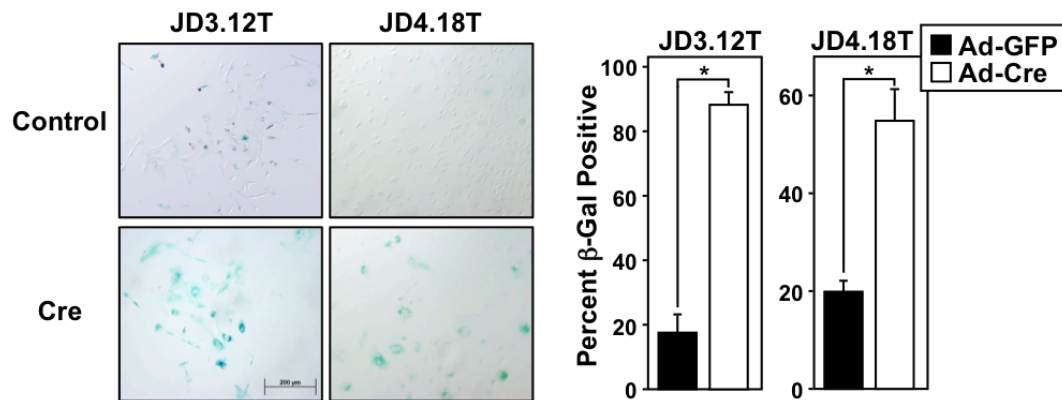
C.
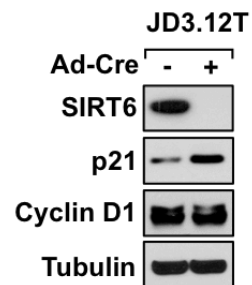
Figure 5. Loss of SIRT6 results the induction of cellular senescence in urethane-derived NSCLC cells. A) Soft agar assay for colony formation reveals that JaDI.3 cells lacking SIRT6 show decreased colony formation with an increase in the overall colony size (n=3, p=0.01). B) Staining JD3.12T and JD4.18T cells with SA-β-Gal 72 hrs. following Ad-GFP or Ad-Cre administration shows that initial loss of SIRT6 induces senescence. Light microscopy photographs show blue staining for SA-β-Gal (10X, n=3, p=0.005). C) Western blot analysis shows that loss of SIRT6 results in induction of p21 expression in the JD3.12T cell line. Work done by Jaclyn D'Innocenzi and Lisa Gray.

Over time, NSCLC cells adapt to the loss of SIRT6 expression to increase proliferation and soft agar growth rates.

Since previous studies have identified SIRT6 as a tumor suppressor using other mouse models of colon, pancreas and liver cancer, we decided to investigate whether chronic loss of SIRT6 changes the tumorigenic properties of urethane cell lines. We were interested in determining whether the acute loss of SIRT6 induced a senescence phenotype in only a subpopulation (≥75%) of JD3.12T cells, while the cells that escape senescence (≤25%) were perhaps more aggressive. JD3.12T, JD4.18T and JD23.77T cell lines treated with Ad-GFP or Ad-Cre were then continuously passaged for approximately 4 weeks, and re-plated for another cell proliferation assay. In contrast to this experiment performed on cells acutely lacking SIRT6 (Fig. 4D), the chronic loss of SIRT6 resulted in cells with increased proliferation rates compared to control (Fig. 6A and Supp. Fig. 2). Additionally, JD3.12T cell line chronically lacking SIRT6 formed soft agar colonies at a higher frequency rate than its counterpart that retained SIRT6 expression (Fig 6B). Thus, while the initial loss of SIRT6 results in an inhibition of cell proliferation and decreased rate of soft agar colonies, the NSCLC cell lines were able to overcome this defect to exceed the proliferative capacity and colony formation potential. This supports the *in vivo* mouse data shown in Figure1B where KPS mice exhibit an initial delay in cell proliferation that results in decreased tumor formation (Fig. 1B and 1C). The fact that these cell lines are able to overcome the loss of SIRT6 by increasing proliferation and colony formation defects supports many previous

studies showing that SIRT6 functions as a tumor suppressor in established and/or

advanced malignant tumors (Fig. 6A and 6B) [1,27].
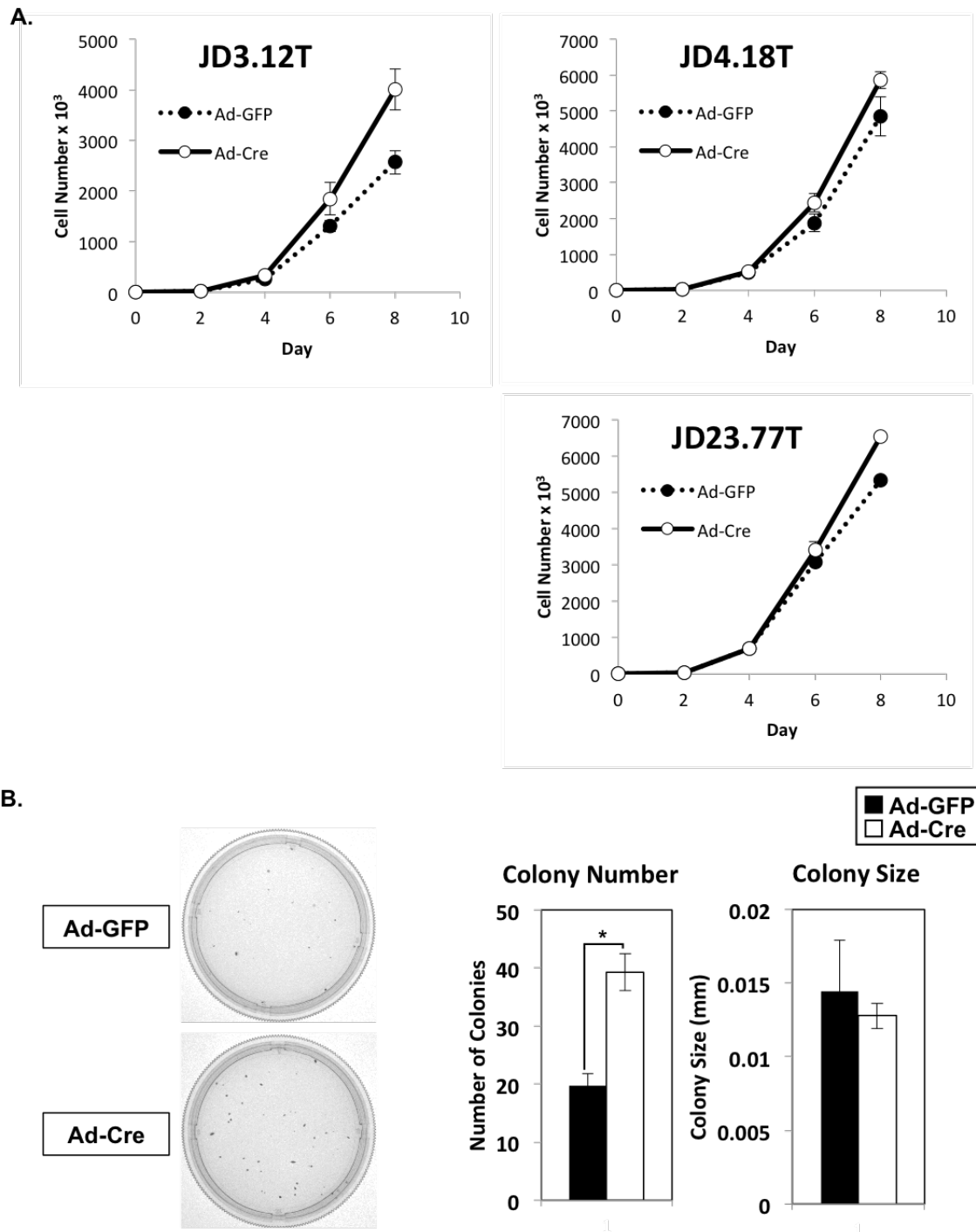
Figure 6. Urethane-induced NSCLC lines escape the initial loss of SIRT6 to display increase tumorigenic characteristics. A) After several cell divisions, JD3.12T, JD4.18T and JD23.77T SIRT6 null cells proliferate at faster rates, compared to control cells (n=3, p<0.05 on days 6 and 8). B) JD3.12T cells exhibit a greater number of soft agar colonies, compared to cells that retain SIRT6 expression. However, colony size is comparable between cell lines assayed. Work done by Jaclyn D'Innocenzi

DISCUSSION

SIRT6 has been known to control many cellular processes relevant to cancer, including glucose metabolism, the DNA damage response (DDR), genomic instability and senescence through telomere maintenance[1,13,21,23-26,28-30]. SIRT6 has been implicated to function as a tumor suppressor in colon, pancreatic and liver cancer through its regulation of glucose metabolism[1,5]. However, its role in the development and progression of lung cancer has not been examined using mouse models. Here, we have uncovered a dual role for SIRT6 in both the initiation and progression of NSCLC. Approximately 30% and 46% of ADCs carry a KRAS and/or p53 mutation respectively[12,14]. Thus, we utilize a well-characterized conditional mouse model of NSCLC in which upon the delivery of intranasal Ad-Cre, oncogenic KRAS[G12D] is expressed in a p53 null background. We were able to show that conditional loss of SIRT6 inhibited lung tumor initiation and formation (Fig. 1). Furthermore, mice lacking SIRT6 showed decreased overall tumor burden at endpoint and increased overall survival. This unexpected result indicates that SIRT6 is necessary for the development of lung tumors, constituting a novel role for SIRT6 in promoting cancer initiation and development in NSCLC (Fig. 1).

To investigate the potential mechanism behind this phenotype, we created three NSCLC cell lines derived from urethane-induced tumors of SIRT6^{fl/fl} mice. Acute knockout of SIRT6 in these lung tumor cell lines induces a phenotype consistent with that seen *in vivo* with KP and KPS mice. Cells lacking SIRT6 initially show slowed proliferation and decreased colony formation in soft agar. However,

SIRT6 null cells that escape senescence continue to divide and eventually have significantly greater rates of proliferation and growth in soft agar. This phenotype seen after a compensation for SIRT6 loss is consistent with previous studies implicating that SIRT6 functions as a tumor suppressor[1,5]. Using both a conditional mouse model along with urethane-derived NSCLC cells we were able to unveil how loss of SIRT6 differentially modulates NSCLC initiation and progression, depending on the timing of SIRT6 loss during the cancer process. Thus, we propose that SIRT6 plays a dual role in lung cancer, where it is necessary for tumor initiation and formation, but later functions to inhibit late-stage cancer progression.

One possible mechanism identified in this study that explains the dual role of SIRT6 loss in lung cancer is senescence. Cancer cells are known to have to overcome replicative senescence, characterized by replication-induced telomere shortening[6]. SIRT6 has been shown to stabilize and maintain telomere length through its ability to deacetylate H3K9Ac to induce heterochromatin formation at telomeric ends[3]. This is consistent with our data presented in Figure 6 showing that mouse lung tumor cells undergo senescence initially in response to loss of SIRT6. The fact that the initial loss of SIRT6 induces senescence is also consistent with data presented in this study showing a delay in cell proliferation, inhibited formation of colonies on soft agar, and a delay in lung tumor initiation and formation in mice lacking SIRT6. There are two major forms of senescence: replicative senescence and premature senescence. Replicative senescence is induced in response to telomere shortening by cellular replication. This is a common form of senescence seen in cancer cells and can be rescued by ectopic hTERT expression[20]. To address this as a

possible mechanism, hTERT was stably expressed in JD3.12T cells and then SIRT6 was knocked out using Ad-Cre. Ectopic expression of hTERT was unable to rescue the senescence phenotype, nor did it rescue cell growth in soft agar following the loss of SIRT6 (Data not shown). These results suggest that loss of SIRT6 does not result in a form of sensescence that can be rescued by increased telomerase activity. Loss of tumor suppressor-induced senescence, along with oncogene-induced senescence (OIS), are both types of premature senescence induced by the loss of a tumor suppressor or activation of an oncogene, respectively[22]. They are further characterized by induction of p21 or p16 in p53 wild type or mutant cells, respectively, to inhibit cell cycle progression[15,16]. Thus, the induction of p21 expression in response to SIRT6 loss (Fig. 5) supports loss of tumor suppressor-induced senescence as a mechanism behind the anti-tumorigenic phenotypes observed in cells lacking SIRT6.

Classically, senescence was characterized by an irreversible decline in proliferative capacity of the cell with sustained viability. However, in recent years, it has been proposed that this process can be reversible. This reversibility has been shown to occur in response to p53 loss or Ras activation, and is p16[INK4A]-dependent. Furthermore, reversible senescence has only been implicated to occur in cells with low p16[INK4A] expression prior to the induction of senescence; in cells with high p16[INK4A] expression, senescence is irreversible[31-33]. Following continuous passaging after an initial loss of SIRT6, all three mouse lung tumor cell lines show a recovery of their initial anti-tumorigenic phenotype and show a more aggressive phenotype in terms of cell proliferation and colony formation on soft agar. The loss of SIRT6 is

compensated for, and the initial senescence phenotype abrogated. Whether or not this data represents a reversal of cellular senescence, or rather a selection process whereby a subset population of cells do not undergo senescence, and survive and persist despite SIRT6 loss is not clear. Future studies on the single cell level or ones aimed at isolating the senescent population of cells in order to observe a reversible recovery would be necessary to further clarify this mechanism. However, it seems that the latter hypothesis whereby a subset of cells are resistant to senescence induced by SIRT6 loss is consistent with the soft agar data presented in Figure 5A. If this was reversible senescence, it would likely be expected that the cells that survived and successfully recovered from senescence would give rise to smaller colonies than those seen in the Ad-GFP group that retain SIRT6 expression. Instead, we have shown that cells lacking SIRT6 formed larger colonies on agar compared to the Ad-GFP group despite slower proliferation rates (Fig. 4D). Thus, it seems reasonable that these cells that overcame the senescence phenotype induced by SIRT6 loss were in fact resistant to it and perhaps are phenotypically more tumorigenic than other cells in the population.

In summary, we have identified a novel function for SIRT6 in lung tumor initiation and development using two mouse models for NSCLC. The role for SIRT6 in NSCLC was previously uncharacterized, and the majority of studies identified this protein as a tumor suppressor in other types of cancer. Furthermore, we show that loss of SIRT6 not only delayed lung tumor formation, but also acted to attenuate cell proliferation and colony formation on soft agar. This resulting phenotype is consistent with the induction of senescence in response to loss of SIRT6. However,

this phenotype was later reversed, and it appears that this initial loss of SIRT6 is compensated for over time. The resulting surviving population of cells lacking SIRT6 have a higher proliferative capacity than their counterparts retaining SIRT6 expression. This dual role for SIRT6 in NSCLC initiation and then progression is a novel finding that SIRT6 may indeed play a role that is stage-dependent in cancer.

REFERENCES

1. Sebastián, C. *et al.* The histone deacetylase SIRT6 is a tumor suppressor that controls cancer metabolism. *Cell* **151,** 1185–1199 (2012).
2. *cancer.org*. Available at: http://www.cancer.org. (Accessed: 22nd December 2016)
3. Michishita, E. *et al.* SIRT6 is a histone H3 lysine 9 deacetylase that modulates telomeric chromatin. *Nature* **452,** 492–496 (2008).
4. Zhong, L. & Mostoslavsky, R. SIRT6: A master epigenetic gatekeeper of glucose metabolism. *Transcription* (2010).
5. Min, L. *et al.* Liver cancer initiation is controlled by AP-1 through SIRT6-dependent inhibition of survivin. *Nature Cell Biology* **14,** 1203–1211 (2012).
6. Kuilman, T. *et al.* Oncogene-Induced Senescence Relayed by an Interleukin-Dependent Inflammatory Network. *Cell* **133,** 1019–1031 (2008).
7. Overview of the treatment of advanced non-small cell lung cancer - UpToDate. *www-uptodate-com.proxy.its.virginia.edu* Available at: https://www-uptodate-com.proxy.its.virginia.edu/contents/overview-of-the-treatment-of-advanced-non-small-cell-lung-cancer?source=search_result&search=NSCLC&selectedTitle=1~150. (Accessed: 28 December 2016)
8. WHO | World Health Organization. *WHO*
9. Zhong, L. *et al.* The Histone Deacetylase Sirt6 Regulates Glucose Homeostasis via Hif1α. *Cell* **140,** 280–293 (2010).
10. Vander Heiden, M. G., Cantley, L. C. & Thompson, C. B. Understanding the Warburg Effect: The Metabolic Requirements of Cell Proliferation. *Science* **324,** 1029–1033 (2009).
11. Cairns, R. A., Harris, I. S. & Mak, T. W. Regulation of cancer cell metabolism. 1–11 (2011). doi:10.1038/nrc2981
12. Aisner, D. L. & Marshall, C. B. Molecular Pathology of Non–Small Cell Lung Cancer. *Am J Clin Pathol* **138,** 332–346 (2012).
13. Kuilman, T., Michaloglou, C., Mooi, W. J. & Peeper, D. S. The essence of senescence. *Genes & Development* **24,** 2463–2479 (2010).
14. Riely, G. J. *et al.* Frequency and Distinctive Spectrum of KRAS Mutations in Never Smokers with Lung Adenocarcinoma. *Clinical Cancer Research* **14,** 5731–5734 (2008).
15. Provokes Premature Cell Senescence Associated with Accumulation of p53 and p16. 1–10 (1997).
16. Tumor Suppression at the Mouse. 1–11 (1997).
17. Chen, Z. *et al.* Crucial role of p53-dependent cellular senescence in suppression of Pten-deficient tumorigenesis. *Nature Cell Biology* **436,** 725–730 (2005).
18. Tissue-specific tumor suppressor activity of retinoblastoma gene homologs p107 and p130. 1–11 (2004).
19. Targeted disruption of the three Rb-related genes leads to loss of G. 1–14 (2000).

20. Nabetani, A. & Ishikawa, F. Alternative lengthening of telomeres pathway: Recombination-mediated telomere maintenance mechanism in human cells. *Journal of Biochemistry* **149,** 5–14 (2010).

21. Young, A. P. *et al.* VHL loss actuates a HIF-independent senescence programme mediated by Rb and p400. *Nature Cell Biology* **10,** 361–369 (2008).

22. Expression of Catalytically Active Telomerase Does Not Prevent Premature Senescence Caused by Overexpression of Oncogenic Ha-Ras in Normal Human Fibroblasts. 1–5 (1999).

23. Shamma, A. *et al.* Rb Regulates DNA Damage Responseand Cellular Senescence throughE2F-Dependent Suppression of N-Ras Isoprenylation. *Cancer Cell* **15,** 255–269 (2009).

24. letters to the editor. 1–3 (2010).

25. Mogi, A. & Kuwano, H. TP53 Mutations in Nonsmall Cell Lung Cancer. *Journal of Biomedicine and Biotechnology* **2011,** 1–9 (2011).

26. occurring andchemically. 1–5 (2007).

27. Van Meter, M., Mao, Z., Gorbunova, V. & Seluanov, A. SIRT6 overexpression induces massive apoptosis in cancer cells but not in normal cells. *cc* **10,** 3153–3158 (2011).

28. Michishita, E., McCord, R. A., Boxer, L. D. & Barber, M. F. Cell cycle-dependent deacetylation of telomeric histone H3 lysine K56 by human SIRT6. *Cell* (2009).

29. Tennen, R. I., Bua, D. J., Wright, W. E. & Chua, K. F. SIRT6 is required for maintenance of telomere position effect in human cells. *Nat Comms* **2,** 433 (2011).

30. Mao, Z. *et al.* SIRT6 Promotes DNA Repair Under Stress by Activating PARP1. *Science* **332,** 1443–1446 (2011).

31. Reversal of human cellular senescence: roles of thep53 and p16 pathways. 1–11 (1912).

32. Dirac, A. M. G. & Bernards, R. Reversal of Senescence in Mouse Fibroblasts through Lentiviral Suppression of p53. *J. Biol. Chem.* **278,** 11731–11734 (2003).

33. Coppé, J.-P. *et al.* Senescence-Associated Secretory Phenotypes Reveal Cell-Nonautonomous Functions of Oncogenic RAS and the p53 Tumor Suppressor. *PLoS Biol* **6,** e301 (2008).

Supplementary Figures

A.
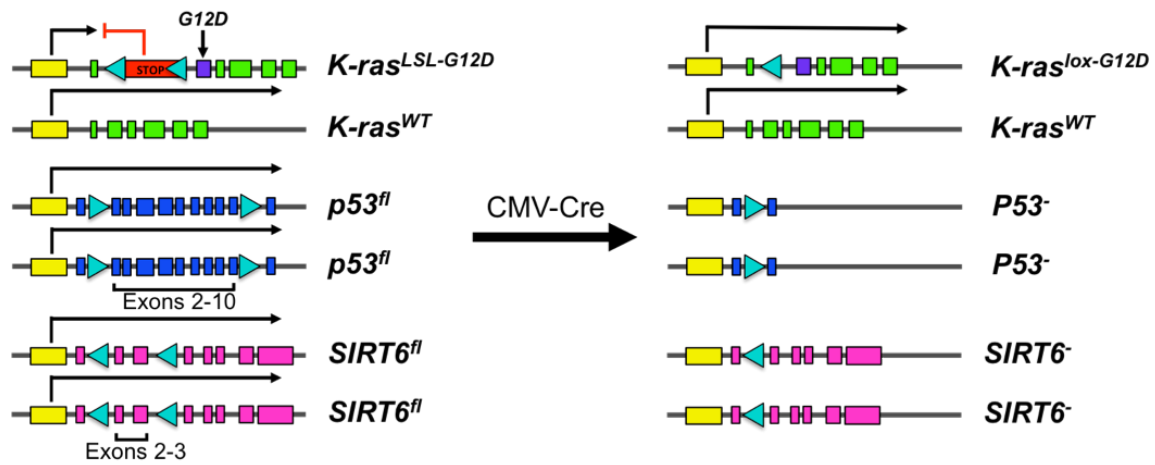
Supplementary Figure 1. Gene map of KP and KPS mice before and after treatment with adenovirus expressing Cre recombinase. Figure created by Jaclyn D'Innocenzi.
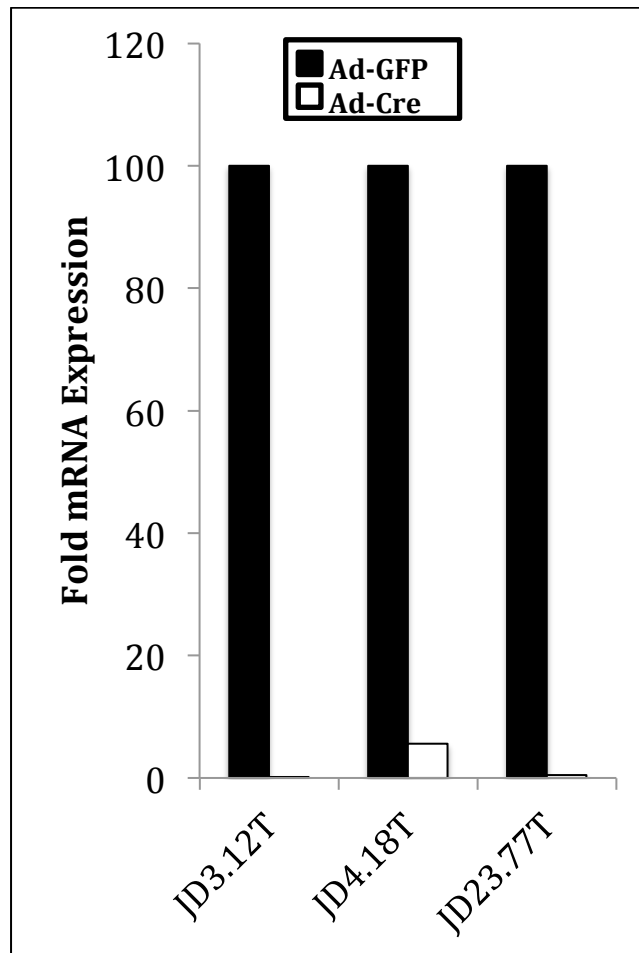
Supplementary Figure 2. SIRT6 is knocked down in JD cells with chronic loss of SIRT6. qRT-PCR for SIRT6 following continuous passaging of JD cells post-Ad-GFP or –Ad-Cre treatment. Work done by Jaclyn D'Innocenzi.

CHAPTER IV

SIRT6 undergoes a glucose- and OGT-dependent N-terminal cleavage

ABSTRACT

Cancer metabolism, characterized by increased glucose uptake and glycolytic flux accompanied by decreased oxidative phosphorylation, is a targetable process of cancer cells as it fuels their ability to survive and proliferate. NSCLC tumors in particular often undergo this metabolic change, as evidenced by their high PET-positivity. The subsequent buildup of glycolytic intermediates under cancer metabolism results in increased flux through anabolic pathways that utilize glycolytic intermediates[1,2]. One such pathway is the hexosamine biosynthesis pathway, which culminates in the production of UDP-GlcNAc, a necessary co-factor for the enzyme OGT. The addition of the O-GlcNAc moiety onto proteins by OGT has been shown to be required for oncogenic programing, as evidenced by its O-GlcNAcylation of the p65 subunit of NF-κB, a necessary step for the full transcriptional activation of this pro-survival protein[3,4]. SIRT6 is a histone deacetylase that has shown to be a key regulator of glucose metabolism and key glycolytic enzymes. While SIRT6 has been identified as a tumor suppressor in several mouse cancer models, its role in lung cancer remains elusive[5,6]. SIRT6 has also been shown to interact with p65, although the nature of this interaction has not been identified[7]. Here, we show that SIRT6 does not deacetylate p65 but rather regulates NF-κB gene targets as a chromatin-associated deacetylase. Furthermore, we found that OGT regulates SIRT6 by promoting its proteasome-mediated N-terminal cleavage, likely resulting in loss of its chromatin localization sequence (CLS). Thus, work presented here indicates that SIRT6 and p65, both of which are

regulated by OGT, may oppose one another when localized to the promoter of

metabolic target genes to regulate cancer metabolism.

INTRODUCTION

Cancer cells have long been identified to have an altered metabolic state, characterized by increased glucose uptake, increased rates of glycolysis and decreased rates of mitochondrial oxidative phosphorylation. This state of Warburg metabolism is thought to allow for a buildup of intermediates of glycolysis that can serve as building blocks for other metabolic processes, such as nucleotide biosynthesis[1,7]. One shunt off of glycolysis that experiences increased flux under these conditions is the hexosamine biosynthesis pathway (HBP). The HBP utilizes glucose and glucosamine, and culminates in production of uridine diphosphate N-acetylglucosamine (UDP-GlcNAc), a molecule that serves as the necessary cofactor for the enzyme O-GlcNAc transferase (OGT). OGT can O-GlcNAcylate hydroxyl groups on serine and threonine residues of proteins and is known to have at least 4000 protein targets. In turn, the protein O-GlcNAcase (OGA), encoded by the *MGEA5* gene, can remove this post-translational modification[3]. In addition to these functions, OGT has also been shown to act as a protease through its ability to cleave host cell factor 1 (HCF-1), a key transcriptional regulator of cell cycle progression[8].

Our laboratory has previously shown that OGT is required to O-GlcNAcylate the T305 residue on the p65 subunit of NF-κB. This is a necessary step that promotes acetylation of p65 at K310, a modification essential for full transcriptional activation of NF-κB[4]. NF-κB has been shown to have an oncogenic role in many cancers and is a key mediator of the pro-inflammatory response, amongst having roles in cell differentiation, proliferation and apoptosis[3,4,8-14]. In addition to having

roles in these key tumorigenic processes, NF-κB has also been shown to be involved in cellular metabolism through positively regulating aerobic glycolysis and potentiating glucose addiction, thus causing cells to be more susceptible to mitochondrial stress and necrosis in response to glucose deprivation[15].

SIRT6 is yet another master regulator of glucose metabolism[5]. It belongs to the Sirtuin family of NAD^+-dependent histone deacetylases. In addition to its deacetylase activity, SIRT6 has also been shown to act as a mono-ADP-ribosyltransferase and a long chain fatty acyl lyase[7,16]j[17,18]. SIRT6 functions to modulate telomere maintenance and aging, DNA damage responses as well as glucose metabolism[5,16,19-21]. Additionally, SIRT6 has been reported to act as a tumor suppressor in pancreatic, liver and colon cancer, at least partially through its metabolic effects[5,6]. More specifically, loss of SIRT6 results in increased glucose uptake and flux through glycolysis through up-regulations of several key glycolytic enzymes, including but not limited to PFK1, PDK1 and LDH[5].

As SIRT6 increases glycolytic flux, it likely could also increase production of UDP-GlcNAc, and thus could possibly serve to regulate O-GlcNAcylation. SIRT6 also has been shown to physically interact with p65 on the promoters of shared metabolic target genes between these two proteins[7,22]. Due to the physical interaction between SIRT6 and p65, and the regulation of p65 by the metabolically regulated OGT enzyme, we were interested in determining whether these two proteins antagonize one another as a result of altered glucose metabolism in the cell – a key process in driving cancer progression[3,4]. Here, we sought to decipher two questions: 1) does SIRT6 post-translationally modify p65 to alter its transcriptional

activity; and/or 2) does SIRT6 and OGT differentially regulate each other to

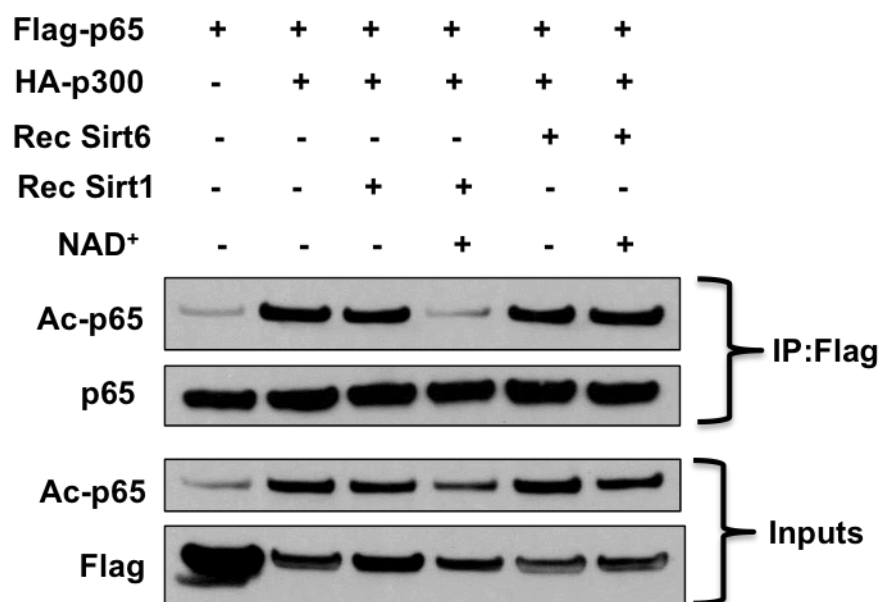modulate p65 transcriptional activity on metabolic target genes?

RESULTS

SIRT6 fails to directly deacetylate the NF-κB subunit of p65.

SIRT6 has previously been shown to be linked to possible NF-κB modulation through several pathways, including regulation of inflammation and senescence[7,19,23]. Kawahara *et al.* 2009 first identified that p65 and SIRT6 physically interact. However, the nature of this physical association remains elusive. In order to further explore this mechanism, we decided to start with verifying if SIRT6 could deacetylate p65 *in vitro*. We performed an *in vitro* deacetylation assay whereby HEK293T cells were transfected with Flag-p65 +/- HA-p300. Flag-p65 was then immunoprecipitated, and combined with recombinant SIRT1 or SIRT6 enzymes in the presence or absence of the NAD^{+} cofactor. The addition of recombinant SIRT1 served as a positive deacetylase control. We found that recombinant SIRT6 on its own did not directly deacetylate p65 (Fig. 7A). Due to this result, other functions of SIRT6 must be explored to determine how SIRT6 may be interacting with p65.

SIRT6 has been largely characterized with regard to its deacetylase activity. However, it also can function as an ADP-ribosyltransferase and mono-ADP-ribosylate target proteins, including PARP1[8,21]. Thus, it is possible that SIRT6 could mono-ADP-ribosylate p65 in order to block the critical acetylation of K310, which is needed for full transcriptional activity of p65. Previously, our lab has also shown that O-GlcNAcylation of T305 of p65 is yet another necessary step for acetylation of K310 to occur[4]. Due to the fact that SIRT6 is a known master regulator of glucose metabolism, and the role of OGT in post-translationally regulating p65, we

postulated that SIRT6 and OGT might oppose one another's function and/or activities [5]. To address this, we performed another *in vitro* acetylation assay whereby HEK293T cells were transfected with HA-p65, V5-SIRT1, Flag-SIRT6 and/or Myc-OGA. HA-p65 was immunoprecipitated and combined with recombinant p300 to allow for acetylation. This assay revealed that SIRT6 dampened full p65 acetylation, perhaps through indirect mechanisms (Fig. 7B). Since SIRT6 has other enzymatic activities, we will in the future aim to determine if SIRT6 was modifying p65 through mono-ADP-ribosyltransferase activity. The attachment of this bulky sugar modification near an acetylation site on p65 could serve to block the acetylation [17].

A.

Flag-p65	+	+	+	+	+	+
HA-p300	-	+	+	+	+	+
Rec Sirt6	-	-	-	-	+	+
Rec Sirt1	-	-	+	+	-	-
NAD⁺	-	-	-	+	-	+

Ac-p65, p65 — IP:Flag

Ac-p65, Flag — Inputs

B.

HA-p65	+	+	+	+	+	+	+
V5-Sirt1	-	-	-	-	+	-	-
Flag-Sirt6	-	-	-	-	-	+	+
Myc-OGA	-	-	+	+	+	-	+
Rec p300	-	+	-	+	+	+	+

K310 Ac-p65, p65 — IP:HA

HA, Myc — Inputs
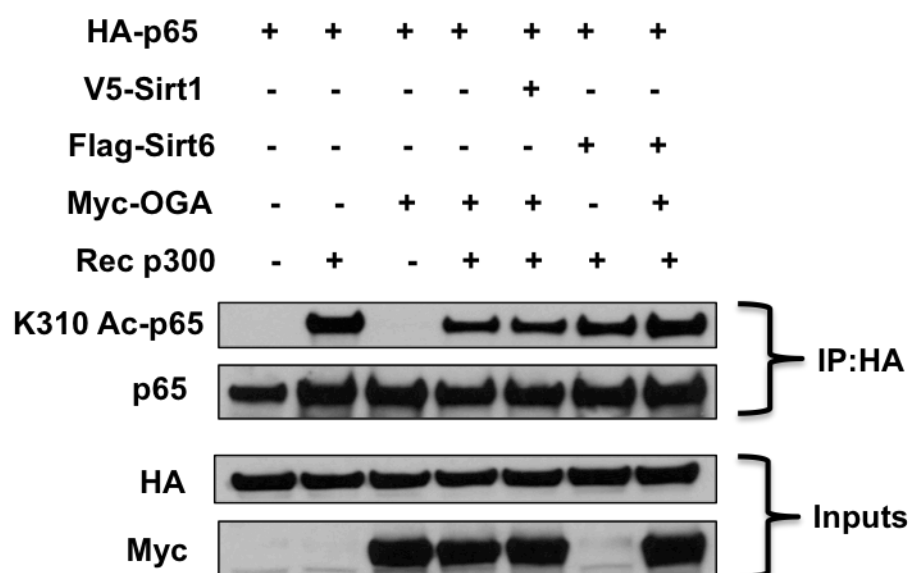
Figure 7. SIRT6 fails to fully deacetylate p65. A) HEK293T cells were transfected with Flag-p65 and/or HA-p300. Immunoprecipitation for Flag and subsequent addition of recombinant (Rec) SIRT6 or SIRT1 +/- NAD$^+$ reveals that SIRT1, but not SIRT6, deacetylates p65. Western blot analysis was performed for acetylated p65 (Ac-p65), p65 and Flag. B) HEK293T cells were transfected with HA-p65, V5-SIRT1, Flag-SIRT6 and/or Myc-OGA. Immunoprecipitation for HA and subsequent addition of Rec p300 reveals that SIRT1 and SIRT6 dampen full p65 acetylation. Western blot analysis was performed for K310 Ac-p65, p65, HA and Myc. Work done by Jaclyn D'Innocenzi.

SIRT6 undergoes a glucose-dependent, OGT-mediated N-terminal cleavage.

Our lab previously identified another metabolic protein that can modify p65. OGT-mediated O-GlcNAcylation of p65 at T305, a nec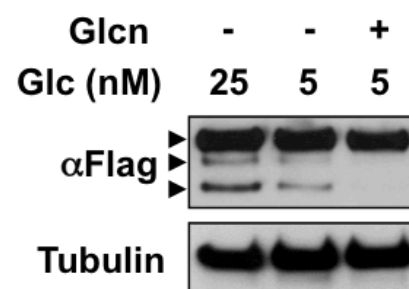essary step to allow for acetylation of p65 at K310 and full transcriptional activation[4]. UDP-GlcNAc serves as the required co-factor for OGT activity, and its production is regulated by flux through the hexosamine biosynthesis pathway (HBP), a shunt off of glycolysis[3]. Because SIRT6 also serves as a master regulator of glucose metabolism and has been shown to also physically interact with p65, we examined whether SIRT6 could be directly regulated by OGT[4,5,7]. To determine whether SIRT6 is O-GlcNAcylated, HEK293T cells were transfected with Flag-SIRT6, V5-OGT and Myc-OGA. SIRT6 was immunoprecipitated and western blot analysis for O-GlcNAc and Flag were performed. Indeed, results showed that SIRT6 is O-GlcNAcylated, and that this O-GlcNAcylation increased in samples over-expressing OGT, and decreased in samples over-expressing OGA (Fig. 8A). Because production of UDP-GlcNAc, the necessary co-factor for OGT, we wanted to determine whether SIRT6 could be regulated by OGT-dependent flux through the HBP[3]. HEK293T cells were transfected with C-terminally tagged Flag- SIRT6 and then grown in both high (25 mM) and low (5 mM) glucose conditions in the presence or absence of glucosamine. Surprisingly, western blot analysis for Flag revealed that SIRT6 undergoes a glucose-responsive N-terminal cleavage, resulting in a ΔN-term SIRT6 (Fig. 3B). As this experiment revealed that the cleavage event was glucose-responsive, we wanted to determine if this cleavage event was regulated by OGT. In order to address this, H1299 cells

were transfected with siRNA to OGT under high (25 mM) or low (5 mM) glucose conditions. Subsequent western blot analysis for SIRT6, OGT and O-GlcNAc revealed that indeed, N-terminal cleavage of SIRT6 resulting in production of ΔN-term SIRT6 was dependent upon OGT expression (Fig. 8C).

A.

Flag-SIRT6	+	+	+
V5-OGT	-	+	-
Myc-OGA	-	-	+

O-GlcNAc

αFlag

B.

Glcn	-	-	+
Glc (nM)	25	5	5

αFlag

Tubulin

C.

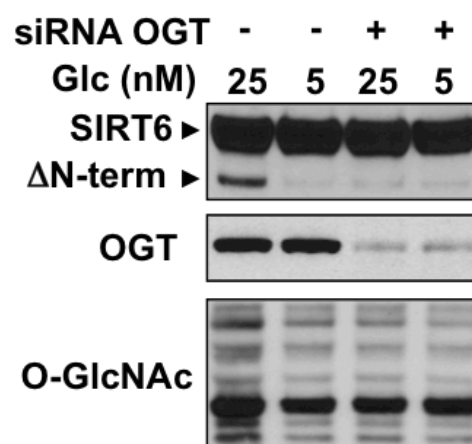| siRNA OGT	-	-	+	+
Glc (nM)	25	5	25	5

SIRT6 ▶
ΔN-term ▶

OGT
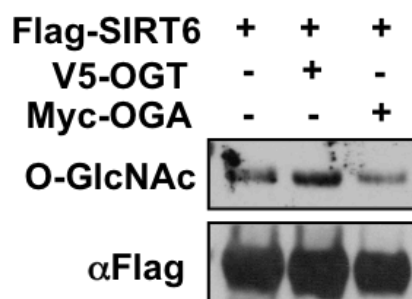
O-GlcNAc

Figure 8. SIRT6 undergoes a glucose-dependent, OGT-mediated N-terminal cleavage. A) HEK293T cells were transfected with Flag-SIRT6, V5-OGT and/or Myc-OGA. Subsequent immunoprecipitation with anti-Flag antibody and western blot analysis for the O-GlcNAc modification reveals that SIRT6 is O-GlcNAcylated. B) SIRT6 undergoes a glucose-dependent N-terminal cleavage. HEK293T cells were transfected with Flag-SIRT6 under high (25mM) and low (5mM) glucose conditions, as well as in the presence and absence of glucosamine. Tubulin is used as a loading control. C) Stability of ΔN-term SIRT6 is mediated by OGT. H1299 cells were transfected with siRNA to OGT or control. Western blot analysis was performed with antibodies to SIRT6, OGT and O-GlcNAc. Work done by Jaclyn D'Innocenzi and Lisa Gray.

The N-terminus of SIRT6 is proteolytically processed and accumulates following inhibition of the 26S proteasome.

To further assess the functional significance and regulation of ΔN-term SIRT6, we first sought to determine if ΔN-term SIRT6 is subject to proteasome-mediated degradation. This could represent a novel regulatory mechanism for SIRT6 expression if such a cleavage event resulted in degradation. To assess this, H1299 cells were treated with the proteasome inhibitor MG132 under high (25 mM) and low (5 mM) glucose conditions in the presence and absence of glucosamine. Indeed, treatment of cells with MG132 rescued the presence of ΔN-term SIRT6, even under low glucose conditions (Fig. 9A). This implies that perhaps it is not only that less ΔN-term SIRT6 is produced under low glucose conditions, but rather that more of it is also degraded under such conditions. However, it does seem that there is still slightly less ΔN-term SIRT6 under low glucose conditions compared to high glucose conditions (Fig. 9A).

Next, we sought to determine if ΔN-term SIRT6 still is localized to the nucleus, or rather is not localized to the cytoplasm. This would lend insight into its functional significance as SIRT6 functions as a nuclear protein that can regulate chromatin. If loss of its N-terminus caused it to re-localize elsewhere, it could represent a novel regulatory mechanism for SIRT6. Protein lysates were collected from the cytoplasm and nucleus of H1299 cells, and subjected to western blot analysis for SIRT6 and HDAC1, which served as a control for sufficient separation of nuclear and cytoplasmic extracts. These results showed that ΔN-term SIRT6 is remains localized to the nucleus with the full length SIRT6 protein (Fig. 9B)

A.

B.
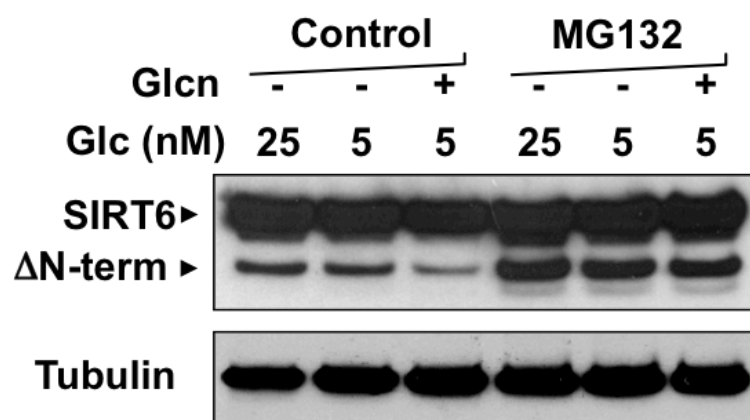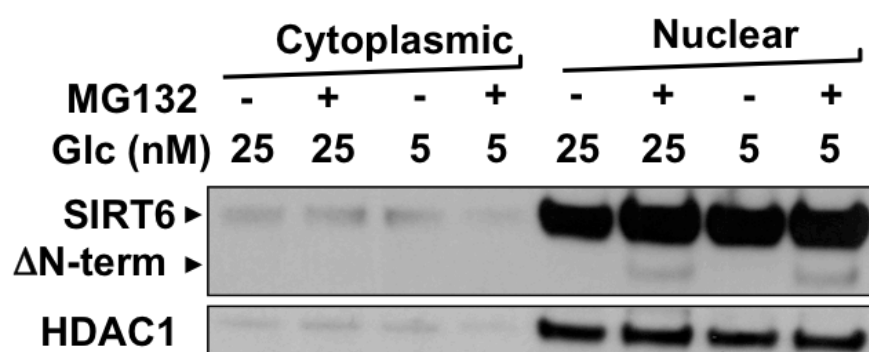
Figure 9. ΔN-term-SIRT6 is nuclear-localized and subject to proteasome-mediated degradation. A) ΔN-term-SIRT6 is subject to proteasome-mediated degradation in response to low glucose levels. H1299 cells were treated with MG-132 to inhibit proteasome-mediated degradation. B) ΔN-term-SIRT6 is nuclear-localized. H1299 cells were treated with gentle lysis to attain cytoplasmic and nuclear protein extracts. Western blotting for SIRT6 and HDAC1 were performed. Work done by Jaclyn D'Innocenzi and Lisa Gray.

DISCUSSION

NF-κB is well established to play a key role in many processes important in cancer, including but not limited to modulation of the pro-inflammatory response, regulation of cell survival and apoptosis, and even metabolism[9-14,21]. p65 is known to be modified by one member of the Sirtuin family, SIRT1[4]. Thus, it seems possible that other Sirtuin family members may be able to modify and regulate this key protein as well. SIRT6 is known to be a key regulator of metabolism, and thus could provide a link of how p65 function can respond to the metabolic state of the cell. Indeed, we show that SIRT6 dampens acetylation of p65 at the key K310 residue potentially through indirect mechanisms. Acetylation at this residue is required for full transcriptional activity of p65. We proposed that this blockage of acetylation occurs through mono-ADP-ribosylation within the lysine-rich Rel homology domain near the K310 residue. Although the deacetylase activity of SIRT6 is more widely studied and applied, SIRT6 has strong mono-ADP-ribosyltransferase activity[17]. Thus, it makes sense that attachment of a bulky ADP-ribose group on a nearby residue could effectively block K310 acetylation of p65. However, we have yet to verify this as the mechanism behind blocked K310 acetylation of p65 by SIRT6.

Furthermore, our lab has previously shown that O-GlcNAcylation of p65 at T305 promotes K310 acetylation of p65. O-GlcNAcylaiton is carried out by the OGT enzyme, which is tightly regulated by the metabolic state of the cell through production of its necessary cofactor, UDP-GlcNAc[4]. As UDP-GlcNAc production by the hexosamine biosynthesis pathway is regulated by glycolytic flux, and SIRT6 is a

key regulator of glucose metabolism, it seems possible that a feedback mechanism could exist where O-GlcNAcylation could regulate SIRT6 function. Indeed we were able to show that SIRT6 is O-GlcNAcylated, and this O-GlcNAcylation triggers an N-terminal cleavage of SIRT6. As loss of the N-terminus of the approximate size seen on western blot corresponds to loss of the chromatin localization sequence (CLS), it looks as though O-GlcNAcylation of SIRT6 may cause SIRT6 to come off of chromatin[24] (Fig. 10). Chromatin immunoprecipitation analysis for both the C-terminus and N-terminus of SIRT6 may be useful in verifying this theory. Furthermore, the fact that ΔN-term SIRT6 is still nuclear localized further supports the theory that is loses its CLS, and not its nuclear localization sequence.

Additionally, it appears that ΔN-term SIRT6 is subject to proteasomal degradation. We were able to show this using the proteasome inhibitor, MG132. Treatment with MG132 rescued the appearance of ΔN-term SIRT6. Thus, it seems under low glucose conditions where ΔN-term SIRT6 is not as present as under high glucose conditions, it may be due to increased degradation of ΔN-term SIRT6 rather than less production of ΔN-term SIRT6. Putting all of this together, we have developed a model for regulation of shared target metabolic genes of p65 and SIRT6. Under normal glucose utilization, SIRT6 is localized to chromatin with p65, and transcription of metabolic gene targets is inhibited by the presence of SIRT6. However, under elevated glucose utilization, OGT is able to O-GlcNAcylate both p65 and SIRT6, thus promoting p65-mediated transcription of metabolic target genes in two ways. First, O-GlcNAcylation of SIRT6 triggers an N-terminal cleavage and loss of its chromatin localization sequence, thus kicking SIRT6 off of chromatin.

Secondly, O-GlcNAcylation of p65 promotes its acetylation at K310, thus allowing for its full transcriptional activation[4] (Fig.10). To verify this theory, we will have to identify shared metabolic gene targets of SIRT6 and p65, and then address if their transcriptional levels change under varying glucose conditions and/or in the presence or absence of SIRT6.

Figure 10. SIRT6 and OGT may co-regulate p65-mediated transcription of metabolic genes. Under normal nutrient utilization conditions, SIRT6 co-localizes to the promoter of NF-κB metabolic target genes to repress transcription. Under elevated nutrient utilization conditions, such as those that occur during Warburg metabolism in the cancer cell, OGT co-localizes to the promoter of these NF-κB metabolic target genes. OGT O-GlcNAcylates p65 at T305, a necessary step to allow for full transcriptional activation of p65 via acetylation at K310 by p300. Simultaneously, OGT O-GlcNAcylates SIRT6, triggering its N-terminal cleavage and loss of its chromatin localization sequence (CLS). Thus, SIRT6 is removed from chromatin and p65 is free to transcribe metabolic target genes. Figure created by Marty Mayo.

REFERENCES

1. Vander Heiden, M. G., Cantley, L. C. & Thompson, C. B. Understanding the Warburg Effect: The Metabolic Requirements of Cell Proliferation. *Science* **324,** 1029–1033 (2009).
2. Cairns, R. A., Harris, I. S. & Mak, T. W. Regulation of cancer cell metabolism. 1–11 (2011). doi:10.1038/nrc2981
3. Abdel Rahman, A. M., Ryczko, M., Pawling, J. & Dennis, J. W. Probing the Hexosamine Biosynthetic Pathway in Human Tumor Cells by Multitargeted Tandem Mass Spectrometry. *ACS Chem. Biol.* **8,** 2053–2062 (2013).
4. Allison, D. F. *et al.* Modification of RelA by O-linked N-acetylglucosamine links glucose metabolism to NF-κB acetylation and transcription. (2012).
5. Sebastián, C. *et al.* The histone deacetylase SIRT6 is a tumor suppressor that controls cancer metabolism. *Cell* **151,** 1185–1199 (2012).
6. Min, L. *et al.* Liver cancer initiation is controlled by AP-1 through SIRT6-dependent inhibition of survivin. *Nature Cell Biology* **14,** 1203–1211 (2012).
7. Kawahara, T. L. A. *et al.* SIRT6 Links Histone H3 Lysine 9 Deacetylation to NF-κB-Dependent Gene Expression and Organismal Life Span. *Cell* **136,** 62–74 (2009).
8. Daou, S. *et al.* Crosstalk between O-GlcNAcylation and proteolytic cleavage regulates the host cell factor-1 maturation pathway. *Proc. Natl. Acad. Sci. U.S.A.* **108,** 2747–2752 (2011).
9. Napetschnig, J. & Wu, H. Molecular Basis of NF-κB Signaling. *Annu. Rev. Biophys.* **42,** 443–468 (2013).
10. Elbein, S. C. *et al.* Molecular screening of the human glutamine–fructose-6-phosphate amidotransferase 1 (GFPT1) gene and association studies with diabetes and diabetic nephropathy. *Molecular Genetics and Metabolism* **82,** 321–328 (2004).
11. Tak, P. P. & Firestein, G. S. NF-κB: a key role in inflammatory diseases. *J. Clin. Invest.* **107,** 7–11 (2001).
12. Perkins, N. D. The diverse and complex roles of NF-κB subunits in cancer. *Nature Publishing Group* (2012). doi:10.1038/nrc3204
13. Karin, M., Cao, Y., Greten, F. R. & Li, Z.-W. NF-κB IN CANCER: FROM INNOCENT BYSTANDER TO MAJOR CULPRIT. *Nat. Rev. Cancer.* **2,** 301–310 (2002).
14. Karin, M. Nuclear factor-κB in cancer development and progression. *Nature Cell Biology* **441,** 431–436 (2006).
15. Huang, X. *et al.* O-GlcNAcylation of Cofilin Promotes Breast Cancer Cell Invasion. *Journal of Biological Chemistry* **288,** 36418–36425 (2013).
16. Michishita, E., McCord, R. A., Boxer, L. D. & Barber, M. F. Cell cycle-dependent deacetylation of telomeric histone H3 lysine K56 by human SIRT6. *Cell* (2009).
17. J. Biol. Chem.-2005-Liszt-jbc.M413296200. 1–19 (2005).
18. Jiang, H. *et al.* SIRT6 regulates TNF-α secretion through hydrolysis of long-chain fatty acyl lysine. *Nature* **496,** 110–113 (2013).
19. Michishita, E. *et al.* SIRT6 is a histone H3 lysine 9 deacetylase that modulates

telomeric chromatin. *Nature* **452,** 492–496 (2008).

20. Tennen, R. I., Bua, D. J., Wright, W. E. & Chua, K. F. SIRT6 is required for maintenance of telomere position effect in human cells. *Nat Comms* **2,** 433 (2011).

21. Mao, Z. *et al.* SIRT6 Promotes DNA Repair Under Stress by Activating PARP1. *Science* **332,** 1443–1446 (2011).

22. Zhong, L. *et al.* The Histone Deacetylase Sirt6 Regulates Glucose Homeostasis via Hif1α. *Cell* **140,** 280–293 (2010).

23. Kawahara, T. L. A. *et al.* Dynamic Chromatin Localization of Sirt6 Shapes Stress- and Aging-Related Transcriptional Networks. *PLoS Genet* **7,** e1002153 (2011).

24. Tennen, R. I., Berber, E. & Chua, K. F. Functional dissection of SIRT6: Identification of domains that regulate histone deacetylase activity and chromatin localization. *Mechanisms of Ageing and Development* **131,** 185–192 (2010).

CHAPTER V

Summary and Future Directions

SUMMARY

Lung cancer causes more cancer-related deaths among men and women than any other type of cancer. Of all the types, non-small cell lung cancer (NSCLC) is the most common. Several cancer-related processes have been shown to have key roles in lung cancer, including DNA damage, aging and altered cancer metabolism[1]. SIRT6 is a histone deacetylase that has previously been shown to play a key role in regulating genomic instability, aging through telomere maintenance and glucose metabolism[2-5]. SIRT6 has been implicated to be a tumor suppressor in pancreatic, colon and liver cancer, although its role in lung cancer remains elusive[2,6]. Here, we created a conditional knockout mouse model for SIRT6 by crossing SIRT6^{fl/fl} mice with KRAS[LSL-G12D]p53^{fl/fl} mice to create KPS mice. Upon intranasal delivery of adenovirus expressing Cre, lung tumor formation is induced selectively via activation of KRAS and knockout of p53 with simultaneous knockout of SIRT6. Unexpectedly, we found that loss of SIRT6 delayed lung tumor initiation and formation, and prolonged overall survival.

To further evaluate the mechanism behind this phenotype, we used murine lung tumor cell lines derived from urethane-induced tumors in SIRT6^{fl/fl} mice. Knockout of SIRT6 via treatment of the cell lines with adenovirus expressing Cre revealed that indeed, initial loss of SIRT6 decreased cell proliferation and colony formation on soft agar. Furthermore, cells lacking SIRT6 were shown to be undergoing an increased amount of senescence, which may account for the delay in tumor formation see *in vivo*. However, with continuous passaging, this phenotype in

response to SIRT6 loss was abrogated and cells lacking SIRT6 showed increased cell proliferation and colony formation on soft agar. After this recovery, it seems as though SIRT6 is acting as a tumor suppressor in more established lung tumors. Its role as a tumor suppressor in other types of cancers is attributed to the ability of SIRT6 to preferentially regulate pathways involved in glucose metabolism and biomass intermediates[2,6]. SIRT6 has been shown to regulate key glycolytic enzymes, and thus, loss of SIRT6 has been shown to potentiate cancer metabolism through increased glucose uptake, increased glycolytic flux and decreased mitochondrial respiration[2]. Under these conditions, flux through other metabolic pathways that utilize glycolytic intermediates is also increased, including the hexosamine biosynthesis pathway (HBP). The HBP culminates in production of UDP-GlcNAc, a necessary cofactor for the enzyme OGT, which has been shown to O-GlcNAcylate key proteins in oncogenesis[7]. This includes the p65 subunit of NF-κB, a modification required for its full transcriptional activation to promote the expression of metabolic target genes[8]. p65 and SIRT6 have also been shown to physically interact, although the nature of this interaction remains elusive[9]. Here we show that SIRT6 indeed does not deacetylate p65 but rather blocks its acetylation. In addition, we found that OGT can regulate not only p65 but also SIRT6 by promoting cleavage of its N-terminus, which likely results in loss of its chromatin localization sequence (CLS). Thus, this implies that OGT may cooperate to induce transcription of key metabolic target genes in cancer metabolism by allowing for full transcriptional activation of p65 while concomitantly inhibiting localization of SIRT6 to these promoter sites.

FUTURE DIRECTIONS

Identify senescence as the mechanism causing a delay in tumor initiation and formation in the KP and KPS mouse model system.

Here, we presented data showing that loss of SIRT6 using the KP lung tumor model resulted in a delay of lung tumor initiation and formation. This delay lead to decreased overall tumor burden and increased overall survival in comparison to their KP counterparts. Using an *in vitro* cell line model system derived from urethane-induced tumors in SIRT6$^{fl/fl}$ mice, we were able to show that initial loss of SIRT6 induced a comparable phenotype, resulting in decreased cell proliferation and decreased colony formation on soft agar. We further verified that initial loss of SIRT6 induced senescence using SA-β-Gal staining. Thus, the implication is that senescence is the mechanism behind the delay in tumor formation seen in the KPS mice. However, to verify this, future experiments would need to perform SA-β-Gal staining on frozen samples derived from lung tumors of KP and KPS mice. To initiate these experiments samples would need to be harvested from mice at several early time points following induction of tumor formation using adenovirus expressing Cre. This is due to the fact that eventually this initial phenotype due to acute SIRT6 loss is overcome, as evidenced by eventual tumor growth in KPS mice and increased cell proliferation and colony formation on soft agar seen after continuous passaging in the urethane-induced lung tumor cell lines lacking SIRT6.

Thus, later-stage, growing, larger tumors may not show the senescence phenotype as it has already been compensated for and overcome.

In addition to confirming that NSCLC cells within KPS tumors are undergoing senescence, it would be equally important to better understand the mechanism by which loss of SIRT6 promotes the senescence phenotype. Perhaps the best potential mechanism is that loss of SIRT6 elevates the SASP (senescence-associated secretory phenotype). This secretory milieu of growth factors, cytokines and chemokines are able to stimulate senescence in an autocrine and paracrine-dependent manner[10-12]. While there are over 50 SAPs identified thus far, many (90%) of these protein targets are transcriptionally regulated by NF-κB[12-14]. Thus, it is quite possible that the loss of SIRT6 promotes inappropriate NF-κB, which then activated the SASP response to promote senescence. To experimentally address this hypothesis we will simply examine cultured supernatant media for its ability to induce senescence in JD cell lines. If supernatants from SIRT6 null cells are able to induce senescence, we will perform ELISAs and qRT-PCR to identify specifically which SAPs are differentially expressed following the knockout of SIRT6 and will examine whether this phenotype is NF-κB-dependent.

Determine how the loss of SIRT6 affects invasion, migration and metastasis in lung tumors.

In this study, we have provided evidence that loss of SIRT6 effectively inhibits lung tumor initiation and formation in KP and KPS mice, a model for NSCLC. Additionally, we show that later on following the initial loss of SIRT6, there is a

recovery and reversion of the original phenotype – KPS tumors did proceed to form and grow at a comparable rate to KP tumors and urethane-induced lung tumor cells lacking SIRT6 started to proliferate faster and form an increased amount of colonies on soft agar. However, we have yet to study the effects of the loss of SIRT6 on invasion and metastasis in NSCLC.

Despite most studies providing evidence that SIRT6 acts as a tumor suppressor in cancer[2,6,15], it seems that its role may be different with regard to metastasis compared to that of tumor size and growth. Indeed, a recent study found that the presence of SIRT6 in NSCLC patient tumors was a poor predictor of prognosis and correlated with advanced TNM staging. This study found that SIRT6 activated matrix metalloproteinase 9 (MMP9) expression via phosphorylation and activation of ERK1/2. This was proposed to be the mechanism behind increased invasion and migration seen in transwell and wound healing assays using established NSCLC cell lines that overexpress SIRT6[16]. Additionally, another study found that overexpression of SIRT6 in pancreatic cancer cell lines resulted in increased cell migration via promotion of a pro-inflammatory phenotype exhibiting elevated IL-8 and TNF expression. It was also found that SIRT6 increased intracellular Ca^{2+} levels via increasing intracellular levels of ADP-ribose, an activator of the Ca^{2+} channel TRPM2. These effects were proposed to be the cause of the pro-inflammatory phenotype driving increased cell migration under overexpression of SIRT6 in pancreatic cancer cells[17].

SIRT6 may also regulate invasion and metastasis through its role in modulating glucose metabolism and glycolytic flux. Loss of SIRT6 has been shown

to increase glucose uptake by up-regulating expression of the glucose transporter, GLUT1. Furthermore, loss of SIRT6 has been shown to induce expression of several key glycolytic enzymes, including PFK1, ALDOC, PDK1 and LDH. This is proposed to be due to its function as a co-repressor of HIF1α, another key regulator of these metabolic gene targets[2,18]. SIRT6 was shown to bind to the promoters of these metabolic gene targets to repress their transcription, but in its absence, H3K9Ac at these locations increases, thus allowing for transcriptional activation of these gene targets via HIF1α. However, it remains un-confirmed if SIRT6 co-localizes with HIF1α on chromatin[2,18].

Although a few studies have examined the effect of SIRT6 on metastatic processes in cancer, they both accomplished this through artificial over-expression of SIRT6, which is not the best way to examine how loss of SIRT6 affects these processes[16,17]. Furthermore, it is yet that this has been examined in an *in vivo* mouse rather than in just cell lines. To address whether loss of SIRT6 affects invasion, migration and/or metastasis using our systems, we can do flank injections of our urethane-induced lung tumor cell lines that have and lack SIRT6 into nude mice to observe and measure metastasis at their survival endpoint. Additionally, we can use invasion and migration transwell assays to observe the effect of loss of SIRT6 on these processes *in vitro* using these same cell lines. However, it is important to note that the soft agar assays performed and presented in this study may give some insight into the metastatic potential of cells lacking SIRT6 vs. those retaining SIRT6 expression, as this assay measures anchorage independent growth and colony

formation. Both of these processes are necessary for successful metastatic tumor
formation.

Determine whether SIRT6 blocks acetylation of p65 at K310 by mono-ADP-ribosylation.

Previous studies have shown that SIRT6 is a strong mono-ADP-ribosyltransferase in addition to deacetylase. However, not many targets of this activity of SIRT6 have been identified. Mao *et al.* 2011 identified PARP1 as a mono-ADP-ribosylation target of SIRT6, resulting in its activation and promotion of repair of DNA damage[5]. Despite a lack of identification of mono-ADP-ribosylation targets of SIRT6, SIRT6 has been identified to physically interact with a number of other proteins, including the p65 subunit of NF-κB[9]. However, the nature of this interaction remains elusive. Here, we showed that SIRT6 does not deacetylate, but rather dampens p300-mediated acetylation of p65 at the key K310 residue, which is required for full transcriptional activation of NF-κB[8,9]. Attachment of a bulky mono-ADP-ribose group onto the lysine-rich Rel homology domain region of p65 may function to effectively block acetylation at the K310 residue close by. To verify this hypothesis, immunoprecipitation of p65 from HEK293T cells transfected with and without a plasmid to overexpress SIRT6 can be performed, and the isolated p65 can be run on a western blot. Probing of this blot with a mono-ADP-ribose antibody can then be used to identify mono-ADP-ribosylation of p65. However, it is important to note that this antibody is not commercially available and would have to be

synthesized. In order to assess which residues are mono-ADP-ribosylated, mass spectrometry can be performed on isolated p65 protein.

Determine whether the loss of SIRT6 results in induction of NF-κB-regulated metabolic genes required for NSCLC growth and metastasis.

SIRT6 has previously been shown to be a master regulator of glucose metabolism in colon cancer cell lines via its inhibitory regulation of key glucose metabolism and glycolytic enzymes, including GLUT1, PFK1, ALDOC, PDK1 and LDH. These have been shown to be shared metabolic targets of SIRT6 and HIF1α, where in the absence of SIRT6, HIF1α can induce expression of these genes to propagate the altered Warburg metabolic state of the cancer cell[2,18]. In addition to this, SIRT6 has been shown to physically interact with the p65 subunit of NF-κB. Additionally, a microarray analysis performed on mouse embryonic fibroblasts (MEFs) showed that SIRT6 and NF-κB share many transcriptional targets, including but not limited to numerous metabolic genes involved in glucose transport and insulin signaling [9,19]. However, it is important to note that this study was performed in MEFs, and thus signaling is likely altered when applied to cancer cells, in particular lung tumor cells. We have identified several metabolic targets of potential interest, most of which could potentially influence flux through the hexosamine biosynthesis pathway (HBP). These include, but are not limited to, GLUT3, DHODH, and HKII. Gene targets that could influence flux through the HBP are of particular interest given the potential for SIRT6 regulation through O-GlcNAcylation by OGT and subsequent N-terminal cleavage of its CLS, shown in data presented earlier (Fig. 8A, 8B and 10).

Thus, it is possible that a feedback mechanism exists where SIRT6 can regulate

transcription of genes that can modulate production of UDP-GlcNAc by the HBP, the

necessary co-factor for the enzyme OGT. To address this, we can use the urethane-

induced lung tumor cell lines, and treat with adenovirus expressing Cre *in vitro* to

knock out SIRT6 and/or shRNAs to target p65. Next, RT-qPCR analysis performed

on these gene targets on both sets of cells can reveal a difference in transcription of

these genes between cells expressing SIRT6 and p65, and those that do not. To take

an unbiased approach, we can also do an expression microarray analysis to identify

possible shared targets between SIRT6 and NF-κB on these cells.

Determine the sequence of ΔSIRT6 and establish whether it no longer

localizes to chromatin.

Our data presented earlier shows that SIRT6 can block acetylation of p65 at

its critical K310 residue; acetylation at this residue allows for full transcriptional

activation of p65 (Fig. 7A and 7B). In turn, data presented here combined with

previously published studies in our lab reveal that both SIRT6 and p65 can be

modified via O-GlcNAcylation by the glucose- and glucosamine-responsive enzyme

OGT. O-GlcNAcylation of p65 at T305 is required for K310 acetylation of p65[8]. We

found that SIRT6 is also O-GlcNAacylated, and this O-GlcNAcylation results in its N-

terminal cleavage to produce ΔSIRT6 (Fig 8A, 8B and 8D). Although we have yet to

perform mass spectrometry analysis on the purified ΔSIRT6 to determine its exact

sequence identity, immunoblot analysis reveals that ΔSIRT6 would have lost a

segment of its N-terminus that corresponds to loss of its chromatin localization

sequence (CLS) (Figure 8B and 10). Thus, it can be inferred that O-GlcNAcylation of SIRT6 causes it to lose its association to chromatin, where it can co-localize to promoters regulated by p65 and OGT (Fig. 10). To verify this model, chromatin immunoprecipitation (ChIP) analysis for p65, SIRT6 and OGT would have to be performed on a shared gene targets. Our lab has identified GFAT2, the rate limiting enzyme of the hexosamine biosynthesis pathway (HBP), as a shared transcriptional target of p65 and SIRT6, and thus can be used for this ChIP analysis. Furthermore, GFAT2 is more actively transcribed under a 3D modeling system with treatment of TNFα, thus allowing us a mechanism to possibly observe the co-localization of SIRT6 and p65 to this gene when it is not stimulated, vs. cleavage of the CLS of SIRT6 and its absence from this gene when GFAT2 is actively being transcribed (Fig. 10). Antibodies directed at both the N-terminus and C-terminus of SIRT6 can be useful in detecting the presence of ΔSIRT6 vs. full-length SIRT6.

REFERENCES

1. *cancer.org*. Available at: http://www.cancer.org. (Accessed: 22nd December 2016)
2. Sebastián, C. *et al.* The histone deacetylase SIRT6 is a tumor suppressor that controls cancer metabolism. *Cell* **151,** 1185–1199 (2012).
3. Michishita, E. *et al.* SIRT6 is a histone H3 lysine 9 deacetylase that modulates telomeric chromatin. *Nature* **452,** 492–496 (2008).
4. Tennen, R. I., Bua, D. J., Wright, W. E. & Chua, K. F. SIRT6 is required for maintenance of telomere position effect in human cells. *Nat Comms* **2,** 433 (2011).
5. Mao, Z. *et al.* SIRT6 Promotes DNA Repair Under Stress by Activating PARP1. *Science* **332,** 1443–1446 (2011).
6. Min, L. *et al.* Liver cancer initiation is controlled by AP-1 through SIRT6-dependent inhibition of survivin. *Nature Cell Biology* **14,** 1203–1211 (2012).
7. Abdel Rahman, A. M., Ryczko, M., Pawling, J. & Dennis, J. W. Probing the Hexosamine Biosynthetic Pathway in Human Tumor Cells by Multitargeted Tandem Mass Spectrometry. *ACS Chem. Biol.* **8,** 2053–2062 (2013).
8. Allison, D. F. *et al.* Modification of RelA by O-linked N-acetylglucosamine links glucose metabolism to NF-κB acetylation and transcription. (2012).
9. Kawahara, T. L. A. *et al.* SIRT6 Links Histone H3 Lysine 9 Deacetylation to NF-κB-Dependent Gene Expression and Organismal Life Span. *Cell* **136,** 62–74 (2009).
10. Xue, W. *et al.* Senescence and tumour clearance is triggered by p53 restoration in murine liver carcinomas. *Nature* **445,** 656–660 (2007).
11. Krizhanovsky, V. *et al.* Senescence of Activated Stellate Cells Limits Liver Fibrosis. *Cell* **134,** 657–667 (2008).
12. Coppé, J.-P. *et al.* Senescence-Associated Secretory Phenotypes Reveal Cell-Nonautonomous Functions of Oncogenic RAS and the p53 Tumor Suppressor. *PLoS Biol* **6,** e301 (2008).
13. Chien, Y. *et al.* Control of the senescence-associated secretory phenotype by NF- B promotes senescence and enhances chemosensitivity. *Genes & Development* **25,** 2125–2136 (2011).
14. Batsi, C. *et al.* Chronic NF-κB activation delays RasV12-induced premature senescence of human fibroblasts by suppressing the DNA damage checkpoint response. *Mechanisms of Ageing and Development* **130,** 409–419 (2009).
15. Van Meter, M., Mao, Z., Gorbunova, V. & Seluanov, A. SIRT6 overexpression induces massive apoptosis in cancer cells but not in normal cells. *cc* **10,** 3153–3158 (2011).
16. Top. Upregulation of SIRT6 predicts poor prognosis and promotes metastasis of non-small cell lung cancer via the ERK1/2/MMP9 pathway. 1–10 (2016).
17. Bauer, I. *et al.* The NAD+-dependent Histone Deacetylase SIRT6 Promotes Cytokine Production and Migration in Pancreatic Cancer Cells by Regulating Ca2+ Responses. *J. Biol. Chem.* **287,** 40924–40937 (2012).

18. Zhong, L. *et al.* The Histone Deacetylase Sirt6 Regulates Glucose Homeostasis via Hif1α. *Cell* **140,** 280–293 (2010).
19. Kawahara, T. L. A. *et al.* Dynamic Chromatin Localization of Sirt6 Shapes Stress- and Aging-Related Transcriptional Networks. *PLoS Genet* **7,** e1002153 (2011).